ESTIMATION OF FLOW PARAMETERS USING LASER ANEMOMETRY

Q. ISA DAUDPOTA

DOCTOR OF PHILOSOPHY

UNIVERSITY OF EDINBURGH

1976

ABSTRACT

The use of a photon count correlator for analysing different flow situations is described. The problem of flow parameter estimation from the correlogram is discussed in some detail. After describing some approximate methods, the least square fitting and Fourier transformation methods are considered. The effect of frequency shifting on parameter estimation is described. The use of high resolution spectral estimators such as the Maximum Entropy and Maximum Likelihood spectra have been considered. An experiment on a sinusoidally fluctuating flow is described. The error involved in uniform random clipping of photon counts in order to make the correlogram independent of the field statistics is derived.

The errors in the determination of the mean and variance of the velocity using a burst counter are derived. This is accomplished by assuming Poisson sampling of a continuous velocity record with a known correlation function. The method of obtaining the turbulence spectra from the burst counter data is described.

KEY WORDS : Laser Doppler Velocimeter, Photon Correlator, Turbulence, Periodic Flow, Parameter Estimation, Least Square Fitting, Fourier Transformation, Maximum Entropy and Maximum Likelihood Spectra, Burst Counter, Poisson Sampling and Error Estimation.

PREFACE

The work presented in this thesis was carried out over the period Dec. '72 - Aug. '76 and is submitted for the Ph.D. degree according to the University regulations.

I would like to thank my project supervisor Dr. Clive A. Greated, Senior Lecturer and Director of the Fluid Dynamics Group in the Physics Dept., for his advice, encouragement and hospitality during my stay in Edinburgh.

It was a pleasure to work with Mr. Graham Dowrick. The fruit of our labour is in chapter 4 §3-8. This collaboration proved to be the most interesting part of my work.

Dr. John Barrow very kindly volunteered to read the initial drafts of the thesis and helped to correct numerous grammatical slips.

Thanks are due to Drs. Francis Barnes and Ian Grant for conducting the experiments in the wind-tunnel described in Appendix A.

The financial support of the Procurement Executive of the Ministry of Defence over the period Dec. '72 - Nov. '75 is gratefully acknowledged.

Rm. 2107, JCM Bldg.,
Edinburgh.
August 1976.

Q.I.D.

CONTENTS

P.T.O.

CONTENTS (cont.)

C H A P T E R 1

INTRODUCTION

Photon counting techniques have been used in various branches of physics, chemistry and biology. It is due to the high sensitivity of these techniques that it has been possible to investigate a large number of interesting light scattering phenomena. The use of high speed clipped digital correlators for analysing the detected photon counts in real time has led to many applications. During the last few years the correlator has been used with a Laser Doppler Velocimeter (LDV). Unlike previous LDV processors, the photon count correlator does not require a continuously varying intensity at the detector when a particle traverses the scattering volume.

In chapter 2 the basic principles of the LDV are described briefly. Different optical configurations are considered, but emphasis is on the cross-beam system which is commonly used with a photon count correlator. Expressions for the correlation functions for sinusoidally fluctuating flow and turbulent flow with Gaussian statistics are obtained. The use of periodic sampling of the detector's output/input for the analysis of periodically fluctuating flows is described. It is shown how the variation in particle density in the flow can be determined using a correlator.

The estimation of flow parameters from a correlogram is discussed in some detail in chapter 3. After describing some approximate methods of parameter estimation the non-linear least square fitting of the correlogram to a model is described. The Fourier transformation of a fully damped correlogram into the spectral plane is shown to be the most convenient method of parameter estimation. By proper frequency shifting most correlograms can be completely damped before the last lag value. The use of high resolution spectral estimators is also illustrated.

The burst counter has been used with considerable success in analysing flows with low particle density. In chapter 4 the errors in estimating the mean and variance of the velocity from the data obtained from the burst counter are derived. It is necessary to assume the form of the velocity correlation function. Exponentially decayed and Gaussian correlation functions are examined. The method of obtaining turbulence spectra is also presented.

In appendix A results are presented of experiments on a sinusoidally fluctuating flow. This involved the investigation of the flow behind a circular cylinder placed in a steady air-flow. A hot-wire anemometer was used to compare results with those obtained from correlograms (a 48 channel Precision Devices photon correlator was used).

Appendix B consists of a paper which discusses the error involved in uniform random clipping of photon counts used in order to make the correlogram independent of field statistics.

A list of reports and papers written during the course of this thesis is presented.

CHAPTER 2

APPLICATION of CORRELATION TECHNIQUE to FLOW MEASUREMENT

§ 1. INTRODUCTION

The statistical and instrumental developments in photon-counting and photon-clipping techniques have been discussed by JAKEMAN('70)Because of the use of digital circuits these methods have a much higher sensitivity than analogue techniques for obtaining the intensity correlation function of scattered light. ABBISS et al (1972) succeeded in measuring the flow velocity using light scattered from naturally occurring dust particles in a wind tunnel using a photon correlator. MENEELY *et al* carried out a similar experiment for measurement of flow in a jet. They identified the "self-beat" and "cross-beat" components in the correlogram.

BOURKE *et al* in an important paper described the spectrum obtained using the reference beam heterodyne technique and the homodyne technique in the measurement of turbulent flows. They discussed the influence of the concentration of scatterers and the strength and coherence of the scattered light on the different components of the spectrum. ADRIAN & GOLDSTEIN have obtained similar results. EDWARDS *et al* (1971, '73) related the spectrum to the Van Hove space-time correlation function and by assuming a Gaussian form for this function they derived expressions for the spectrum and its moments. All the papers mentioned in this paragraph discuss the analysis of the reference-beam system used in conjunction with a sweep frequency analyser to obtain the spectrum.

The sweep mode slows the response of the frequency analyser and it is therefore advantageous to use a filter bank or a phase lock loop. The phase lock loop requires a continuous signal input and hence cannot be used when there are few particles in the flow while the filter bank is very expensive and difficult to construct. Therefore, for low seeding conditions there are only two efficient LDV processors at the moment i. burst counter system

and ii. photon correlation system.

The photon correlation system, while more sensitive than the burst counter system, has not yet been used for obtaining turbulence spectra. In order to obtain the spectrum it would be necessary to measure the inter-arrival times of particles and also analyse the correlation function due to each particle to obtain its velocity. The velocity can be obtained by one of the following methods:

i. zero-crossing analysis of the correlation function after passing it through a digital high-pass filter or

ii. by detecting the peak of the Fourier transform of the correlogram, which can be obtained by using a hardware FFT analyser (BERGLAND).

The use of these methods has not been reported in the literature.

In Chapter 4 the burst counter is discussed and it is shown how the turbulence spectra can be obtained using it.

In § 2 the principle of Doppler shift and its application to LDV is described. It is shown that the cross-beam configuration can be analysed by a real figure model. When the number of particles in the flow is high, the reference-beam system is generally preferred to the

cross-beam system. Both these systems are discussed in § 3.

In § 4 the spatial resolution of the LDV is considered. In a cross-beam system it is useful to have a large angle between the beams and also between the principal bisector of the beams and the line of the detector. This arrangement accompanied by a suitable field stop in front of the detector improves the spatial resolution. In the reference-beam system the scattering volume is defined principally by the size of the detector's field stop.

In § 5, the relation between the count correlation function (which would be obtained when an ideal full digital correlator is used) and the intensity correlation function is given. Since these two functions are related linearly, only expressions for the intensity correlation function are derived in the succeeding sections.

In § 6, there is a discussion on the statistics of random pulse trains. It is shown that the general expression for the correlation function obtained by BEUTLER & LENEMAN reduces to Campbell's theorem under certain conditions. It is shown in § 7 how Campbell's theorem can be used to obtain the correlation function for a constant flow. In § 7.1 it is indicated how the results in § 7 can be applied to the measurement of particle concentration.

In § 8 the correlation function for the case of turbulent flow is derived. An attempt has been made in this section to explain the approaches taken by different authors in analysing this flow situation.

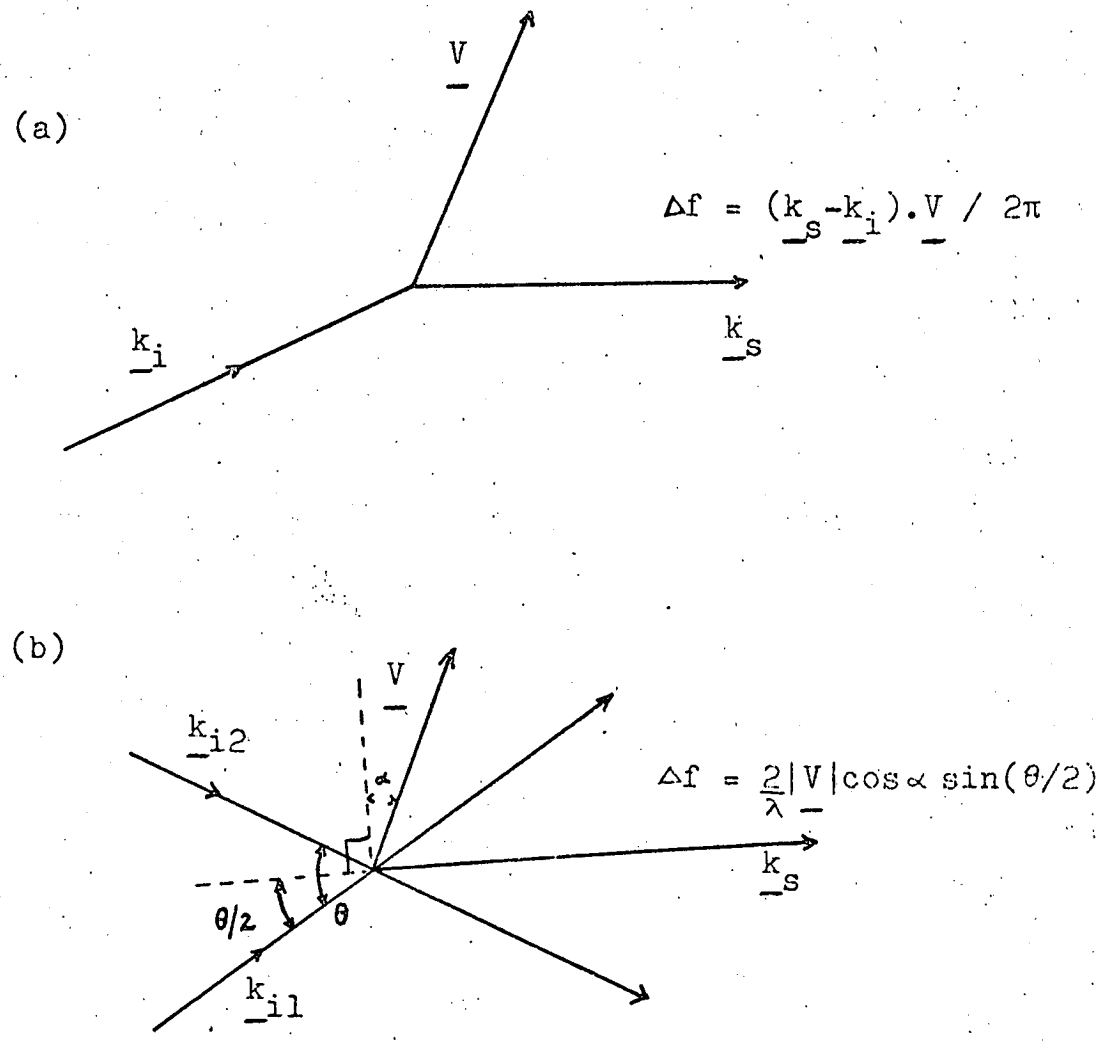

Fig.(1) Principle of Doppler shift.

Measurement of periodic flows is possible using correlation techniques. The procedure, which depends on periodically sampling the scattered light, is described in §9.

The correlation function for a sinusoidally fluctuating velocity is discussed in some detail in § 10. Details of experiments performed in order to verify the expressions obtained in §10 are given in Appendix A.

§ 11 presents a brief review of the cross-correlation technique. It is indicated how this method can be used to study diffusive motion.

§ 2. PRINCIPLE of the DOPPLER EFFECT

The laser anemometer is based on the principle of the Doppler shift; the frequency of light scattered by an object moving relative to a radiating light source is changed by an amount which depends on the velocity and the scattering geometry. In fig.(1a), $\underline{k}_i$ and $\underline{k}_s$ are the incident and scattered wave vectors respectively. The magnitudes of these vectors are given by $\left|\underline{k}_g\right| = 2\pi/\lambda_g$, $(g \equiv i,s)$, where λ_g represents the wavelength of the incident and scattered light. For a particle travelling with velocity $\underline{V}$, the Doppler shift is given by the dot product, $\Delta f = (\underline{k}_s - \underline{k}_i).\ \underline{V}\ /2\pi$ Hz.

For high speed flows the Doppler shift is usually very large and so a Fabry Perot interferometer can be used to determine the flow velocity. The finite spectral resolution of the interferometer presents a lower bound on the velocity that can be measured accurately. Typically one might have a frequency shift of 500 MHz at

supersonic velocities which would require an instrumental bandwidth of the order of 5 MHz; this corresponds to a very high resolution instrument. Conventional plane Fabry-Perot interferometers have resolutions of the order of 100 MHz and even this is difficult to maintain except under carefully controlled conditions. Confocal systems such as described by AVIDOR can have resolutions of the order of 1 MHz. Even at such high resolutions, the interferometer is essentially a high velocity measuring instrument.

The principle of light beating was demonstrated by FORRESTER *et al* about 20 years ago. YEH & CUMMINS using this principle and the Doppler effect showed that it was possible to measure very low frequency shifts in light and hence determine a large range of velocities which are not accessible to the Fabry Perot.

Consider the cross-beam geometry in fig.(1b). Two convergent beams with wave vectors $\underline{k}_{i1}$ and $\underline{k}_{i2}$ illuminate a particle moving with velocity $\underline{V}$. The frequency shift of the light scattered from each of these vectors in the direction of $\underline{k}_s$ is $\Delta\nu_1 = (\underline{k}_s - \underline{k}_{i1}).\ \underline{V}$ and $\Delta\nu_2 = (\underline{k}_s - \underline{k}_{i2}).\ \underline{V}$. The difference of these frequencies is obtained when a square-law detector is used to observe the scattered light.

$$\Delta\nu_1 - \Delta\nu_2 = (\underline{k}_{i2} - \underline{k}_{i1}).\underline{V} = \underline{K}.\underline{V} \qquad (1)$$

Now

$$\left|\underline{k}_{i1}\right| = \left|\underline{k}_{i2}\right| = 2\pi/\lambda,$$

hence
$$\Delta f = (\Delta\nu_1 - \Delta\nu_2)/2\pi = \{2\ u \sin \left(\frac{\theta}{2}\right)\}/\lambda \qquad (2)$$

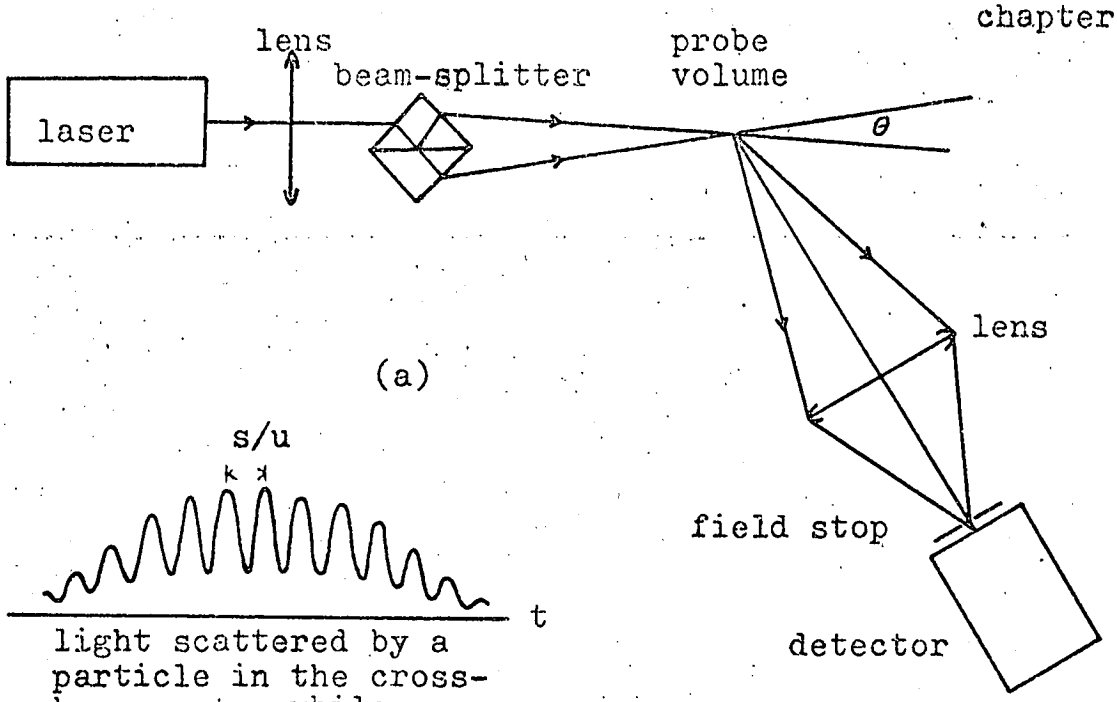

(a)

light scattered by a particle in the cross-beam system while traversing the probe volume

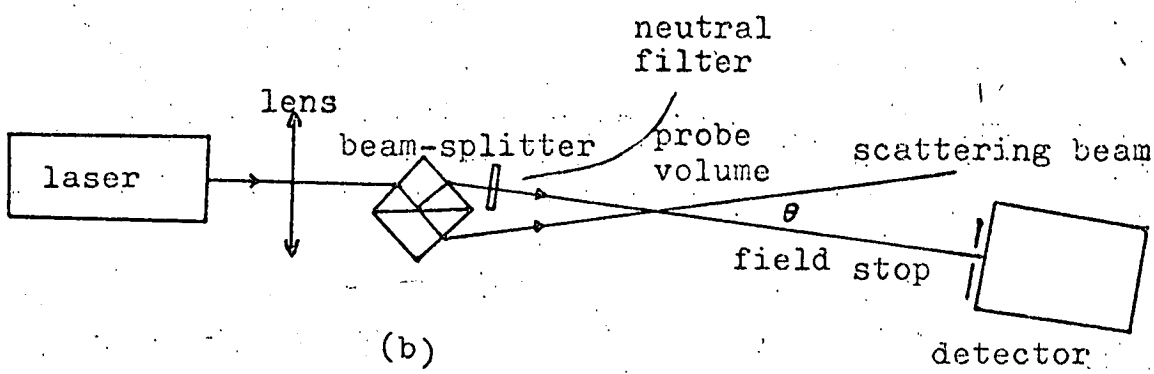

(b)

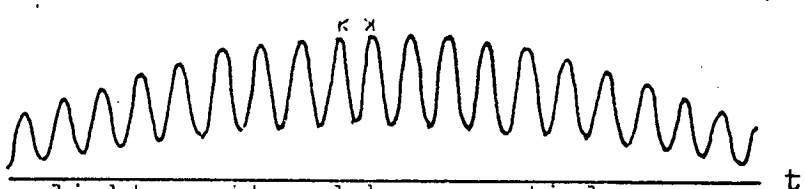

light scattered by a particle in the reference-beam system while traversing the probe volume

Fig.(2) Optical arrangements

(a) cross-beam system

(b) reference-beam system

u = velocity of particle, s = fringe spacing,

Doppler frequency = $u/s = 2u \sin(\theta/2)/\lambda$,

where $u = |\underline{V}| \cos \alpha$ is the component of $\underline{V}$ in the direction of $\underline{K}$, and u is perpendicular to the planes of interference fringes formed at the intersection of the two beams of equal intensity. The relationship between the spatial frequency of the interference pattern and the Doppler frequency Δf will be discussed later. Eq.(2) indicates that Δf is independent of the scattering direction. Consequently, the collecting efficiency can be enhanced by using a large collecting lens. It is also worth noting that Δf is not direction sensitive, ie. it depends on the speed u.

The reference beam system which will be discussed in the next section also measures a frequency shift as given in eq.(2). This system however cannot be described by a real fringe geometry and has an upper limit on size of the collection aperture.

§ 3. OPTICAL ARRANGEMENTS and COHERENCE CONSIDERATIONS

The cross-beam system, fig.(2a), and reference-beam system, fig.(2b), will be described in this section. Only the salient features will be discussed here while the practical details will be left to the next section.

In a cross-beam system, fig.(2a), the laser beam is split by a beam splitter into two beams of equal intensity which are focussed to a point in the flow by a lens. The region in space where the two beams cross, together with the field stop on the face of the detector, define the scattering volume from which the velocity information is

obtained. This region will also be referred to as the probe volume. The scattered light due to particle traversing the probe which falls on the detector is collected by a large aperture lens, (c.f. pg 2.11).

The cross-beam method is particularly well suited to flows in which the density of scatterers is low. Ideally there should be not more than one particle present in the probe volume at any instant. The S/N ratio decreases with increasing number of particles because the signals from individual particles are of random phases. DRAIN has likened the presence of a large number of particles to a "cloud" with the effect of blurring the contrast between the light and dark fringes of the interference pattern in the probe volume. This argument is justifiable since the cross-beam anemometer can be explained by a fringe model which helps to clarify the working of the anemometer. Since fringe spacing in the scattering volume is $s = \lambda/\{2.\sin(\theta/2)\}$, a particle with velocity u moving perpendicular to the fringes results in a fluctuating scattered intensity with frequency $2u.\sin(\theta/2)/\lambda$. This is identical to the result in eq.(2) of the previous section, obtained by using only the Doppler shift principle. This is a result that is explained by either of two different physical processes, namely, Doppler frequency shift and interference pattern formed in Young's double-shift experiment. This observation has been discussed in some detail by PENNER *et al.*

When the average number of particles in the probe volume is significantly greater than unity, the reference-beam system is to be preferred to the cross-beam system. This has also been noted in DRAIN's paper in which the important features of the cross-beam and

the reference-beam systems have been summarised.

The reference-beam system, fig.(2b), requires the aperture of the field stop in front of the detector to be sufficiently small so the scattered light from any point in the scattering volume arrives with approximately the same phase as the reference-beam. This ensures that the cancellation of the cross-beam signal due to random phases of the particles does not occur in the reference-beam system. The criterion for such coherent detection is that the solid angle subtended at the scattering volume by the detector aperture be at most λ^2/w^2, where w is the largest dimension of the scattering volume. It is necessary for the intensity of the scattered light to be much lower than that of the reference-beam. It is recommended that the intensity of the reference beam be one tenth the intensity of the scattering beam. This generally ensures good mixing at the detector.

Several optical configurations have been devised for LDV. Take for instance the system with one incident beam and two scattering directions which WANG labelled the symmetric heterodyne arrangement and showed that the signal analysis for this system was identical to that used for the cross-beam system. This system however is inferior to the cross-beam system since the scattered light is collected over a comparatively small area. Such systems are not used widely and will not be discussed further.

A unified analysis of cross-beam and reference-beam systems has been carried out by SHE & WALL. Their article is a very important contribution to the LDV literature. They have considered the effect of parameters such as spatial coherence and scatterer density fluctuations on the autocorrelation function and the power spectrum of the observed signal. Their analysis of the cross-beam and the reference-beam system is an extension of the results of DRAIN and ADRIAN & GOLDSTEIN respectively. The results for the S/N ratios of the two systems obtained by SHE & WALL are however more practical than those of WANG , DRAIN and ADRIAN & GOLDSTEIN.

SHE & WALL have presented a comprehensive description of the use of an LDV for the measurement of turbulence. A tabulated comparison of the S/N ratios for different modes of operation (reference-beam vs. cross-beam) and for different methods of analysis (spectral measurement vs. correlation function analysis) has been given. The unified character of their work relies on the reference-beam and cross-beam systems both being analysed by adding the scattered fields incident at the detector. By using different coherence factors, expressions for the spectrum and the correlation function for these two systems are obtained. It has been shown that for the reference-beam system the form of the correlation function, which is independent of the particle density in this case, is the same as that of the correlation function for the cross-beam system with low particle density. When the particle density in a cross-beam system increases there can be significant interference between fields scattered by different particles and this gives a low frequency

contribution to the spectrum. The reason why this effect is insignificant in the reference-beam system is that the intensity of the detected scattered light is very small compared with that in the cross-beam system. The cross-beam system is used when the scattered intensity is low (this usually occurs when there are few particles in the probe volume) and hence is generally used in conjunction with a photon correlator. When the collection-lens aperture is large, as is usual in a cross-beam system, it is reasonable to assume that the photomultiplier in this situation acts as a linear detector of intensity, ie the scattered intensity due to each particle adds at the detector surface. When the number of scatterers is large, and a small collection aperture, however, the rigorous analysis of SHE & WALL is necessary in order to explain the total photocurrent and the correlogram which contains a low frequency contribution due to interference between fields scattered by different particles. This effect will not be considered further in this thesis. It is however worth noting that this term can be used to determine the particle concentration. This has been demonstrated by SHE & LUCERO. Their method is however rather complicated and is not of great practical significance (SHE, private communication).

Although the form of correlation function for the reference-beam system and the cross-beam system (for low particle density) is the same, the correlogram damps more quickly in the case of the cross-beam system than for the reference-beam system. This effect can be understood by noticing the form of signal detected due to a single

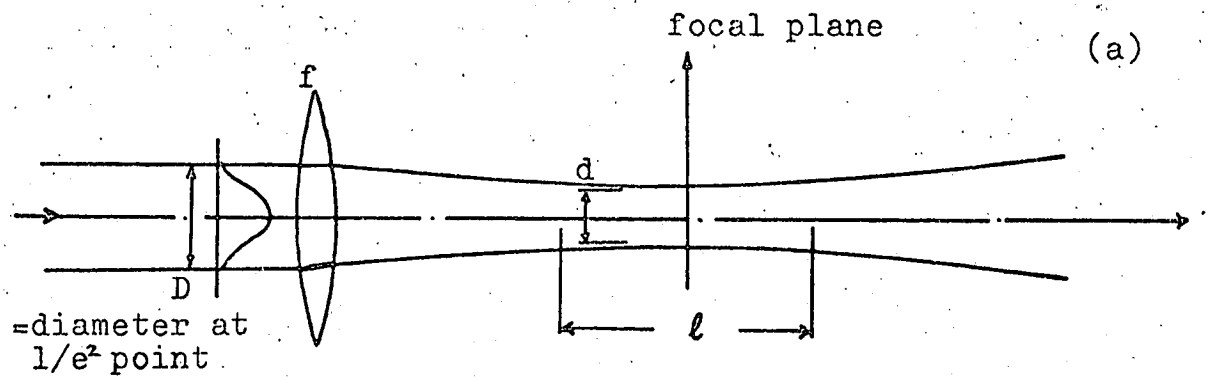

d=diameter at $= 4\lambda f/\pi D$
$1/e^2$ point

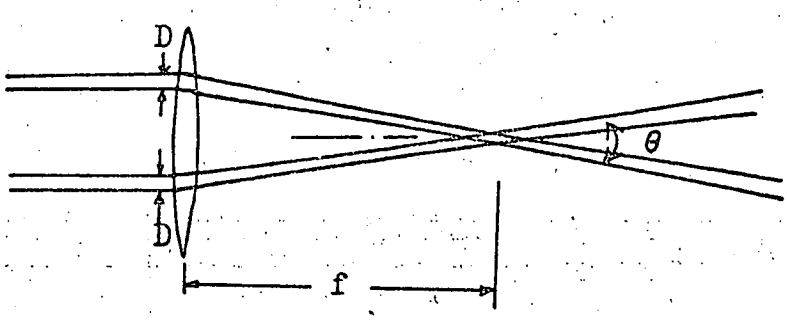

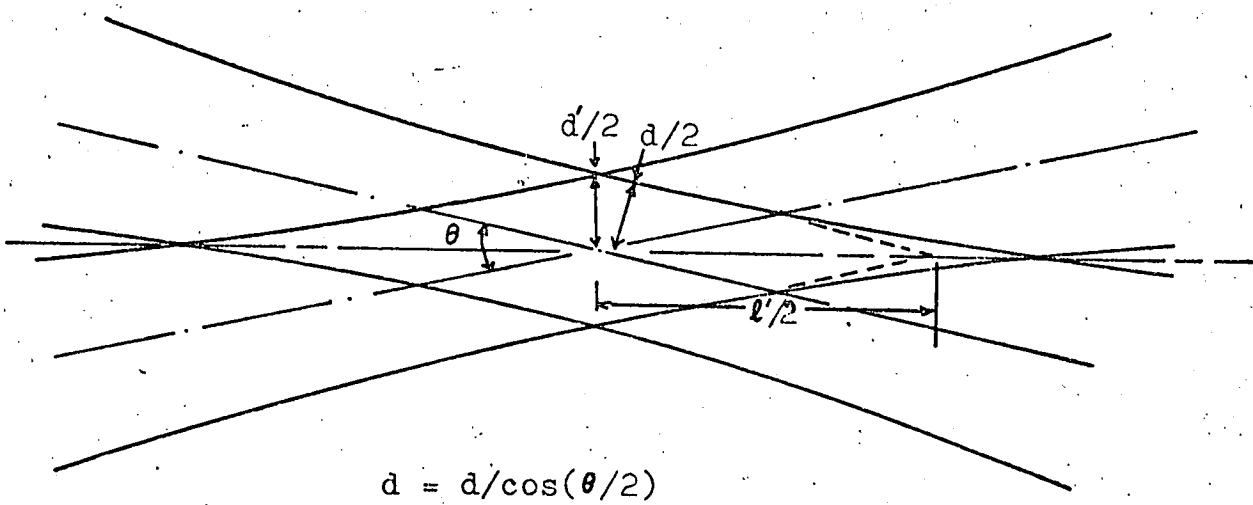

$$d = d/\cos(\theta/2)$$
$$\ell' = d/\sin(\theta/2)$$

Fig. (3) Details of the probe volume:

(a) Geometry of a focused laser beam with a Gaussian intensity profile.

(b) Probe volume formed by using a thin lens assuming no phase distortion. The length of the intersection ℓ' is obtained by neglecting the beam divergence in the vicinity of the focal point.

particle traversing each system (see fig.(2)). It is also borne out by the analysis of SHE & WALL. As mentioned in § 1, however, the S/N ratios of the two systems are different.

§ 4. SCATTERING VOLUME GEOMETRY and SPATIAL RESOLUTION

The size of the probe volume is in important consideration because it determines the dimensions over which any velocity fluctuations and gradients in the flow are averaged. The probe volume is determined by the optics of the transmitter and the collection lens and by the size of the laser beam. As shown in fig.(2a), two beams are focussed to a spot to minimise the scattering volume. Under these conditions, the spot size is determined by the diffraction limit of the focussing lens. The effect of placing the beam splitter before the lens will be discussed later.

Consider a parallel, monochromatic beam, of uniform intensity, diameter D and wavelength λ passing through a thin lens of focal length f. At the focal point of the lens a diffraction pattern is formed and the diameter, d, of the central bright spot (Airy disc) is given by the relation $d = 1.22\lambda f/D$ (KLEIN).

For a laser beam incident on a lens of focal length f, the intensity of the laser beam is not uniform but has a Gaussian profile as shown in fig.(3a), and the wave front is usually spherical. The diameter of the beam at the focal point is (CHU)

$$d = (4/\pi)\lambda f/D \qquad (3)$$

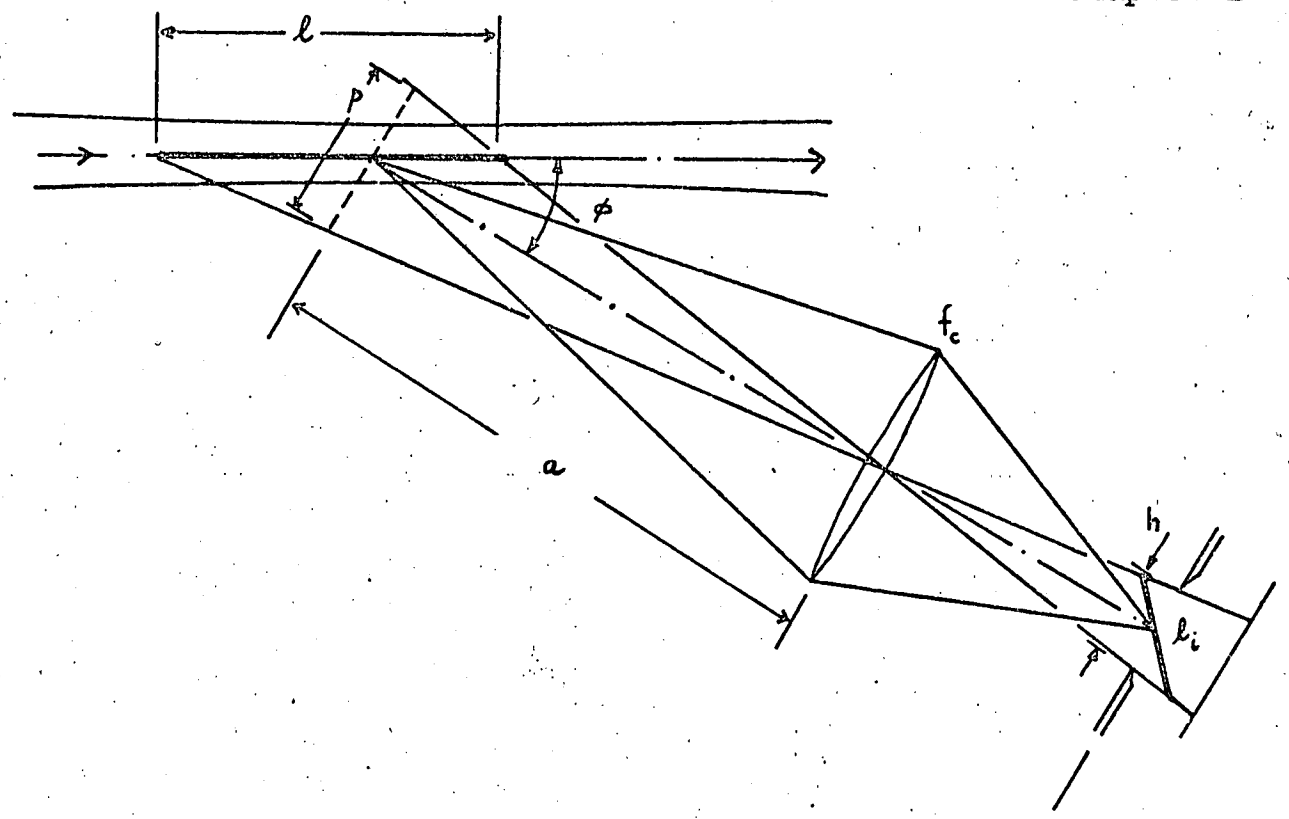

Fig. (4) Receiver optics for a cross-beam system. For the sake of clarity only one beam is shown. The four free parameters a, f_c, h and ϕ should be selected carefully in order to keep the probe volume as small as possible. See eq.(4).

The significance of d and D is shown in fig.(3a). It is noted that the diameter in this case is almost equal to the Airy disc and also that d can be reduced by beam expansion in the transmission optics.

In the cross-beam system, the two beams intersect at the focal point of the transmission lens and the interference fringes are formed only where the beams intersect. When the two beams of diameter D are focussed as in fig.(3b), the width of the probe volume d' is $d/\cos(\theta/2)$, where d is given by eq.(3). Although real fringes are not formed in the reference-beam system, the width of the scattering volume is also d'.

As previously mentioned, stops and apertures in the collector optics are normally used to limit the size of the scattering volume to a small probe volume because generally the dimension (ℓ or ℓ') of the scattering volume along the optical axis is too long for good spatial resolution in the flow. A simple means of reducing this dimension by using the collector optics for a cross-beam system is shown in fig.(4) where for clarity, only one beam is shown. A pinhole of diameter h is placed in front of the detector so that it is in the image plane of the collector lens with focal length f_c. In this arrangement, the length of the probe volume ℓ seen by the detector is $\ell = p/\sin\phi$, where ϕ is the mean scattering angle. By using the lens formula we obtain

$$\ell \simeq (a/f_c - 1)\, h/\sin\phi \qquad (4)$$

Thus the length of the probe volume can be controlled by a judicious choice of collector optics and the scattering angle. Usually not all the parameters in eq.(4) will be free since there will be constraints due

to the experimental geometry. For the sake of clarity only one beam is shown in fig.(4).

HANSON has considered the broadening in the power spectrum due to improper alignment of the beams forming the interference pattern. A number of investigators have used the laser-beam splitter-lens transmission arrangement. In this set-up the lens is not used paraxially, hence the waists of the two beams may not coincide with the cross-over point where the interference pattern is formed. This leads to a variable fringe spacing which can lead to a spectral broadening which under certain conditions can be greater than the transit time broadening, HANSON. It is for this reason that the laser-lens-beam splitter configuration in figs.(2a,b) is recommended.

§5. DETECTION of SCATTERED LIGHT

Photodiodes or photomultipliers are generally used for the detection of scattered light. When there is a high scattered intensity, the signal at the output of these devices varies continuously because the detection system has a finite bandwidth. In a photo-multiplier, the absorption of a photon creates individual photo-

electrons at the cathode which after multiplication appear as discrete pulses at the output. These discrete pulses can be observed if the incident light levels are low so that pulses do not overlap and the finite bandwidth effect is not dominant. In flows with low or very little seeding the scattered intensity is inevitably low and hence it is necessary to detect (count) these discrete pulses in order to obtain information about the flow. This is the basis of the photon correlation method (ABBISS *et al*), for which a photon counting photomultiplier is necessary. This type of photomultiplier has a high temporal resolution and a discriminator unit attached to it outputs a sequence of pulses of equal height which can then be analysed by a digital correlator.

It can be shown (PIKE) that the count correlation is proportional to the intensity correlation function for non-zero time lags if the fluctuations of the scattered field are 'stationary', ie

$$E\left[n(o;\Delta t).n(\tau;\Delta t)\right] = (\eta\Delta t)^2 R_I(\tau) + \eta\Delta t.E\left[I(0)\right]\delta_{\tau 0} \qquad (5)$$

where $n(\tau;\Delta t)$ is the number of pulses output from the discriminator at the time τ in an interval Δt short enough for the intensity to remain constant over this interval; η is the quantum efficiency of the photomultiplier; $R_I(\tau) = E\left[I(0)I(\tau)\right]$ is the intensity correlation function and $\delta_{\tau 0}$ is the Kronecker delta. Since the digital correlator, (Precision Devices) used in the experiments to be described, does not compute the correlation function for $\tau = 0$, the second term $\eta\Delta t\, E\left[I(0)\right]\delta_{\tau 0}$ in eq.(5) will not be considered any further. From now on only expressions for $R_I(\tau)$ the intensity correlation function will be given since the count correlation function is proportional to it.

§ 6. STATISTICS of RANDOM PULSE TRAIN

There has been a considerable interest in the analysis of random pulse trains since there are a number of physical processes that can be represented by such a model. Notable among the publications is the work of BEUTLER & LENEMAN. A brief account of their results will be given in this section while the application to the LDV will be discussed in the following sections.

Consider a general pulse train of the form

$$y(t) = \sum_{-\infty}^{+\infty} i_n(t-t_n) \tag{6}$$

in which $\{t_n\}$ is a random time base (a stationary point process) and $i_n(.)$ is the n-th pulse. The mean of $y(t)$ in eq.(6) is computed by averaging successively over $\{i_n(.)\}$ and $\{t_n\}$ (these are assumed to be independent random variables) thus,

$$E\left[y(t)\right] = E_t\left[E_i\left[\sum_{-\infty}^{\infty} i_n(t-t_n)\right]\right] = E_t\left[\sum_{-\infty}^{+\infty} m(t-t_n)\right] \tag{7}$$

If $g(t) = \sum \delta(t-t_n)$, it is possible to write

$$m(t-t_n) = \int_{-\infty}^{\infty} m(t-\tau)g(\tau)d\tau \tag{8}$$

and hence

$$E\left[y(t)\right] = E\left[\int_{-\infty}^{\infty} m(t-\tau)g(\tau)d\tau\right] \tag{9}$$

By interchanging the order of expectation and integration in eq.(9):

$$E\left[y(t)\right] = \nu\int_{-\infty}^{\infty} m(u)du \tag{10}$$

where $E[g(\tau)] = \nu$, which is the average number of pulses per unit time.

It can be shown that autocorrelation of y(t) is

$$R_y(\tau) = E[y(t)y(t+\tau)] = \nu\{\int_{-\infty}^{\infty}\Gamma_o(\tau+u,u)du + \sum_{k=1}^{\infty}\int\int_{-\infty}^{\infty}\Gamma_k(\tau+v,u) \cdot f_k(|u-v|)du\ dv\} \tag{11}$$

in which

$$\Gamma_k(u,v) = E[i(u)\ i_{m+k}(v)] \tag{12}$$

and $f_k(t_{m+k}-t_m)$ is the probability density of the interval $t_{m+k}-t_m$ between k successive intervals.

In the second integral of eq.(11), by assuming independence of the $\{i_n(t)\}$

$$\Gamma_k(u,v) = E[i_n(u)]\ E[i_n(v)],\ k \neq 0. \tag{13}$$

Thus Γ_k does not depend on its index and the summation may be applied only to f_k. For a Poisson point process $\{t_n\}$ it follows that whenever $u \neq v$

$$\sum_{k=1}^{\infty} f_k(|u-v|) = \sum_{k=1}^{\infty} \frac{\nu^k|u-v|^{k-1}}{(k-1)!}\exp(-\nu|u-v|) = \nu, \tag{14}$$

accordingly in this case the autocorrelation is

$$R_y(\nu) = \nu\int_{-\infty}^{\infty}E[i_m(u+\tau)i_m(u)]du + \nu^2\left(\int_{-\infty}^{\infty}E[i_m(u)]du\right)^2 \tag{15}$$

where the first term is τ dependent and the second term contributes

only to the d.c. . When i_m is deterministic, the expectation operator E can be removed and the result is Campbell's theorem. In this case the characteristic function of the pulse process can also be determined and hence any statistic of y(t) is available in principle.

From eq.(12) it can be seen that the second term in eq.(11) will contribute to the fluctuation in the correlation function if $\{i_n(t)\}$ is a correlated sequence.

Eq.(11) will be discussed further in § 8 where the correlation function for a turbulent flow will be considered.

§ 7. INTENSITY CORRELATION FUNCTION for CONSTANT VELOCITY

Consider a typical cross-beam arrangement as shown in fig.(2a). For simplicity it is assumed that particles traverse the scattering volume in the plane of maximum fringe contrast or in other words, pass through all the fringes. A particle with velocity u produces a scattered intensity

$$I(t) = I_o \exp\{-\frac{(t-t_o)^2 u^2}{2r^2}\} \cos^2(\frac{\pi u t}{s}) \qquad (16)$$

where I_o is the peak scattered intensity, t_o is the time of arrival of the particle at the centre of the scattering volume where it scatters I_o, $r = (d/4)/\cos(\theta/2)$ and s is the fringe spacing (see § 3 and eq.(3)). After normalizing I(t), it can also be regarded as the probability of absorption of a scattered photon by the photomultiplier.

When a number of particles pass through, the resultant scattered intensity is the sum of the contributions due to each particle, ie

$$I(t) = \sum_{k=1}^{N} I_{ok} \exp\{-\frac{u^2(t-t_{ok})^2}{2r^2}\} \cdot \tfrac{1}{2}\{1+\cos(2\pi ut/s)\} \qquad (17)$$

By assuming that the arrival times $\{t_{ok}\}$ of the particles form a Poisson sequence, the autocorrelation function of I(t) can be evaluated using eqs.(15) and (17) after a simple but rather tedious calculation:

$$R_I(\tau) = \frac{\nu}{4} E\left[I_{ok}^2\right] \cdot \left[\frac{\sqrt{\pi}r}{u} \exp\left(\frac{-u^2\tau^2}{4r^2}\right) \left(1 + 2 \exp\left\{\frac{-\pi r^2}{s^2}\right\} \cos\left(\frac{\pi u\tau}{s}\right) + \tfrac{1}{2}\cos\left(\frac{2\pi u\tau}{s}\right) + \tfrac{1}{2}\exp\left\{\frac{-4\pi^2 r^2}{s^2}\right\} \right)\right] + \frac{\nu^2}{4}\left(E\left[I_{ok}\right]\right)^2 \left[\frac{2\pi r^2}{u^2} \cdot \left(1 + 2 \exp\left\{\frac{-2\pi^2 r^2}{s^2}\right\} + \exp\left\{\frac{-4\pi^2 r^2}{s^2}\right\}\right)\right] \qquad (18)$$

where $\nu = E\left[N/T\right]$ and $\nu^2 = E\left[N(N-1)/T\right]$, (T = total experimental time).

A similar expression has been obtained by ABBISS *et al* (1974). There seem to be three errors in their formula noticeable when it is converted to the form of eq.(18). They have $E\left[I_{ok}\right]$ and $2\sqrt{\pi}r/u$ instead of $E\left[I_{ok}^2\right]$ and $\sqrt{\pi}r/u$ respectively in the term multiplied by ν. Instead of $E^2\left[I_{ok}\right]$ as in the term multiplied by ν^2, they have $E\left[I_{ok}^2\right]$; this too seems to be incorrect.

For the successful operation of an LDV there should be at least two fringes inside the probe volume, ie $r > s$. Therefore eq.(18) can be greatly simplified to give

$$R_I(\tau) = \frac{\nu}{4} E\left[I_{ok}^2\right] . \frac{\sqrt{\pi} r}{u} . \exp\left(\frac{-u^2\tau^2}{4r^2}\right)\left[1 + \tfrac{1}{2} m^2 \cos\left(\frac{2\pi u\tau}{s}\right)\right] +$$

$$\frac{\nu^2}{4} E^2\left[I_{ok}\right] . \frac{2\pi r^2}{u^2} \qquad (19)$$

where a fringe visibility constant ($o<m<1$) has been introduced to take account of less than 100% contrast between light and dark fringes. The value of m is due only to the optics and not to the number of particles in the probe volume.

There can be some confusion when comparing eqs.(17) and (19). The τ dependent terms in the two equations appear to be the same except that, while the amplitude I_o of a pulse in eq.(17) is independent of the velocity, the amplitude of $R_I(\tau)$ seems to be proportional to u^{-1}. This is obviously incorrect since it suggests that the amplitude of $R_I(\tau)$ approaches infinity as the velocity approaches zero. This fact has however not been noted by ABBISS *et al* (1974) who expressed the fluctuating part of the correlation function as $\frac{a_o}{u} \exp(.)\left[1+. m^2\cos(.)\right]$, (their eq.11), having implicitly absorbed ν in the constant a_o. Since ν is proportional to the velocity (ν = d.u, where d is proportional to the number of particles per unit volume), the amplitude of the correlation function, like the amplitude I_o, is independent of the velocity.

Before discussing some aspects of particle concentration determination some consequences of the Poisson arrival times will be described. Inherent in the Poisson assumption is that no two particles arrive at the same time in the middle of the probe volume.

This consequence is often not stated in the LDV literature. DURRANI & GREATED (1974), using the formulation of the shot noise introduced by COX & MILLER have used concentration constants γ and κ instead of ν and ν^2 respectively and have hence considered a non-Poisson point process in which coinciding points are allowed. In eq.(11) by assuming an arbitrary distribution for $\{t_n\}$, noting of course the independence of the occurrence times, the two concentration constants γ and κ would become ν and $\nu.\sum_k f_k$ respectively. This suggests that $\sum_k f_k = \kappa/\gamma$. Even when the Poisson assumption is not valid, as when the particle density is high, $\nu \simeq N/T$ and $\nu\sum_k f_k \simeq N^2/T$. This aspect will be discussed further in § 7.1.

§ 7.1 Determination of particle concentration

Assume that identical particles (size < fringe width) used for seeding in a flow are mono-disperse and are moving with a constant velocity. The correlation function given by eq.(19) can now be written as

$$R_I(\tau) = \frac{K}{4} N I_o^2 \exp\left(\frac{-u^2\tau^2}{4r^2}\right)\left\{1 + \frac{m^2}{2}\cos\left(\frac{2\pi u\tau}{s}\right)\right\}, + 2\frac{K^2}{4} N^2 I_o^2 \qquad (20)$$

where $K = \frac{\sqrt{\pi}r}{uT}$ and $E\left[I_{ok}^2\right] = E^2\left[I_{ok}\right] = I_o^2$ since the particles are identical.

By using a large number of fringes or by frequency shifting, the term $\exp(-u^2\tau^2/4r^2)$ in eq.(20) can be made approximately equal to unity and by proper optical alignment m can be made very close to

units. Eq.(20) can now be further simplified to give

$$R_I(\tau) = \frac{KNI_o^2}{4}\{1 + \tfrac{1}{2}\cos(\frac{2\pi u\tau}{s})\} + \tfrac{1}{2}K^2N^2I_o^2 \qquad (21)$$

$$= \tfrac{1}{8}KNI_o^2\cos(\frac{2\pi u\tau}{s}) + \tfrac{1}{2}K^2N^2I_o^2, \quad (N >> 1) \qquad (22)$$

The first and second terms in eq.(22) give the a.c. and d.c. contribution to the power of the scattered intensity. The total power is the sum of the mean square a.c. and d.c. power. It can be shown easily that the ratio (a.c./d.c.) of these two components varies as N^{-1}. This result has been obtained before by LADING (1973a) and FARMER. The result in eq.(22), however, shows that a correlator can be used to detect the effect of particle concentration in the flow. The only practical drawback with this method is the inevitable contribution of background light to the d.c. power. This contribution can however be removed either by clipping or averaging the background contribution with no flow. The clipping procedure will be described in the next chapter.

The N^{-1} variation is common to all situations where quantities with random phases are summed. When using this relationship to determine the variation in particle concentration with a correlator it should be borne in mind that it is only true for a constant flow with $N >> 1$. FARMER has indicated that in theory the particle number density can be calculated in a turbulent flow if the velocity distribution is available, however no analytical proof is given. He has also not considered the fact that a larger number of particles with

high velocities pass through the probe volume than those with low velocities. Leaving aside this complication, it is still felt that the complex scattering process and flow characteristics can only permit, at the very best, not more than an approximate N^{-1} relationship.

§ 8. INTENSITY CORRELATION FUNCTION for TURBULENT FLOW

A number of authors have derived expressions for the intensity correlation function without stating clearly the underlying assumptions. The complete analysis in this case needs to take into account the fact that the time of arrival of particles $\{t_n\}$ is modulated by the velocity of the fluid and the light scattered by a particle is correlated with that scattered by other particles. Under these conditions the methods of derivation adopted by the authors will be discussed.

Two models of point processes have been discussed at considerable length in the literature of applied stochastic processes. PAPOULIS has derived the correlation function of a non-homogenous Poisson process (rate = $\nu(t)$) with a deterministic pulse shape. This model is inapplicable to the LDV since the time dependent rate $\nu(t)$ can only occur with a fluctuating velocity and this in turn means that the centre frequencies of the Doppler bursts becomes random. The model described in § 7 is more appropriate to the LDV, however, it does not take into account the time dependent rate of the point process. By deriving an expression for the correlation function from first principles it will become clearer what assumptions are necessary in the process of obtaining the result.

Let the signal input to the correlator at time t due to N particles be

$$y(t) = \sum_{n=1}^{N} i_n(t-t_n) \tag{23}$$

where unlike the uniform velocity case N, i_n and t_n are correlated with the velocity $\{v_n\}$, n=1,...,N, of each particle in the probe volume. The correlation function is $R(\tau) = A(\tau) + B(\tau)$ where

$$A(\tau) = E\left[\sum_{n=1}^{N} i_n(t-t_n)\, i_n(t+\tau-t_n)\right] \tag{24a}$$

and

$$B(\tau) = E\left[\sum_{p\neq q}^{N}\sum^{N} i_p(t-t_p)\, i_q(t+\tau-t_q)\right] \tag{24b}$$

Eq.(24) gives the complete expression for the correlation function. The single particle contribution is given by $A(\tau)$, and $B(\tau)$ represents the two particle contribution. Only the single particle contribution is considered by ABBISS *et al* (1974) while DURRANI & GREATED (1974) and SHE have considered both the contributions. SHE has pointed out thet in order to evaluate $B(\tau)$ it is necessary to assume that the velocities of the particles are uncorrelated which is not stated but is implicit in the derivation of DURRANI & GREATED (1974). As mentioned earlier ABBISS *et al* (1974) consider only the case when there is not more than one particle in the probe volume; here $B(\tau) = 0$. CROSIGNANI *et al* have derived an expression for $B(\tau)$ assuming a jointGaussian probability density function for the velocities of the particles. They have not considered, however, the finite transit time effect which does play a significant part in damping the influence of the correlated velocity effects. It can be shown

qualitatively (also analytically but this would be rather tedious) that $B(\tau)$ contributes a low frequency component to the correlation function when the number of particles in the probe volume is greater than unity and if the velocities are correlated. It does not contribute a d.c. component as suggested by DURRANI & GREATED (1974); their result for $B(\tau)$ is true only when the velocities are uncorrelated. It should be noted that the two particle contribution $B(\tau)$, in SHE's analysis contains an extra time dependent term due to coherent detection which is neglected in the above discussion since a large detection aperture is used generally in a cross-beam system. For a detailed discussion on $B(\tau)$ refer to chap.6 of the book by CROSIGNANI *et al.* If all contributory effects were taken into account, assuming that all the statistics were available, the complete result would be extremely complicated and not very useful for parameter estimation.

An expression for $A(\tau)$ will now be derived. Let the velocity of the N particles in the flow be $\{v_n\}$, $n = 1,\ldots,N$. In eq.(24a) the averaging has to be over $\{v_n\}$, $\{t_n\}$ and N. First, taking expectation over $\{t_n\}$ gives

$$A(\tau) = E\left[\int_o^T \frac{Kv_1}{T}\, dt_1 \ldots \int_o^T \frac{Kv_n}{T}\, dt_N \sum_{n=1}^{N} i_n(t-t_n)\, i_n(t+\tau-t_n)\right] \quad (25a)$$

where the probability of a particle arriving at time t_n is $Kv_n dt_n/T$; T is the total experimental time and K is a normalization constant.

This is equivalent to saying that the higher the velocity of the particle the more likely it is to be present at time t_n. This modulated Poisson process was first discussed by McLAUGHLIN & TIEDERMAN. Eq.(25a) can be simplified (for a similar manipulation see pg.148 of WAX)

$$A(\tau) = E\left[\sum_{n=1}^{N} \frac{Kv_n}{T} \int_o^T i_n(t-t_n) i_n(t+\tau-t_n) dt_n\right] \tag{25b}$$

The integral w.r.t. t_n has already been evaluated in eq.(19) and the result will be represented as a function $g(\tau,v_n)$. Averaging eq.(25b) w.r.t. the velocities $\{v_n\}$ gives

$$A(\tau) = E\left[\int_{-\infty}^{\infty} dv_1 \ldots \int_{-\infty}^{\infty} dv_N \, f(v_1 \ldots, v_N) \sum_{n=1}^{N} \frac{Kv_n}{T} g(\tau,v_n)\right] \tag{25c}$$

where $f(v_1,\ldots,v_N)$ is the joint velocity probability density function. On further simplification eq.(25c) becomes

$$A(\tau) = E\left[\sum_{n=1}^{N} \int_{-\infty}^{\infty} \frac{Kv_n}{T} g(\tau,v_n) \, f(v_n) \, dv_n\right] \tag{25d}$$

where $f(v_n)$ is the probability density of velocity of the n-th particle. Since it is assumed that the particles "track" the fluid perfectly, v_n can be replaced in eq.(25d) by v the velocity of the fluid. Before averaging over N, it should be noted that the previous expectations w.r.t. $\{t_n\}$ and $\{v_n\}$ assumed that these sequences were independent of N. This is justifiable if T is much greater than the inverse of the velocity fluctuation bandwidth. Now, averaging over N gives

$$A(\tau) = E[N].\frac{K}{T}\int_{-\infty}^{\infty} v\ g(\tau,v)f(v)dv \qquad (25e)$$

(see pg.248 of PAPOULIS for a discussion on "random sums"). The form of $g(\tau,v)$ is (from eq.19)

$$g(\tau,v) = \frac{a}{u}\exp(\frac{-v\tau^2}{4r^2})\{1+\frac{m^2}{2}\cos(\frac{2\pi v\tau}{s})\} \qquad (26)$$

Eq.(25e) can be evaluated now if the velocity probability density is known. By assuming a Gaussian probability density eq.(25e) becomes

$$A(\tau) = D\exp\{\frac{u^2}{2\sigma C} - \frac{u^2}{2\sigma}\}\left[1 + \frac{m^2}{2}\exp\{-\frac{2\pi^2\sigma^2}{s^2C}\tau^2\}\cos(\frac{2\pi u}{sC}\tau)\right] \qquad (25f)$$

where u and σ^2 are the mean and variance of the flow velocity respectively, D is a constant and $C = 1 + \sigma^2\tau^2/(2r^2)$. This formula is similar to that quoted by FOORD *et al* and applies for an arbitrary turbulence intensity. When the turbulence intensity is low ($\sigma/u<<1$) and assuming that the velocities of the particles do not change while traversing the probe volume ($\sigma\tau_m<<r$, where τ_m is the maximum correlation lag value of the order of the mean transit time) eq.(25f) can be simplified ($1/C \simeq 1-\sigma^2\tau^2/(2r^2)$) to give

$$A(\tau) = D\exp\{\frac{-u^2\tau^2}{4r^2}\}\left[1 + \frac{m^2}{2}\exp\{\frac{-2\pi^2\sigma^2}{s^2}\tau^2\}\cos(\frac{2\pi u\tau}{s})\right] \qquad (27)$$

For experiments conducted in a flow with no or very little artificial seeding, the correlation function will have the form given by eq.(27). This expression has been derived by a number of authors. SHE and DURRANI & GREATED (1974) for example do not

consider the modulated Poisson process $\{t_n\}$ and hence effectively end up with a relationship with D in eq.(27) replaced by D/u. SHE has avoided this sticky point by dividing the autocorrelation of the weighting function (the weighting function function defines the transit time effect) by its value at zero lag hence cancelling the $1/u$ in the numerator and denominator. After this has been done, the expectation over $\{v_n\}$ is taken assuming a Poisson distribution of particles. GRANT *et al* use a method similar to DURRANI & GREATED (1974) and hence also arrive at the surprising $1/u$ dependence. ABBISS *et al* (1974) arrive at an identical expression to eq.(27). Their method is similar to that used in this section. It is felt however that the derivation given here gives a clearer picture of the necessary assumptions required in arriving at the solution.

§ 9. PERIODIC FLOW ANALYSIS by SAMPLING

The investigation of periodic flows is of considerable interest to the fluid dynamicist. In such flows it is sufficient to determine the velocity of the fluid over one period. In such flows the excitor, which for example could be a wave-paddle, a peristaltic pump or a lung machine, stimulates the flow in a periodic fashion. The frequency of this motion is generally linked to the frequency of the observed periodic response of the fluid. Such flows can be measured by using a gated cathode photomultiplier which is triggered by periodic pulses derived from the excitor, such that the photomultiplier always "sees" the same velocity. The duty cycle of the gating pulses should there-

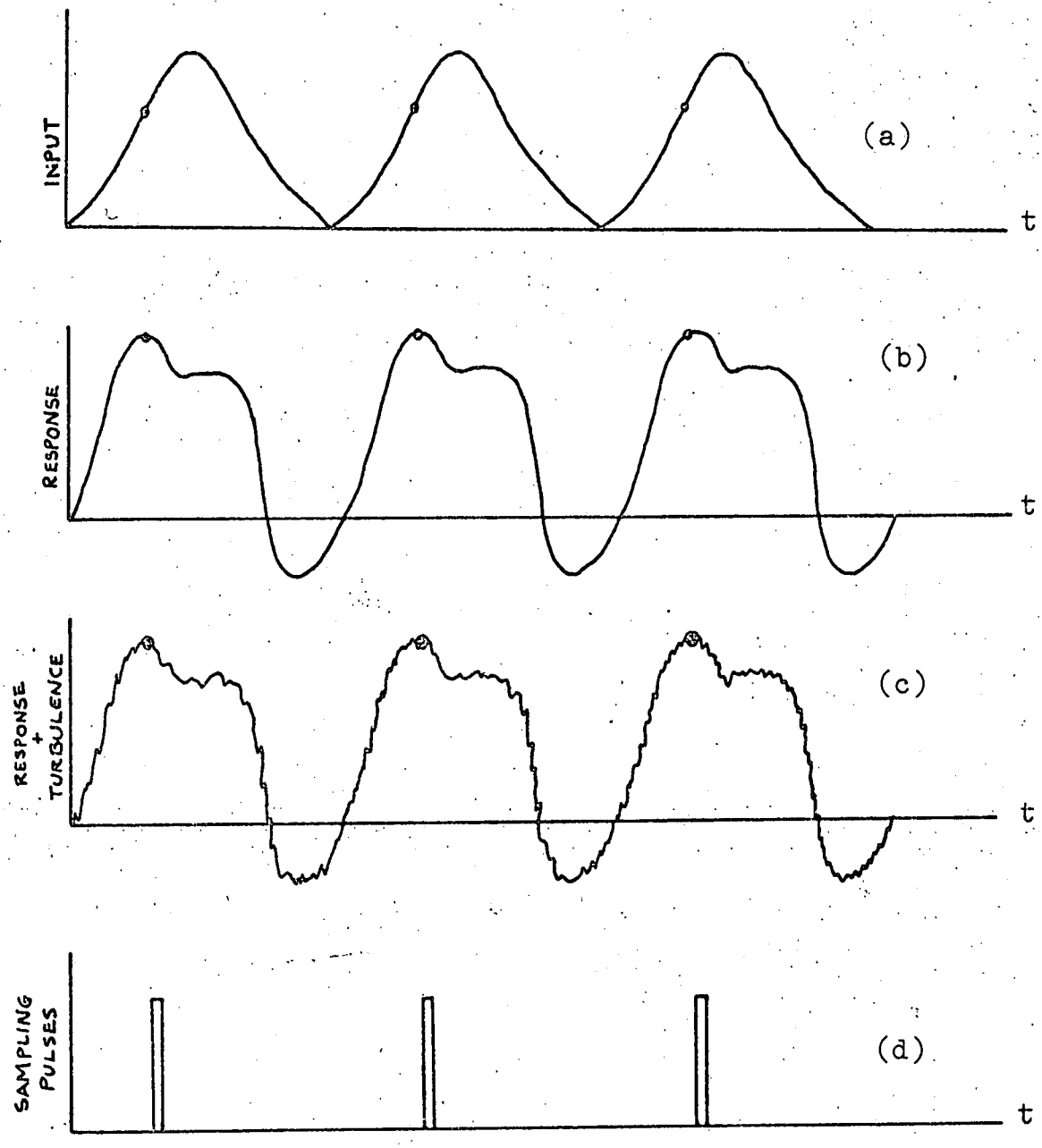

Fig.(5) Principle of periodic sampling

(a) periodic excitation applied to the system

(b) velocity (system's response) due to periodic excitation shown in (a)

(c) response + background turbulence

(d) sampling wave-form used to gate the detector.

fore be very short compared to the period. By varying the phase of the gating waveform and observing the correlograms for each of these different phases, the fluctuating velocity of the fluid can be mapped completely by using eq.(9). See fig.(5).

In certain cases there might be some background turbulence which will add to the periodic signal. Using the procedure mentioned in the previous paragraph, but in this case using eq.(13), the mean and variance of the velocities can be determined. See fig.(5).

The procedures that have been suggested can be used to analyse any periodic flow. Since the photomultiplier "sees" the velocity only for a short time the disadvantage of this method is that the correlogram takes a long time to build up. This method is therefore susceptible to extraneous low frequency fluctuations.

§ 10. SINUSOIDAL FLOW

Simple periodic flows can be analysed by the correlation method withoutthe need for periodic sampling, hence improving the response time of the technique. It is necessary in such situations to know the form of the fluctuation a priori.

In this section the form of the correlation function for a mean velocity with a sinusoidal fluctuation will be derived. The fluctuation will be assumed to be small in comparison with the mean velocity.

Let the velocity in the mean flow direction be

$$v(t) = u + a\cos(\omega_o t + \phi) \tag{28}$$

where u is the mean velocity; a, ω_o are the amplitude and frequency of the fluctuation respectively and ϕ is uniformly distributed over $(0, 2\pi)$.

The velocity probability density function is then

$$p(v) = \frac{1}{\pi\sqrt{a^2-(v-u)^2}} \quad ; \quad |v-u| \lesssim a \tag{29}$$

$$= o \quad ; \quad \text{otherwise}$$

By using eqs.(25e) and (26) and the procedure of averaging suggested in § 8, the correlation function for this flow can be obtained:

$$R_I(\tau) = \frac{A}{\pi}\int_{u-a}^{u+a} \frac{\exp\{-v^2\tau^2/(4r^2)\}}{\sqrt{a^2-(v-u)^2}}\left[1 + \frac{m^2}{2}\cos\left(\frac{2\pi v}{s}\tau\right)\right]dv \tag{30}$$

By assuming that $u >> a$,† the Gaussian term can be taken outside the integral to give

$$R_I(\tau) = \frac{A}{\pi}\exp\left\{\frac{-u^2\tau^2}{4r^2}\right\}\int_{u-a}^{u+a} \frac{1}{\sqrt{a^2-(v-u)^2}}\left[1 + \frac{m^2}{2}\cos\left(\frac{2\pi v}{s}\tau\right)\right]dv \tag{31}$$

Eq.(16) can be simplified to give

$$R_I(\tau) = F\exp\left\{\frac{-u^2\tau^2}{4r^2}\right\}\left[1 + \frac{m^2}{2}J_o\left(\frac{2\pi a}{s}\tau\right)\cos\left(\frac{2\pi u}{s}\tau\right)\right] \tag{32}$$

† for arbitrary a/u ratio a closed form result is not possible. See eq.(25f) which is valid for any turbulence intensity.

Notice the similarity in form with eq.(27). For the turbulent flow case the cosine term is damped by a Gaussian factor whereas for a periodic flow this damping is replaced by J_o, the zero order Bessel function. This causes a beating effect in the correlation function.

Experiments were carried out to verify eq.(32) and are discussed in Appendix A where a simple method of estimating the parameters u and a is described.

§ 11. CROSSCORRELATION TECHNIQUES

Crosscorrelation techniques have been applied extensively in the analysis of signals from various types of transducers used for flow measurements. For example BECK *et al* have described how the fluid velocity and the particle size distribution can be determined by cross-correlating signals arising from two conductivity probes placed a short distance apart in a pipeline. For industrial applications cross-correlation techniques are particularly powerful because of their simplicity and the case with which the results can be interpreted. The mean velocity of the flow can be determined directly from the lag value of the peak of the correlation function. The ratio of the distance between the probes and the lag value of the peak gives the mean velocity.

A distinctive peak can be observed even with a low S/N ratio. A peak detection circuit (TAI *et al*) or a delay lock loops (HAYKIN & THORSTEINSON) can be used to keep track of the peak of the cross-correlation function. If the separation between the transducers is

made extremely small the crosscorrelation methods can be made to be almost as effective as the frequence trackers commonly used in LDV work.

The crosscorrelator is analogous to the time-of-flight measuring counter used in nuclear physics experiments. A distribution of the time-of-flight of particles is obtained by using a multichannel pulse height analyser, into which is fed the flight time of each particle. The output of this instrument is then the probability density of the times of flight. Similarly the output of the cross-correlator is the probability density of the transit time of particles passing from one beam to the other. The area under the crosscorrelation function can be normalised to unity.

LADING (1973b) and DURRANI & GREATED (1975) have derived expressions for the crosscorrelation function in a turbulent fluid when the probability density function of the velocity is assumed to be Gaussian. It can be shown easily that when the separation between the probe volumes (or transducers) is small the crosscorrelation function approximates closely the velocity probability density function.

A possible interesting application of the crosscorrelation technique is the investigation of diffusive motion. WASAN has discussed the first-passage-time probability density of Brownian motion with a positive drift. This probability density has also been considered in the statistical literature under the heading " Gaussian (Wald) Distributions", JOHNSON & KOTZ. Based on the results of WASAN it can be shown easily that the diffusion constant can be

determined from the correlation function. A more accessible reference than WASAN's monograph is a paper by ROY & WASAN to which the reader may refer for details.

C H A P T E R 3

PARAMETER ESTIMATION from COUNT CORRELATION FUNCTION

§ 1. INTRODUCTION

To obtain a photon count correlogram the number of counts occurring in consecutive non-overlapping intervals of length T are measured. If n_k is the number of counts in the time interval $(kT, \overline{k+1}\,T)$, then a digital correlator computes the correlation function $N^{-1}\sum_{k=1}^{N} n_k n_{k+s}$, s=0,1..,M-1, where M-1 is the maximun lag value and NT is the total experimental time. In practice digital photon correlators often use some form of clipping procedure which results in an approximation to correlation function described above.

The Precision Devices correlator which was used in the experiments, in addition to other statistics, computes the single clipped correlation function for 48 correlation lag values. The values computed are $\sum_{k=1}^{N}[n_k]^c n_{k+s}$ (s=1,2..,48), N, $\sum_{k=1}^{N}[n_k]^c$ and $\sum_{k=1}^{N} n_k$ where

$$[n_k]^c = 1 \quad \text{if} \quad n_k \geqslant c \quad \text{and}$$

$$[n_k]^c = 0 \quad \text{if} \quad n_k < c \ .$$

The clipping level c, sample time T and total number of samples N can be set by the experimenter.

Before estimating the flow parameters it is convenient to normalize the correlation function to give

$$R(sT) = \frac{N^{-1}\sum_{k=1}^{N}[n_k]^c\, n_{k+s}}{(N^{-1}\sum_{k=1}^{N}[n_k]^c)(N^{-1}\sum_{k=1}^{N} n_k)} - 1$$

which can be simplified by cancelling the N^{-1} factors. This form of normalization is useful in that the effect of slow

extraneous variations in the mean count rate can be minimized and also that the first term on the r.h.s. approaches unity as $sT \to \infty$, hence $R(sT) \to 0$. This ensures that there is no pedestal in the correlation function and this reduces by one the number of free parameters required in parameterizing the correlation function. It is noted that the effect of background light, which otherwise leads to a pedestal, is also eliminated. The constant pedestal term included in the expressions for the correlation function for the different flows discussed in chapter 2 will be neglected for the rest of this chapter.

Associated with the discriminator (attached to the photon counting photomultiplier) there is normally a dead time which is introduced into the circuitry to inhibit the formation of two pulses in very rapid succession. This is necessary because of ringing effects associated with the signal which reaches the discriminators. Dead times are typically of the order of 50 ns. and result in a reduced correlation between counts at delay times of this order. This does not generally cause any serious problems but sometimes means means that the first point (s=1) on a correlogram has to be ignored when sample times of the order of 50 ns. are used.

In order to simplify the notation, $R(sT)$ will be replaced by $R(\tau)$, where τ now takes discrete values: $\tau=1,2...,48$ if the sample time $T=1$.

It was noted on pg. 2.14, eq.(5) , that the full count correlation function is related very simply to the intensity correlation function. This result is independent of the statistics of the incident field. Since the use of clipping techniques can considerably reduce the hardware and time necessary to compute the count correlation function, it is reasonible to enquire how the clipped correlation function is related to the intensity correlation function. For Gaussian fields these two functions are again simply related. There is however no simple relationship for an arbitrary field.

When the field scattered by a fluid has a non-Gaussian probability density, the reference-beam system gives the spectrum of the field if a full correlator is used with $N_r \gg N_s$, where N_r and N_s are the average photon counts per sample time due to the reference beam and scattered beam respectively. For a weak signal ($N_s \ll 1$ and $N_r \gg N_s$) the effect of non- Gaussian statistics is dominated by the shot noise due to the reference beam so that the single clipped correlator may be used in this case without distortion. For details see JAKEMAN(1972). The use of the reference-beam system with photon correlation to measure fluid velocities has however not been reported.

For a large particle density and a constant velocity the field and intensity detected in a cross-beam system has a Gaussian probability density because of the central limit theorem. In general, for low particle density and and turbulent flow the detected field is non-Gaussian. Uniform random clipping can be used here to make the count

correlation function independent of the signal statistics. In Appendix B there is a discussion on the use of uniform random clipping while the error associated with this method is derived and also articles relevant to this topic are referenced. As mentioned earlier, for a low count rate ($E[n]<0.1$) the single-clipped correlation function is essentially undistorted so that non-Gaussian signals can always be handled at these low light levels. For a general review of correlation techniques refer to the article by Oliver referenced in Appendix B.

In the following sections it will be assumed that the count correlation function is proportional to the intensity correlation function.

§2. GENERAL FORM of CORRELATION FUNCTION

The intensity correlation function for a fluctuating flow with a finite mean velocity and a perturbation which is small compared with the mean is given by

$$R(\tau)=T(\tau)\left[1+1/2.m^2\ f(\tau)\ \cos\left(\frac{2\pi u}{s}\ \tau\right)\right] \qquad (1)$$

where u is the mean velocity, $T(\tau)$ is the transit time effect term and can be replaced by a constant when there are a large number of fringes, m accounts for for the imperfect visibility and the Fourier transform of $f(\tau)$ is proportional to the probability density of the fluctuating velocity. Note that there is no constant pedestal in eq.(1). A closed form such as eq.(1) is in general not possible when the fluctuation is comparable with or greater than the mean velocity, however, an accurate expression for the correlation function can be derived for a velocity with a Gaussian probability density with arbitrary turbulent

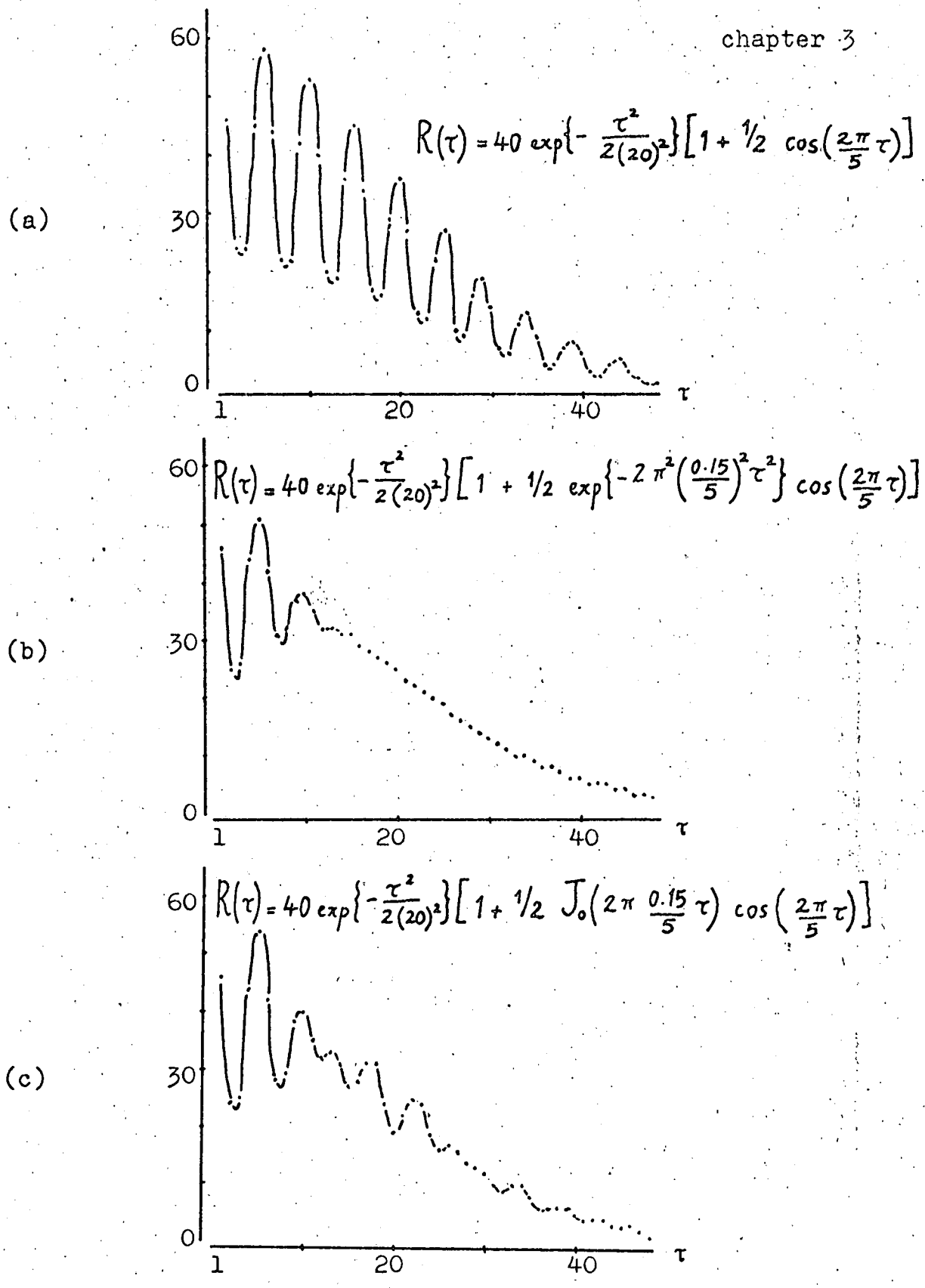

Fig.(1) Correlograms for (a) constant flow (b) turbulent flow with intensity $\sigma/u = 0.15$ and (c) sinusoidally fluctuating flow with $a/u = 0.15$.

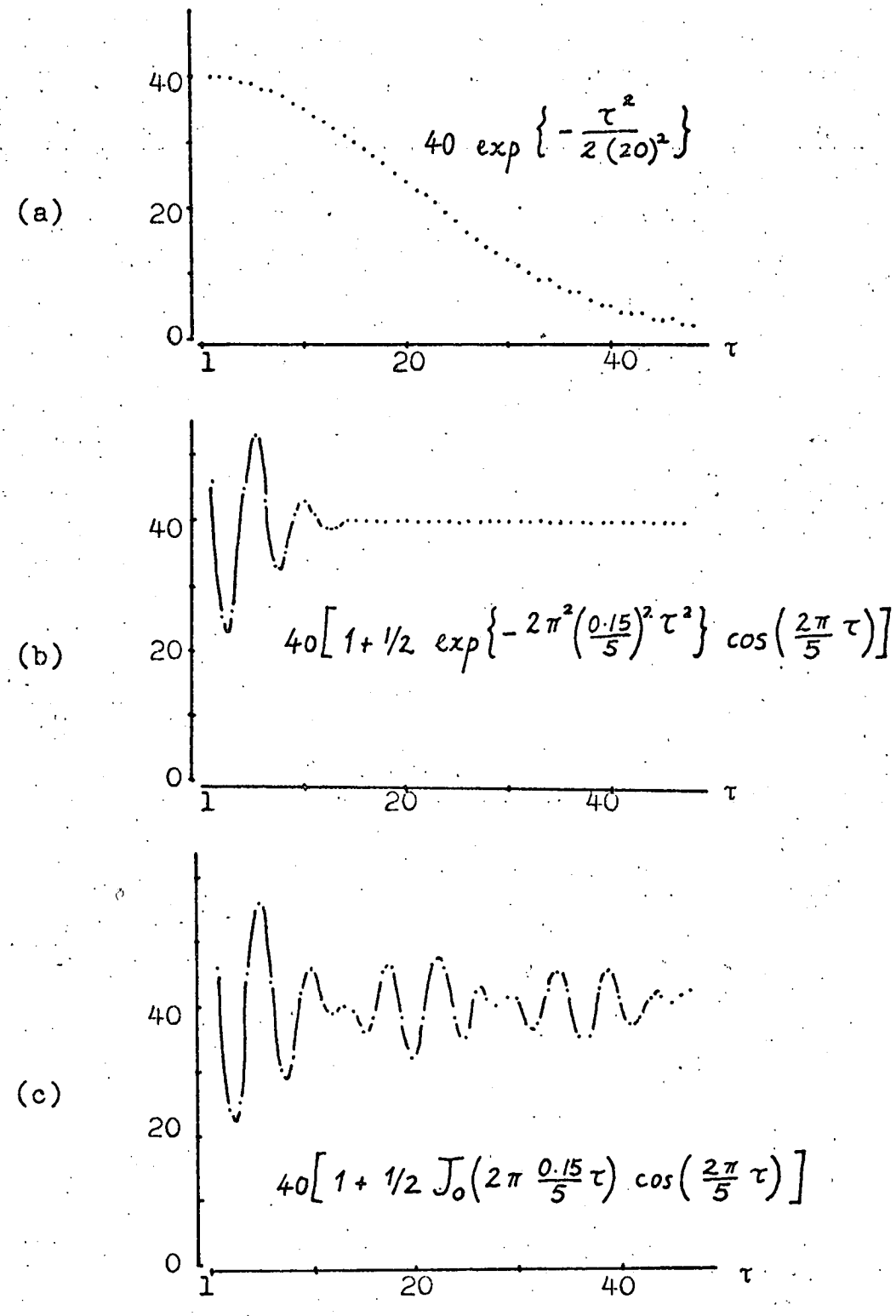

Fig.(2) (a) Transit time effect in the correlograms shown in fig.(1).

(b) and (c) show the correlograms of figs.(1b and c) with the transit time effect removed. The constant pedestal (=40) can be easily removed.

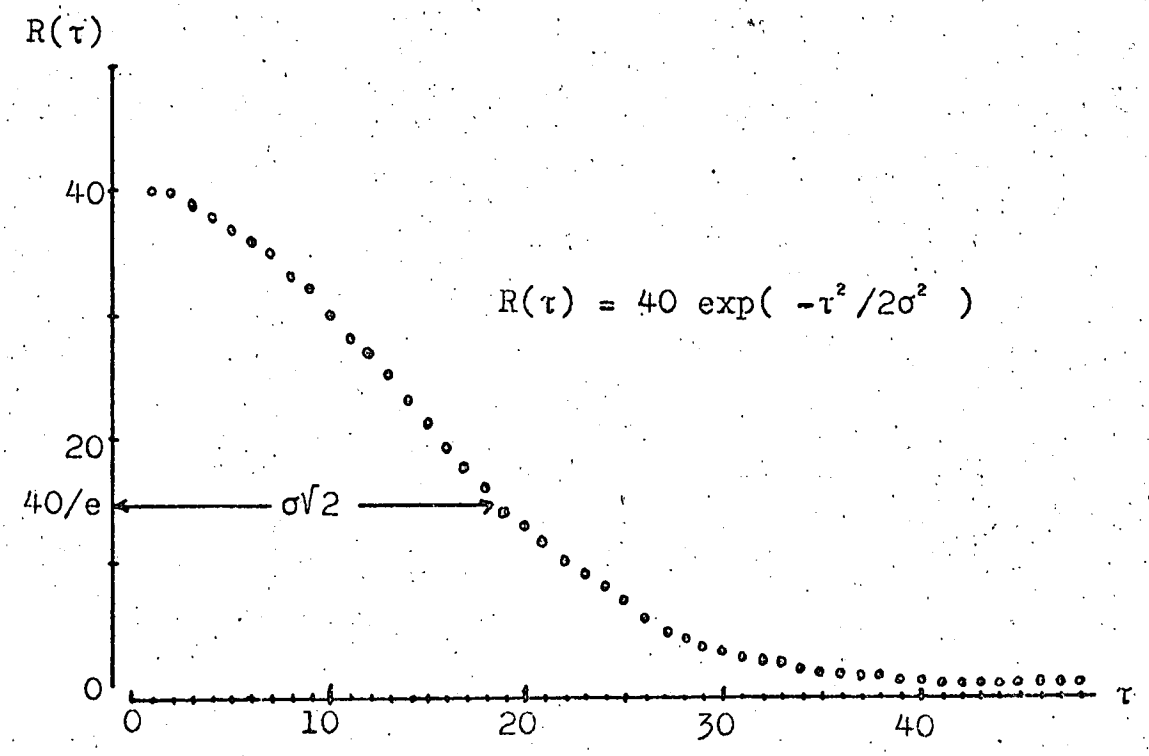

Fig.(3) A correlogram of this form should be obtained in order to remove the transit time effect. The ordinates of this correlogram become zero before the last lag.

Knowing that the form of the correlogram is a Gaussian, the variance of the Gaussian function can be found by using the width of the function at its 1/e point or by fitting.

If a separate experiment for the determination of the transit time effect is not possible, it should be ensured that the transit time effect is low. The transit time effect can now be removed by fitting a low order polynomial to the correlogram. Polynomial $P(\tau)=A(1+B\tau^2+C\tau^4+ \ldots)$

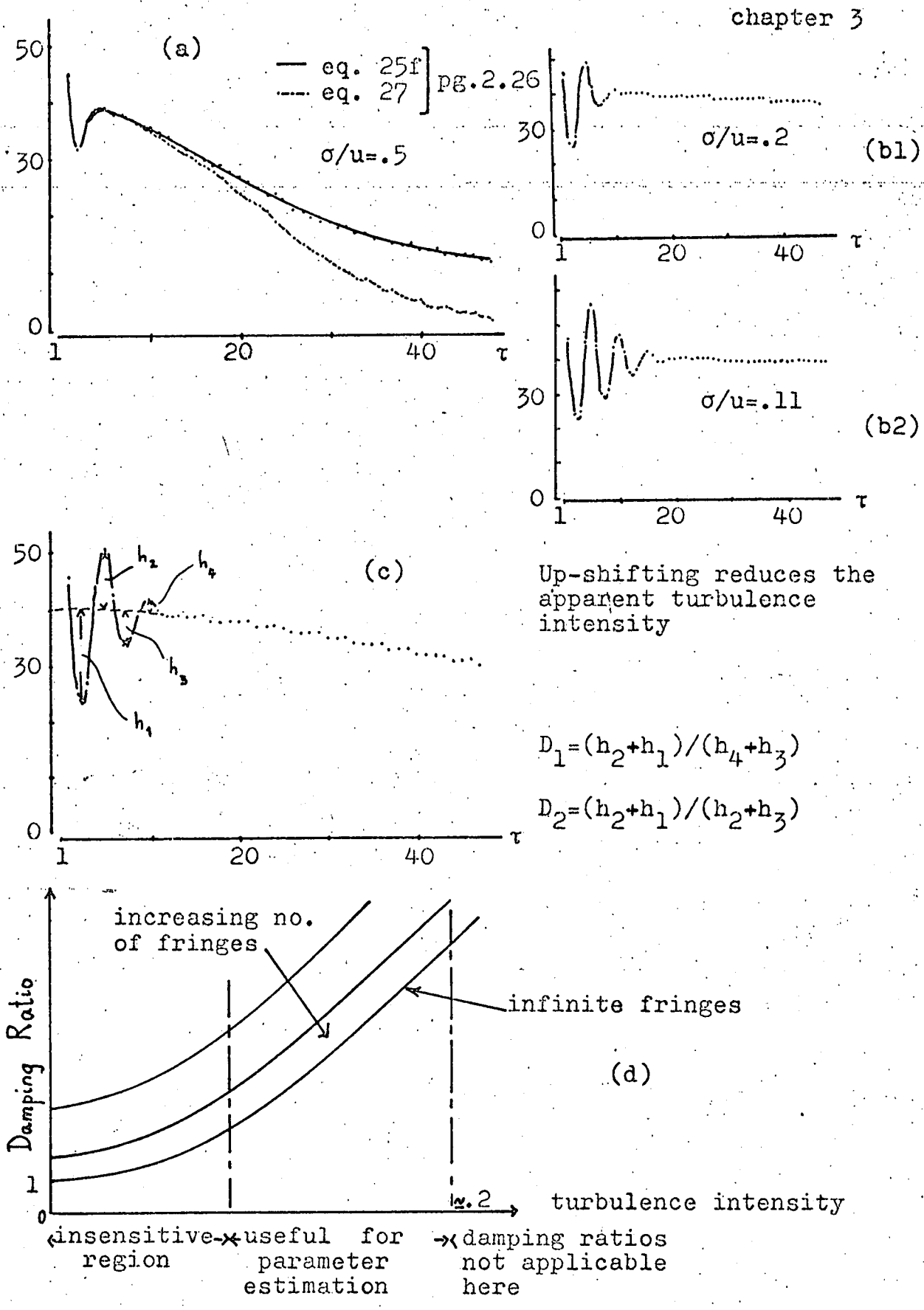

Fig.(4) (a) Difference between the accurate (eq.25f) and approximate (eq.27) formulae. See pg.(2.26) for these formulae.
(b1 and b2) Effect of frequency up-shifting.
(c) Method of obtaining damping ratios. Note that for D_1 and D_2 it is not necessary to draw in the low frequency line.
(d) Graph (schematic) of damping ratio vs. turbulence intensity.

intensity σ/u, c.f. eq.(25f) on pg. 2.26 . Although the form of eq.(25f) on pg. 2.26 is not like that of eq.(1), the mean and variance of the velocity can be estimated from it. It should be noted that for low turbulence intensity this expression reduces to the form of eq.(1).

In fig.(1) three correlation functions are shown for which expressions were derived in chapter 2. Forty eight ordinates are shown since this is the number of channels on the Precision Devices correlator. The zeroth lag value is not computed. The separation between the ordinates equals the sample time T.

It is useful to remove the transit time effect before parameter estimation. The transit time effect can be found by using a large sample time ($>s/2u$) so that the periodic part of the correlation function is smeared out. Frequency up-shifting can be used here to further reduce the periodic component. Frequency shifting is described in §4. Another method is to mask one of the incident beams so that the interference pattern is not formed and hence the correlation function becomes $T(\tau)$. See fig.(2). Some methods of removing the transit time effect are shown in fig.(3). When the turbulent intensity is high the same procedure can be used to find the transit time effect . It can however be seen from fig.(4a) that the approximate formula indicates a greater transit time effect (smaller transit time) than that for the more accurate formula.

§3. SIMPLE METHODS of PARAMETER ESTIMATION

Unless stated otherwise in this section it will be assumed that the transit time effect has not been removed.

The estimation of the mean velocity is fairly simple since one needs to measure only the time interval between successive crests and/or troughs of the correlogram to obtain the mean Doppler frequency. The positions of these turning points are shifted towards towards the origin due to $f(\tau)$ and $T(\tau)$. It is advisible therefore to measure the the time interval between any two maxima/minima with the exception of the maxima at the origin (WATRASIEWICZ & RUDD). Within the accuracy expected of the approximate methods to be discussed in this section, it can be said that the error involved in using the interval between the origin and the first maxima will not be too significant.

Generally speaking the time lag corresponding to a crest or trough will not fall at an exact multiple of the sample time so one must interpolate between the ordinates to improve the estimation of the positions of these turning points i.e. a parabola can be made to pass the three ordinates which form the troughs/crests.

The rate of damping of the periodic component of the correlogram is related to the turbulent intensity and can be measured easily by noting the rate at which the relative heights of successive crests and troughs decrease. BIRCH et al. (1973) have suggested that this can be done by drawing in first the line that corresponds to the low frequency component of the LDV signal, fig.(4c). The heights of the first trough h_1 and crest h_2 are measured relative to this line. From eq.(27),pg.(2.26), assuming that the transit time effect is

negligible compared with the damping due to the turbulence, it can be shown easily that the turbulence intensity is given by

$$\sigma/u = 1/\pi \cdot \left[\frac{2}{3} \ln(h_1/h_2) \right]^{1/2} . \qquad (2)$$

By removing the transit time effect it is easy to show that that the value of turbulence intensity using eq.(2) approaches the expected value. The only error then is in the estimation of h_1 and h_2. See fig.(4c).

Although eq.(2) is convenient in that it gives an explicit expression for the turbulent intensity in terms of quantities which can be measured directly from the correlogram, it tends to be too inaccurate for all but the most approximate estimates, especially when the number of fringes is small. A more accurate method is to measure damping ratios such as $D_1 = (h_2+h_1)/(h_4+h_3)$ or $D_2=(h_2+h_1)/(h_2+h_3)$. For a particular optical configuration with a known number of fringes a nomogram can be constructed relating the damping ratio to the turbulent intensity, figs.(4c,d).

It should be noted that the approximate formulae discussed in this section are only applicable for low turbulence intensity (20 %). The damping ratios will however be insensitive to very low turbulent intensity and here it is necessary to increase the apparent turbulence intensity by down-shifting the frequency in order to facilitate accurate parameter estimation. On the other hand, if the turbulence intensity is so high that the correlogram is highly damped, then, up-shifting the frequency until a reasonable damping ratio is obtained is recommended. The effect of frequency shifting on the accuracy of parameter

estimation will be discussed in the next section.

4. FREQUENCY SHIFTING

Optical frequency shifting techniques are as powerful when applied with photon correlation as they are when used for shifting the frequency of the analogue (continuous) Doppler signal.

Fig.(4a) shows the difference in the two formulae for turbulent flow. For such high turbulence intensity (50 %) it is not possible to estimate the mean velocity or the turbulence intensity accurately. By properly up-shifting the frequency, parameter estimation can be made possible.

The expressions for the correlation functions after frequency shifting by f_s can be obtained by replacing u/s in the previous chapter by $u/s + f_s$. When f_s is positive the fringes move in a direction opposite to the mean flow and hence effectively increase the frequency of the fluctuating part of the correlogram, fig.(4b). Since the number of channels (lags) available on a correlator is limited this means that the maximum correlation lag for which the correlation function fluctuates is reduced (for the same number of points per cycle on the correlogram) when up-shifting and vice versa. The effect of frequency up-shifting is therefore to reduce the effect of turbulence and transit time damping. Since $\sigma\tau/r \ll 1$, then eq.(25f) on pg.(2.26) reverts to

$$R(\tau) = D \exp\left(-\frac{u^2}{4r^2}\tau^2\right)\left[1+m^2/2.\exp\left(-\frac{2\pi^2\sigma^2}{s^2}\tau^2\right).\right.$$
$$\left.\cos\left\{2\pi(u/s+f_s)\tau\right\}\right] . \qquad (3)$$

This equation is different from eq.(27) on pg.(2.26) only in that it contains a different frequency. It is now not possible to use all the curves in fig.(4d) relating the damping ratio to the turbulence intensity because now the the damping ratio not only depends on the number of fringes in the probe volume but also on the amount and direction of the frequency shift. If the number of fringes or the amount of frequency shift are high enough for the transit time effect to be negligible, the curve for infinite number of fringes in fig.(4d) can be used. The turbulence intensity σ/u can be obtained directly from the apparent turbulent intensity $(\sigma/s)/(u/s+f_s)$ which is extracted from fig.(4d) .

Frequency shifting affects the accuracy with which the mean frequency can be estimated visually. Consider a correlogam which is a pure cosine of Doppler frequency f_o. By assuming that the number of points n in each cycle can be estimated to within ± 1 , it can be shown easily that the % error $\delta f_o/f_o = 1/M$, where M is the total number of correlation lags. Since the mean frequency is $(\bar{n}T)^{-1}$, the frequency resolution δf_o is $(M\bar{n}T)^{-1}$, where $\bar{n}$ is the average number of points per cycle and T is the sample time. With a frequency shift f_s it can be shown easily that the % error in the estimation of the Doppler frequency is

$$|\delta f_o/f_o| = M^{-1}|1 + f_s/f_o| .$$

It can be seen that down-shifting ($f_s < 0$) improves the accuracy of the mean velocity (f_o) estimate and deteriorates when up-shifting. For example a 50 point correlogram with no frequency shift ($f_s = 0$) has an error in the mean velocity of 2 %.

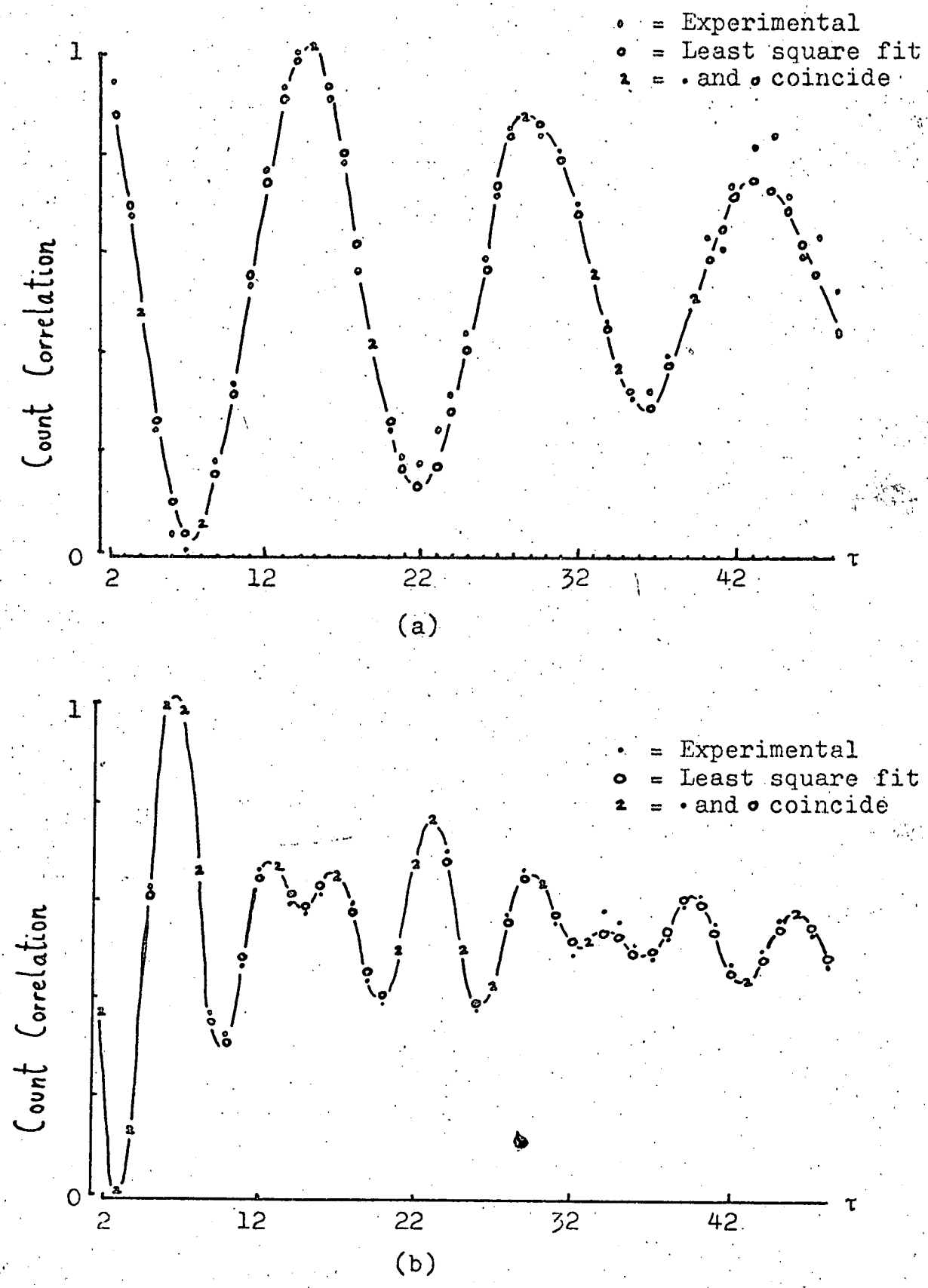

Fig.(5) Least square fitting of experimental correlograms:

(a) Correlogram for turbulent flow with Gaussian velocity probability density function.

(b) Correlogram for a sinusoidally fluctuating flow.

Although the preceding results are applicable only to a pure cosine, the ideas are also relevant to correlation functions for arbitrary fluctuations.

§5. CURVE FITTING

In this section it will be shown how by fitting a model to the correlogram the flow parameters can be obtained. Because of the highly non-linear forms of the correlation functions obtained in the previous chapter, it is recommended that some simplification should be carried out in order to determine the useful parameters before fitting. This means that the transit time effect (nuisance term) is removed and then the fitting is performed. Some methods of removing the transit time effect are shown in fig.(3). After the transit time term is removed the functions that remain are of the form $A\, f(\tau) \cos(2\pi\{u/s + f_s\}\, \tau)$, fig(2).

Before much experience was gained with the least square fitting procedure, the complete correlation function (with transit time term) was fitted. It was found that the objective function to be minimized was highly sensitive to some parameters while not being affected very much by others. If the initial guess values of the parameters were close to the true values, however, the parameters values did converge. It was found that the Nelder Mead method (routine) was most suitable for this type of fitting in comparison with others that were tried. The Marquardt and Powell methods usually tended to diverge significantly from the expected values. Two examples of curve fitting using the Nelder Mead method are shown in fig.(5). The transit time effect was

not removed before fitting here. Parameter values are not given since the only purpose is to show the closeness of the fit. When the transit time effect is removed before fitting, however, the Marquardt method may prove to be the most efficient. See HIMMELBLAU for details of methods.

BIRCH et al. (1975) have used the non-linear least square fitting method to determine parameters assuming a Gaussian and a Gram-Charlier velocity probability density. They found that the Gram-Charlier model gave a better fit than the Gaussian model. The closeness of fit was judged by the final value of the objective function. The confidence bound on the parameters were not computed. It was also not indicated how initial guess values for the skewness, kurtosis and higher moments can be made from the correlograms. The estimation of the confidence bounds on the parameters cannot be over-emphasised when using a model such as the Gram-Charlier since it is not known exactly where the Gram-Charlier series has to be truncated and the estimation of third and higher velocity moments must present difficulty. Although the information regarding the higher moments is present in the correlation function, their estimation will be considerably easier if the Fourier transform of a damped correlogram is used. This opinion is contrary to that put forward by BIRCH et al. (1975).

When the average count per sample time is low, the errors in the ordinates of the correlogram are independent. By using the first partial derivatives with respect to the parameters, the confidence bounds on the parameters can be obtained by forming the variance-covariance matrix. Details

of this standard procedure which was carried out in the the fitting programs is described by BEVINGTON. For an arbitrary count rate this procedure gives lower bounds on the errors of the estimated parameters.

The main drawback of the non-linear least square fitting method is that the initial guess values of the parameters need to be provided by the experimenter. An alternative method which was not tried is to use an initial Fourier transformation in order to obtain the initial guess values. This method is not without its drawbacks because it would increase the amount of computation required and also the unambiguous automatic extraction of the initial guess values from the spectrum would be quite difficult. If the correlogram is dead before the last lag, there will be no need for least square fitting of the correlogram since now the spectrum is proportional to the velocity probability density. The method of obtaining the spectrum is described in the next section.

§6. TRANSFORMATION of CORRELATION FUNCTION

The main advantage of the transformation method over the least square fitting method of §5 is that no a priori model for the velocity probability density is necessary. When a large number of correlograms have to be analysed, the least square fitting method would be very time consuming since initial guess values of the parameters have to be provided by the experimenter for each correlogram. This is overcome by using the transformation method.

(a)

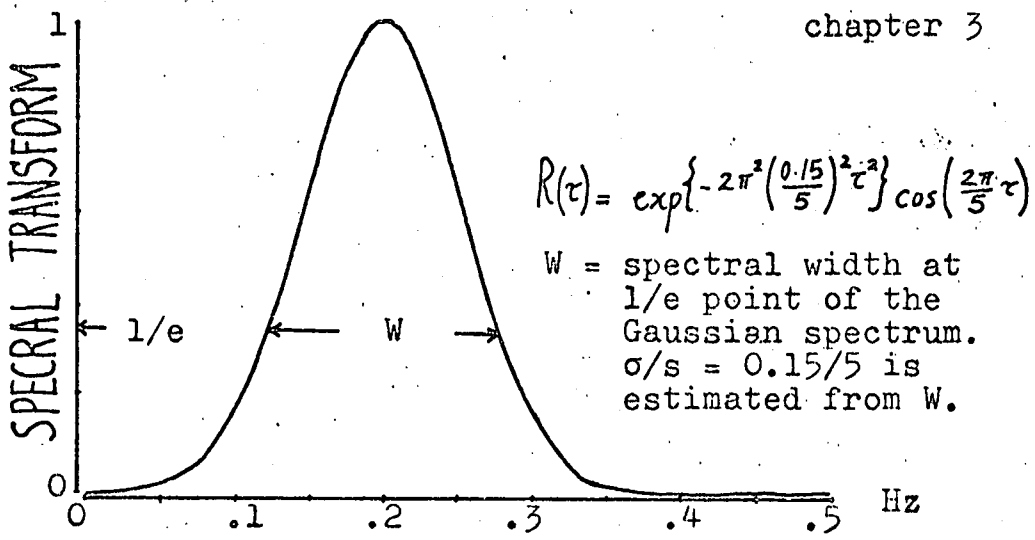

(b)

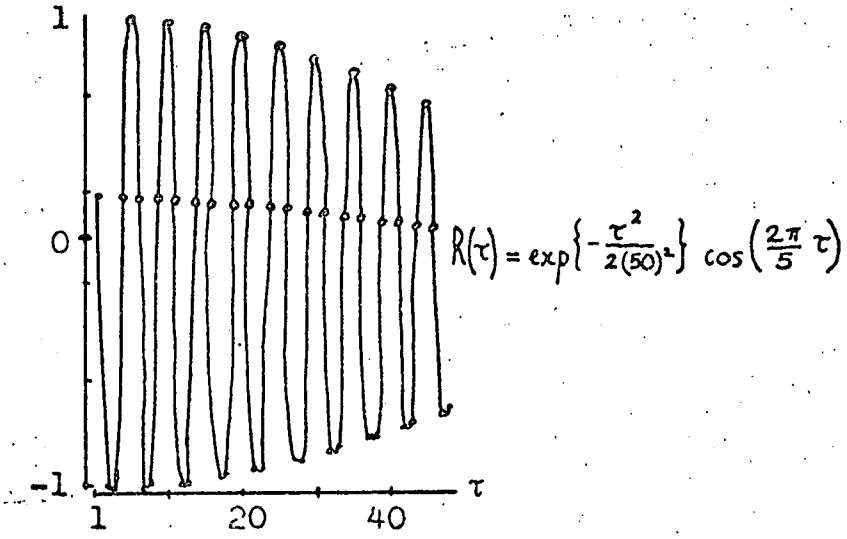

(c)

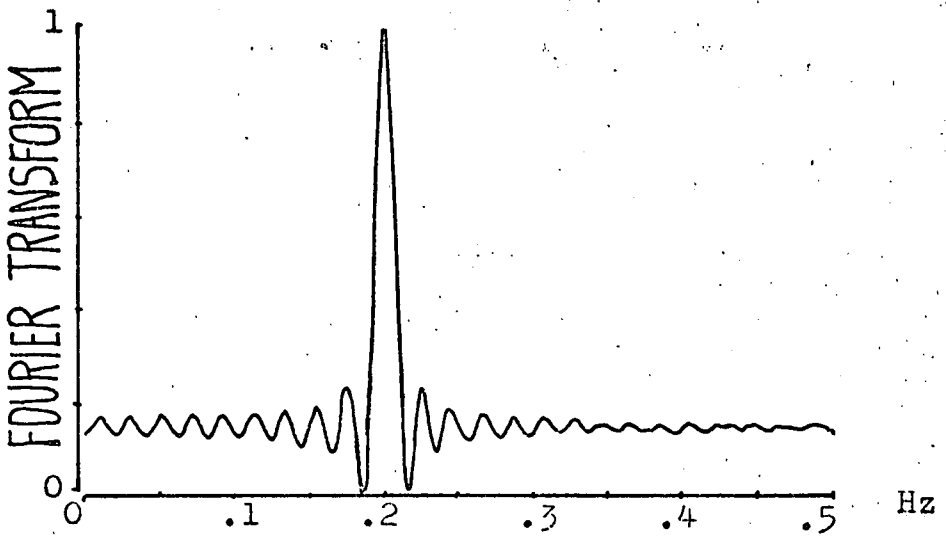

Fig.(6) (a) Spectrum obtained from a correlogram which is completely damped before its last lag. See fig.(2b). The spectral forms are identical for the 3 transformation methods investigated.
(b) A lightly damped correlogram.
(c) Fourier transform of correlogram in (b).

As in §5 it will be assumed that the correlation function being dealt with is of the form

$$R(\tau) = A\, f(\tau) \cos(2\pi\{u/s + f_s\}\,\tau)$$

where the Fourier transform of $f(\tau)\cos(2\pi u/s.\tau)$ is proportional to the velocity probability density function and f_s is the frequency shift. Note that the transit time effect $T(\tau)$ has been removed from the correlogram.

The spectrum which is the Fourier transform of the correlation function $R(sT)$, $s=0,1,..,M-1$, is given by

$$S(f) = R(0)T + 2T \sum_{s=1}^{M-1} R(sT)\cos(2\pi f s T) \qquad |f| \leq 1/2T \qquad . \quad (4)$$

Since $R(0)$ is not available on the Precision Devices correlator, it has to be determined in order to compute $S(f)$. $R(0)$ only introduces a constant pedestal in the spectrum and hence it is sufficient to ensure that $R(0) > R(sT)$ for $s>0$.

In eq.(4) if $f(\tau) = \exp(-2\pi^2\sigma^2/s^2.\tau^2)$ with finite σ/s and $M=\infty$

$$S(f) = A \exp\left[-s^2/2\sigma^2 \,.\, \{f-(u/s+f_s)\}^2\right] \quad , \quad f \leq 1/2T \,.$$

Here the constant pedestal is neglected and the multiplicative constants are absorbed in A. In this case there is no windowing problem. In practice, however, it is not possible to have an infinitely long correlogram but windowing can still be avoided by using frequency shifting to damp out the correlogram before the last correlation lag, fig.(2b). The spectrum of this correlogram in fig.(6a) gives values of u/s and σ/s consistent with the correlogram.

When the correlogram is not dead as in fig.(6b) the effect of the window will cause a broadening of the spectrum and the occurrence of side-lobes, fig.(6c). The spectrum in this case has a resolution of 1/MT where M is the total number of correlation lags and T is the sample time. This limited resolution is due to windowing which is common to all conventional Fourier transformation methods. Despite the broadening the position of the spectral peak is not affected. It can be deduced that the mean velocity (frequency) obtained from the spectrum for a velocity with symmetric probability density is unaffected by the windowing.

For a sinusoidally fluctuating flow it was shown on on pg.(2.29) that

$$f(\tau) = J_o(2\pi a/s \cdot \tau).$$

For an infinitely long correlogram the spectrum is given by

$$S(f) = A\left[a^2 - \left\{f-(u/s+f_s)\right\}^2\right]^{-1/2}, \quad \left|f-(u/s+f_s)\right| \leqslant a$$

$$= 0, \quad \text{otherwise}$$

where $|f| \leqslant 1/2T$.

The envelope of the correlogram in this case is oscillatory (fig.(2c)) and hence its Fourier transform will have a limited resolution. While the Gaussian can be considered dead after two standard deviations the Bessel function $J_o(x)$ oscillates approximately like $\sqrt{2/\pi x}\cos(x-\pi/4)$, (SNEDDON) hence frequency shifting does not help very much in damping out this correlogram. In this case it was found that estimation of the amplitude of fluctuation is best determined by finding the zero crossing of the envelope J_o of the correlogram, c.f. Appendix A. The value of the mean velocity can be determined by the midway point between the

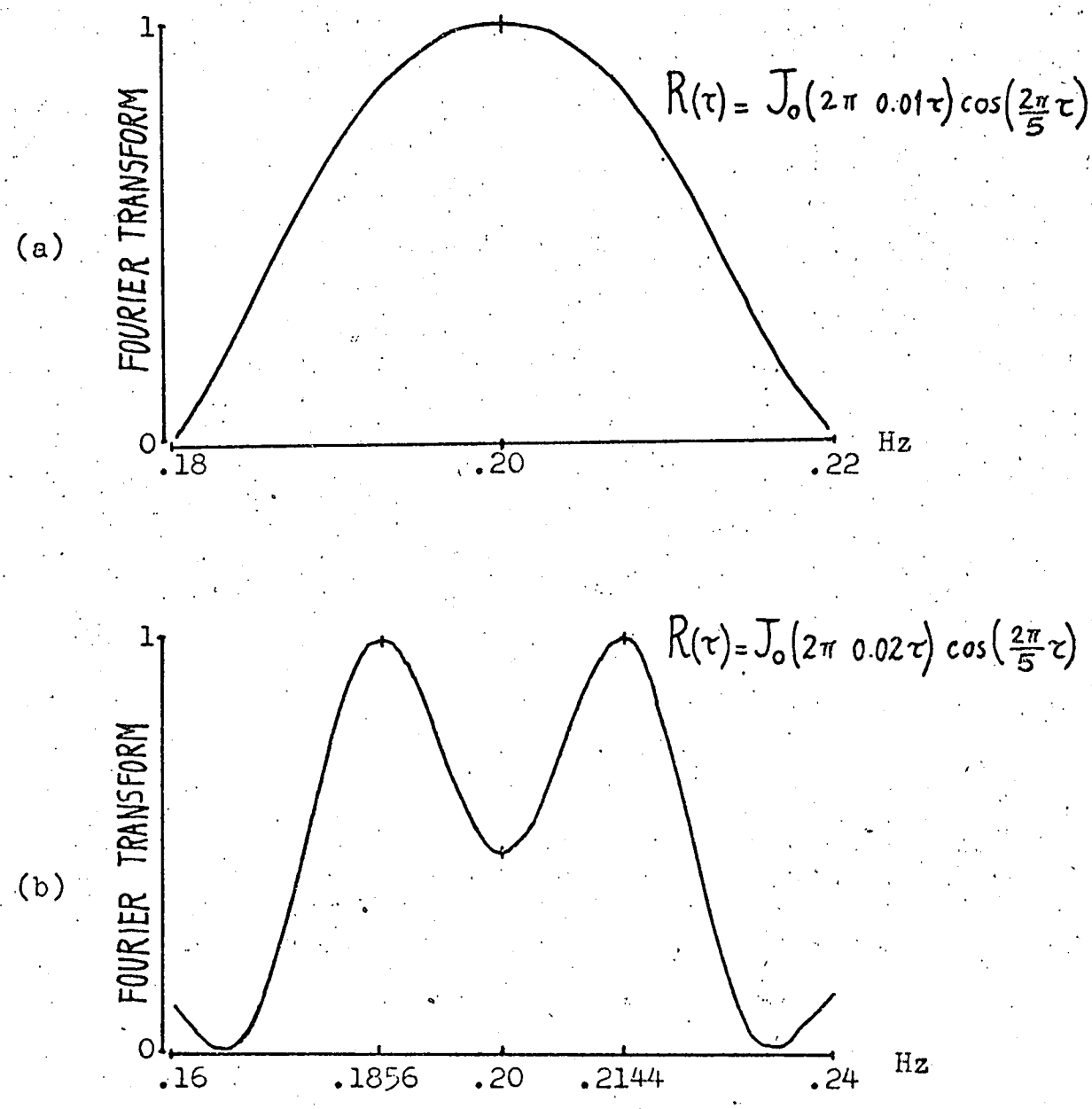

Fig.(7) (a) Spectrum with peaks not resolved.

(b) The two peaks are resolved in this spectrum. The peaks should theoretically occur at 0.18 Hz and 0.22 Hz for an infinitely long correlogram.

two peaks of the spectrum. In case the peaks are not resolved, the position of the single peak determines the mean velocity u, c.f. fig.(7).

The use of regression spectral estimators in geophysics has shown their superiority in detecting spectral peaks which would otherwise be masked by conventional spectral analysis (LACOSS). Two such techniques referred to as the Maximum Entropy (ME) Method and the Maximum Likelihood (ML) Method were used to see their effect in resolving the two peaks in the spectrum for sinusoidally fluctuating flow and on the single peak for turbulent flow.

The ME spectrum at frequency f is given by

$$S_{ME}(f) = pT/E^{T}\Gamma\,\Gamma^{T}E^{*}$$

and the ML spectrum is

$$S_{ML}(f) = 1/E^{T}R^{-1}E^{*}$$

where E and Γ are column vectors $(1, e^{i2\pi fT}, e^{i4\pi fT}, .., e^{i2(M-1)\pi fT})^{T}$ and $(1, \gamma_1, \gamma_2, .., \gamma_{M-1})^{T}$ respectively. * denotes complex conjugate. The components of Γ and the Mx1 column vector $P = (p, 0, .., 0)$ are found by solving the set of linear equations $R\Gamma = P$. R^{-1} is the inverse of the MxM correlation matrix R.

For these two high resolution methods it is necessary to obtain the inverse matrix R^{-1}. Since R is a Toeplitz matrix, i.e., the value of its elements r_{km} are dependant only on $|k-m|$, special iterative methods which use only N^2 operations (general matrix inversion requires N^3 operations) can be used to find the inverse. One 'multiply and add' is

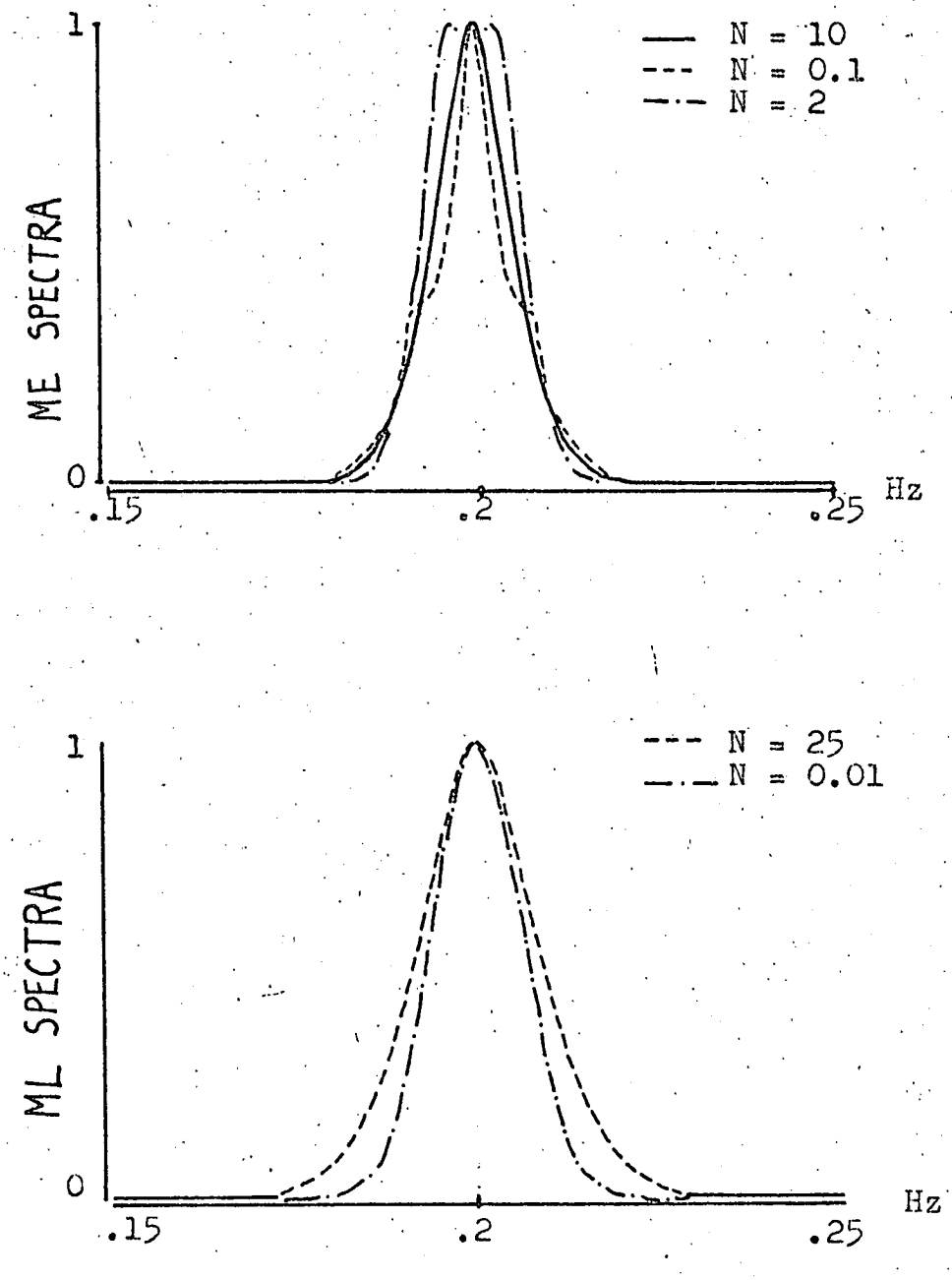

Fig.(8) Effect of the origin value R(0) of the correlogram on the ME and ML spectra. The correlogram is:

$$R(\tau) = N\,\delta_{\tau 0} + 2\,\exp\left\{-\frac{\tau^2}{2(27)^2}\right\}\cos\left(\frac{2\pi}{5}\tau\right)$$

equivalent to one operation. Algorithms given by MARKEL & GRAY were used to obtain the spectra shown in this chapter. Since only the shape of the spectra is of interest, the scale of the ordinates is unimportant.

Unlike the Fourier transform, the value of the correlation function at the origin does not simply transform to a constant pedestal in the high resolution spectra. It has been shown by PISARENKO that the higher the value of origin value R(0) the smoother the ME spectrum obtained. A similar though less marked behaviour was noted in the ML spectrum. The effect of R(0) on the spectral shape makes the two methods unreliable for the estimation of spectral widths. The effect of R(0) on the two spectra is shown in fig.(8).

Based on PISARENKO's paper the following method for the determination of R(0) is suggested (R(0) is not provided by the Precision Devices correlator). Introduce a trial value $R(0) > R(\tau)$, $\tau \neq 0$, and determine the smallest eigenvalue of the correlation matrix. The value of this eigenvalue is the noise n. Note that all eigenvalues should be positive. The value of the correlogram at the origin can now be put as R(0)-n. Sometimes this might lead to an unstable inverse and so it will be necessary to add a small amount of noise δ so that the origin value becomes $R(0)-n+\delta$. Further discussion on the effect of origin value is given by MAKHOUL.

Tests were carried out with simulated correlation functions for turbulent and sinusoidally fluctuating flows. In the turbulent flows cases the three method: Fourier transformation, ME and ML methods gave identical and accurate results for the mean velocity u and standard deviation σ

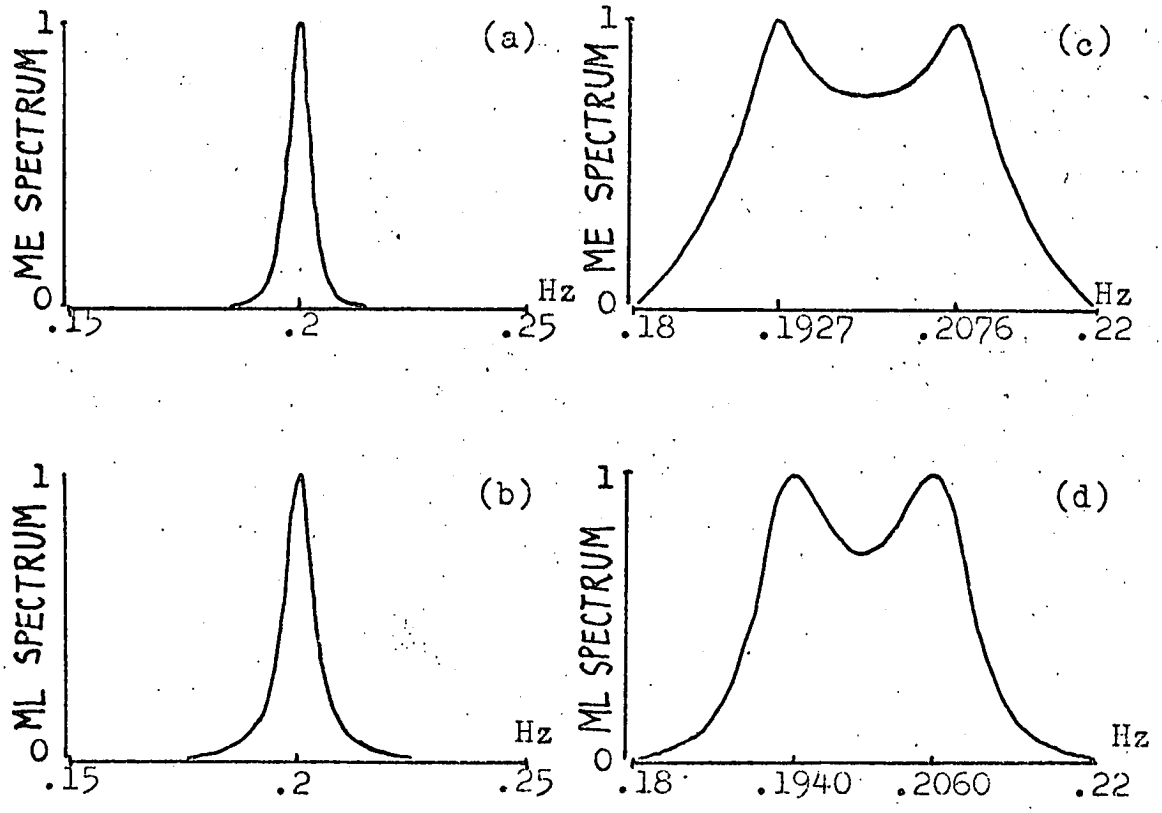

$$R(\tau) = \delta_{\tau 0} + \exp\left\{-\frac{\tau^2}{2(50)^2}\right\} \cos\left(\frac{2\pi}{5}\tau\right) \qquad R(\tau) = \delta_{\tau 0} + J_0(2\pi\ 0.01\tau) \cos\left(\frac{2\pi}{5}\tau\right)$$

Fig.(9) (a) and (b) show the ME and ML spectra for a partially damped correlogram. See figs.(6b,c). The standard deviation of the Gaussian envelope of the correlogram $\sigma=50$. The value of σ obtained from (a) = 62 and (b) =46. From the Fourier transform in fig.(6c), $\sigma=30$.

(c) and (d) show the ME and ML spectra for a sinusoidally fluctuating flow. Compare with fig.(7a).

of the velocity for correlograms with σ/u high enough for the correlograms to be zero before the last correlation lag as in fig.(2b). The ME and ML spectra for the correlogram in fig.(6b) are shown in figs.(9a,b). Here the correlogram is not dead before the last lag. Although the peaks of these spectra are narrower than the peak in fig.(6c), only an approximate estimate of σ is obtained from these high resolution spectra. The ML spectra gave consistently better values of σ than obtained by the ME method for such correlograms; the mean velocity estimate being accurate for all methods.

For a correlogram of length M the resolution of the Fourier transform is $(MT)^{-1}$ Hz while the ME and ML spectra have resolutions of approximately $(M^2T)^{-1}$ Hz and $(M^{3/2}T)^{-1}$ Hz respectively. It can be seen from fig.(9c,d) that although the high resolution methods resolve the two peaks in the spectrum of the correlogram for sinusoidal fluctuation the effect of the finite correlogram leads to the separation between the peaks to be reduced. Measurement of the amplitude of oscillation(a)from the separation will in general be lower than its true value.

The results obtained in this section point to the importance of using frequency shifting in order to damp the correlogram and then using Fourier transformation, hence avoiding the use of high resolution spectral estimators. For periodic flows the shape of the correlogram should either be related directly to the flow parameters of interest as was done for the sinusoidal fluctuation or use periodic sampling in order to find the form of the fluctuation as was shown on pg.(2.27).

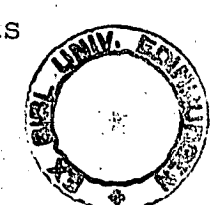

DURRANI & GREATED (1975) have applied the Fourier transformation, ME and ML methods to correlograms which were not completely damped and concluded that the ME spectrum gives an accurate estimate of σ and hence the turbulence intensity σ/u. They also suggested that the ML method because of its limited resolution in comparison with the ME spectrum does not give good estimates of the turbulence intensity. Both these points are contradicted by the results of the tests carried out in this section.

Various other tests on the extention of the correlogram were carried out (DUBROFF). It was shown that by increasing R(0) extention of the correlogram deteriorated. These results, however, are not relevant to the estimation of flow parameters and are therefore not presented here.

§7. CONCLUSIONS

By a proper choice of frequency shift a damped correlogram should be obtained if possible. After normalization of the correlogram the transit time effect should be removed.

When analysing periodically fluctuating flows of unknown form it is best to use the periodic sampling method described in chapter 2.

The estimation of parameters from the spectrum is much easier than by using least square fitting of a model to the correlogram.

Generally there should be no need to use the high resolution spectral estimators for the transformation of the correlograms in a properly designed experiment. The Fourier transform will give a good estimate of the velocity probability density if the correlogram is damped.

CHAPTER 4

BURST COUNTER PROCESSING

§ 1. INTRODUCTION

Several systems have been proposed for processing LDV signals in order to provide a voltage proportional to the instantaneous signal frequency, and to track variations in this frequency. Most of these systems rely on frequency demodulation by locking on to the phase of the input signal. The necessary requirement for such systems to perform efficiently is that the LDV signal is continuous, which is possible only if the particle distribution is homogeneous and the particle density is high. In applications such as wind tunnel measurements, or other gas flows, where artificial seeding is either not possible or undesirable the scatterer density is extremely low. Such experimental conditions demand more sensitive measurement techniques. The burst counter has been used with considerable success in such situations.

In this chapter the burst counter technique will be described. The application of this method to the measurement of flow parameters such as mean velocity, mean square turbulence level†, probability density of velocity and turbulence spectra will be discussed.

§ 2. DESCRIPTION of the BURST COUNTER

The principle of the burst counter is very simple. Imagine a particle passing through a scattering volume such that the scattered intensity detected gives a continuous variation of the current at the output of the photo multiplier while the particle is traversing the probe volume.

† equivalent to mean square turbulence intensity c.f. chapter 2

If the scattered intensity is sufficiently high the current variation effectively reproduces the intensity variation in the scattering volume, ie the frequency of the signal burst is proportional to the velocity of the particle. The frequency is usually determined by the rate of level crossings of the burst. The velocity of each particle can therefore be obtained since the constant of proportionality linking it to the frequency of the detected signal is pre-determined by the optical geometry and the wavelength of the laser light. See § 2 & § 3 of Chapter 2. As each particle passes through the scattering volume, velocity and time of passing through the centre of the scattering volume is measured and recorded. The information regarding the time of passing is only necessary if the turbulence spectrum is required.

Some practical details of the data acquisition and pre-conditioning will be discussed. The signal burst for each particle consists of a low-frequency pedestal and a high frequency component which contains the desired information. The burst counter operates by passing the received bursts through a high-pass filter and timing the consecutive intervals between the zero-crossings of the output bursts and assigns a frequency tag to each burst. The effect of lower scattered photon flux, finite fringe numbers and residual pedestal renders the level-crossing spacings non-uniform. Most burst counter processors include some logic circuits to ensure that errors due to spurious or missing zero-crossings are avoided. Experimenters have used different criteria (hence different logic circuitry) for accepting "genuine" bursts. For the purpose of this chapter it will

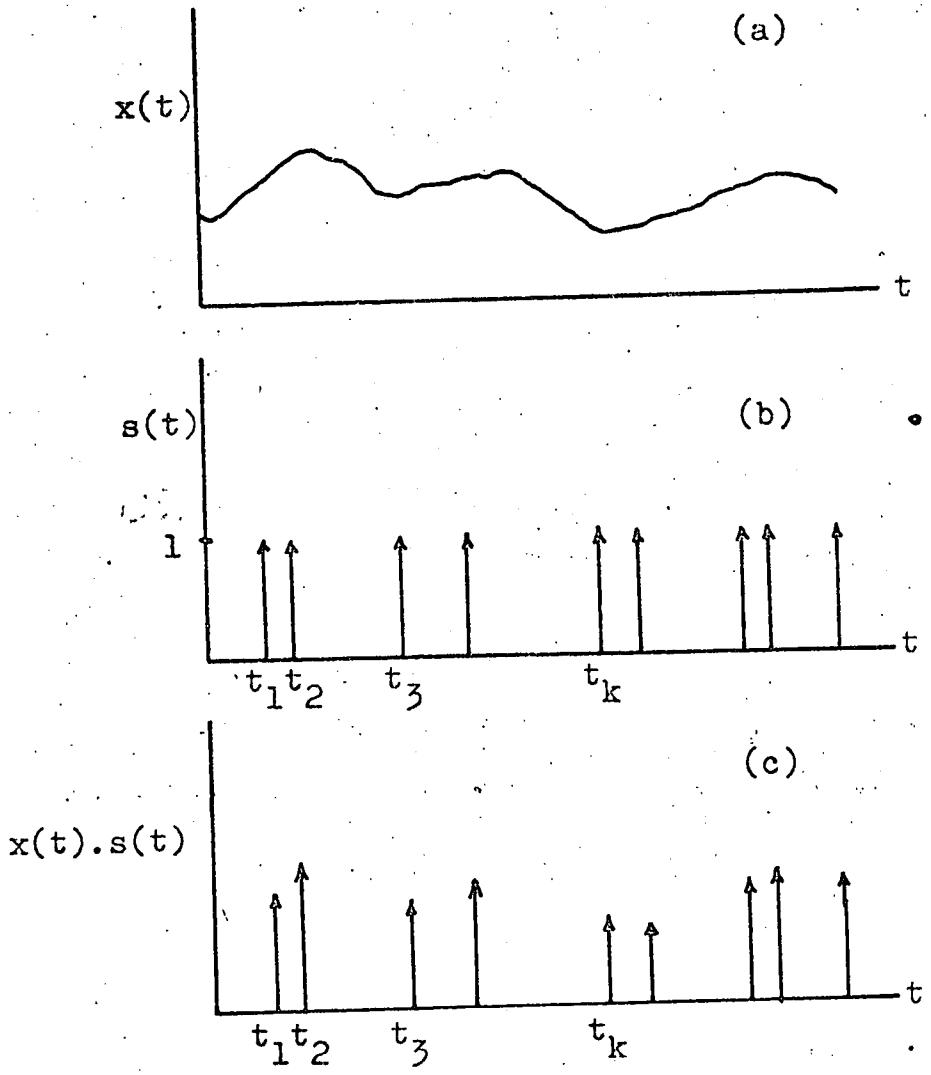

Fig.(1) (a) Fluid velocity.

(b) Poisson sampling signal of unity impulses. An impulse corresponds to the time of arrival of a particle in the scattering volume. Since the transit time is usually short compared with the inter-arrival times of the particles, the unity impulses are justifiable.

(c) The data x(t).s(t) output by a burst counter.

be assumed that all particles passing through the fringe volume will be detected and that their velocity and arrival times will be measured accurately.

In this section the principle of the burst counter has been described. For details of practical systems, the reader is referred to BRAYTON *et al* . The continued interest in this technique is illustrated by the number of articles about it in the Proc. of the Second International Workshop on Laser Velocimetry, Purdue University, '74.

§ 3. SAMPLING MODEL of VELOCITY

Since the transit time of the particle in the scattering volume is very small compared to the time interval between the arrival of two consecutive particles it is reasonable to consider the velocity sequence $\{x(t_k)\}$ where $k = 1, 2, \ldots, n$, as a Poisson sampling process with a mean rate ν which would depend on the scatterer density and be a constant for any experiment. SMITH & MEADOWS have experimentally verified this model by showing that the inter-arrival time τ of two consecutive particles has an exponential probability density function $\nu \exp(-\nu\tau)$. Figure 1 shows the fluid velocity and the sampling process which is used as a model in the analysis that follows. There are a host of examples in other branches of physics where the events of interest occur sporadically as in Figure 1.

The experimenter is often faced with the problem of deciding how many samples n of the velocity are necessary in order to achieve a required accuracy for the mean and turbulence level of the fluctuating velocity. DONOHUE *et al* have calculated the value of n that is required in order to obtain a certain desired accuracy. Their calculations are, however, based on the sum of independent random variables argument since they assume that $\{x_k\}$ is an uncorrelated sequence. In flows with more than one particle passing through the fringe volume in less than the Eulerian time scale, the velocities $\{x_k\}$ can be highly correlated. Under such conditions the results of DONOHUE *et al* under-estimate the value of n required to achieve the desired accuracy.

In order to take into account the correlated behaviour of the velocity fluctuations and its effect on the necessary value of n, it is necessary to assume a functional form for the velocity correlation function (c.f.). Three specific c.fs will be considered:

$$\exp(-\alpha|\tau|), \quad \exp(-\alpha|\tau|)\cos(\omega\tau) \quad \text{and} \quad \exp(-\lambda\tau^2).$$

Considering each c.f. in turn, the unbiased mean and variance estimators of the correlated sequence $\{x(t_k)\}$ will be derived. The sampling will be assumed to be Poissonian, ie the number of samples (velocity samples) in a fixed time has a Poisson probability density function with rate ν.

The only statistics of the velocity x(t) required for the derivation of the variance of the mean estimators (for the three c.fs) is the a priori knowledge of the c.fs.

In order to evaluate the variance of the variance estimators, however, Gaussian statistics for x(t) have to be assumed. The results for the c.f. $\exp(-\alpha|\tau|)\cos(\omega\tau)$ can be obtained directly from the exponentially decaying c.f. $\exp(-\alpha|\tau|)$ as will be explained later. Hence, only the c.f. $\exp(-\alpha|\tau|)$ will be discussed in detail and expressions will be obtained for the limiting cases of this c.f. when the number of samples n is large. Although the form of the variance of the estimators for the Gaussian c.f. $\exp(-\lambda\tau^2)$ is similar to that obtained for the c.f. $\exp(-\alpha|\tau|)$, the results cannot be obtained analytically. With the aid of a recurrence formula, however, numerical results can be obtained easily. For large n, the variance of the mean estimators is obtained analytically for the Gaussian c.f.

§ 4. POISSON SAMPLING

If the number of samples in a fixed time has a Poisson probability density, then the interval τ between adjacent samples has an exponential probability density and the probability density of any two non-overlapping intervals is independent. The probability density of τ is:

$$p(\tau) = \nu\exp(-\nu\tau) \qquad (\tau \geq 0)$$
$$p(\tau) = 0 \qquad (\tau < 0) \tag{1}$$

where ν is the rate parameter of the Poisson probability density. From this it follows that the probability density of the interval between any two samples $x(t_m)$ and $x(t_{m+n})$ separated by n independent intervals is

$$p_n(\tau) = \int_{-\infty}^{+\infty} p(u)p_{n-1}(\tau-u)du = \int_o^{\tau} p(u)p_{n-1}(\tau-u)du$$
$$p_1(\tau) \equiv p(\tau) \tag{2}$$

ie $p_n(\tau)$, $n \geq 2$, is obtained by successively convolving $p(\tau)$ with itself (n - 1) times. This leads to

$$p_n(\tau) = \frac{\nu^n \tau^{n-1}}{(n-1)!}\exp(-\nu\tau) \qquad (\tau \geq 0)$$
$$p_n(\tau) = 0 \qquad (\tau < 0) \tag{3}$$

The c.f. of the sampled process $\{x(t_K)\}$ is given by

$$C(n) = E\left[(x(t_i)-\mu)\ (x(t_j)-\mu)\right]$$
$$= E\left[E\left[(x(t_i)-\mu)(x(t_j)-\mu), \text{for } t_i \text{ and } t_j \text{ fixed}\right]\right] \tag{4}$$

where $\mu = E\left[x\right]$, $\sigma^2 = E\left[(x-\mu)^2\right]$ and $n = |i-j|$ is the number of intervals between the samples $x(t_i)$ and $x(t_j)$. $E[.]$ denotes expectation. In, eq. (4) the two expectations are with respect to x

and the exponentially distributed random variable $|t_i - t_j|$.

Consider a process x(t) with an exponentially decaying c.f. $\sigma^2 \exp\left[-\alpha|\tau|\right]$, where σ^2 is the variance of x(t) and $\alpha > 0$. The c.f. of the sequence $\{x(t_K)\}$ can now be found using equation (4).

$$C(n) = E\left[\sigma^2 \exp(-\alpha|\tau|)\right] \qquad (\tau \geq 0) \tag{5}$$

where $|\tau| = |t_i - t_j|$ is the random variable. Using equations (3) and (5)

$$C(n) = \sigma^2 \int_0^\infty \exp(-\alpha\tau)\, \frac{\nu^n \tau^{n-1} \exp(-\nu\tau)}{(n-1)!} d\tau \tag{6}$$

Since the Gamma function is defined as

$$\Gamma(n+1) = \int_0^\infty \phi^n \exp(-\phi) d\phi = n! \quad \text{(n is a natural number)}$$

then

$$C(n) = \sigma^2 \left(\frac{\nu}{\alpha+\nu}\right)^n \tag{7}$$

By considering the exponentially decaying c.f. as $\mathrm{Re}\left[\exp\{-(\alpha+i\omega)|\tau|\}\right]$, $(i = \sqrt{-1})$, the c.f. of the sampled sequence is simply

$$C(n) = \mathrm{Re}\left[\frac{\nu}{\nu+(\alpha+i\omega)}\right]^n \tag{8}$$

where $\mathrm{Re}[.]$ denotes real part.

For the Gaussian c.f. $\sigma^2\exp(-\lambda\tau^2)$, the covariance of the sequence now becomes

$$C(n) = \int_0^\infty \sigma^2\exp(-\lambda\tau^2)\ \frac{\nu^n\tau^{n-1}}{\Gamma(n)}\ \exp(-\nu\tau)d\tau \qquad (9)$$

From GRADSHTEYN & RHYSIK

$$\int_0^\infty x^{\nu-1}\exp(-\beta x^2-\gamma x)dx = (2\beta)^{-\nu/2}\Gamma(\nu)\exp(\frac{\gamma^2}{8\beta})\ D_{-\nu}(\frac{\gamma}{\sqrt{2\beta}}),(\beta,\nu>0) \qquad (10)$$

$$\therefore \quad C(n) = \sigma^2(\frac{\nu}{\sqrt{2\lambda}})^n\exp(\frac{\nu^2}{8\lambda})D_{-n}(\frac{\nu}{\sqrt{2\lambda}}) = \sigma^2 z^n\exp(z^2/4)D_{-n}(z) \qquad (11)$$

where $D_{-n}(z)$ is a parabolic cylinder function and $z=(\frac{\nu}{\sqrt{2\lambda}})$.

§ 5. C.F. $= \sigma^2\exp[-a|\tau|]$

5.1 Mean Estimate and its Variance

We shall now consider the mean estimate $\hat{x}$ of the sequence of variables $\{x(t_i)\}$, $i = 1,\ldots,n$. Representing $x(t_i)$ by x_i, a reasonable estimate is

$$\hat{x} = \sum_{i=1}^{n} x_i/n \qquad (12)$$

Unless specified, all summations that follow will be from 1 to n. Since we know a priori that $E[x(t)] = \mu$, then,

$$E\left[\hat{x}\right] = E\left[\sum_i x_i/n\right] = \sum_i E\left[x_i\right]/n = \mu \tag{13}$$

We shall now determine the variance of the unbiased mean estimator $\hat{x}$: ie

$$V(\hat{x}) = E\left[\hat{x}-\mu\right]^2 = \frac{1}{n^2} E\left[\sum_i (x_i-\mu)\right]^2 \tag{14}$$

$$= \frac{1}{n^2} E\left[\sum_i (x_i-\mu)^2 + \sum_{i\neq j}\sum (x_i-\mu)\ (x_j-\mu)\right] \tag{15}$$

$$= \frac{1}{n^2}\left[\sum_i E(x_i-\mu)^2 + \sum_{i\neq j}\sum E(x_i-\mu)\cdot(x_j-\mu)\right] \tag{16}$$

The definition of variance is

$$E(x_i-\mu)^2 = C(0) = \sigma^2 \tag{17}$$

Using equations (7) and (17) gives

$$V(\hat{x}) = \frac{1}{n^2}\left[n\sigma^2 + \sigma^2 \sum_{i\neq j}\sum \left(\frac{\nu}{\nu+\alpha}\right)^{|i-j|}\right] \tag{18}$$

Letting $a = \left(\frac{\nu}{\nu+\alpha}\right) < 1$ and removing the modulus sign we get

$$\sum_{i\neq j}\sum \left(\frac{\nu}{\nu+\alpha}\right)^{|i-j|} = 2\sum_{i>j}\sum a^{i-j} \tag{19a}$$

$$= 2\sum_r (n-r)a^r \tag{19b}$$

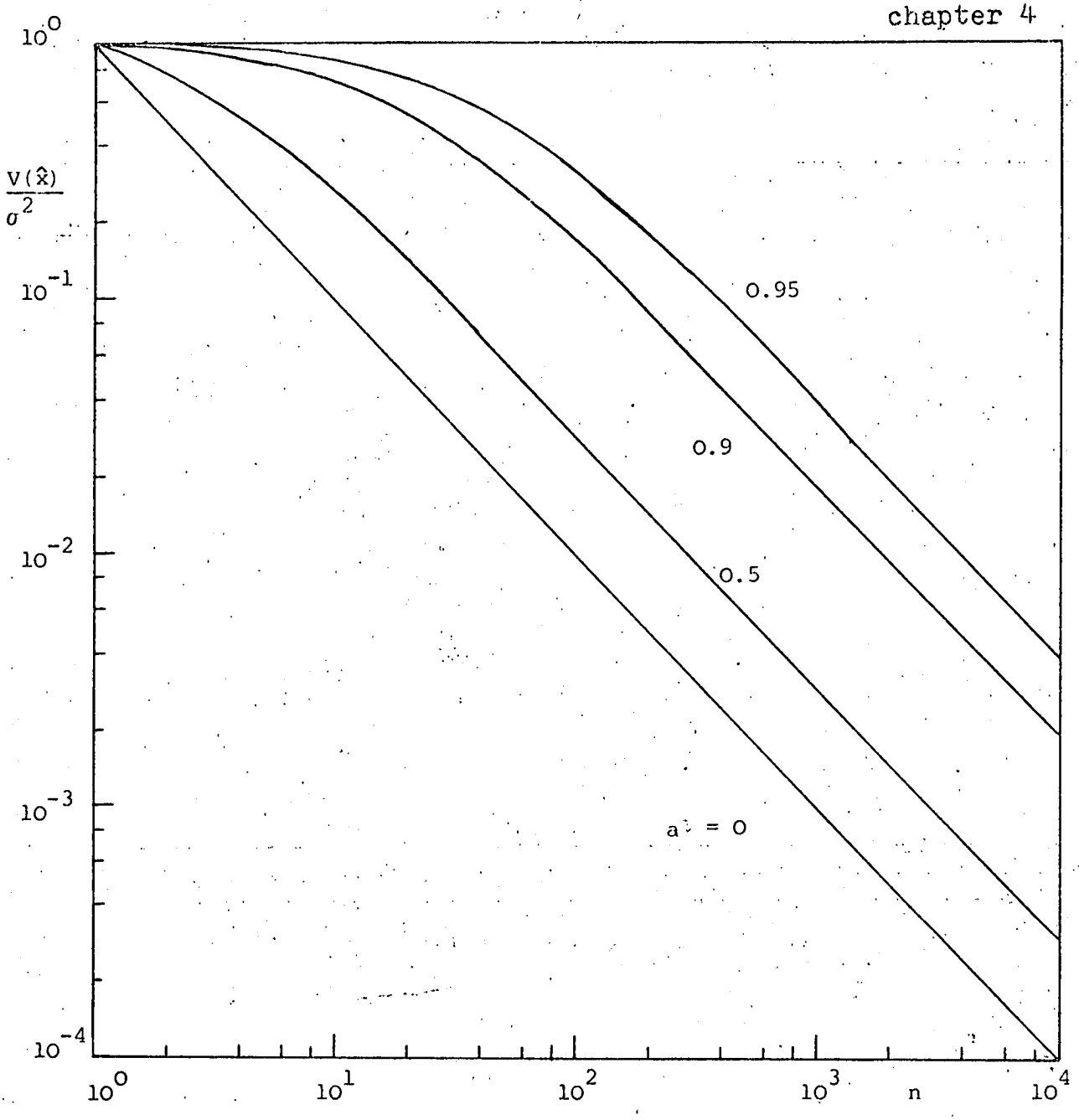

FIG (2) $\frac{V(\hat{x})}{\sigma^2}$ versus n for various values of $a = \frac{\nu}{\nu+\alpha}$

c.f. = $\sigma^2 \exp(-\alpha|\tau|)$

In expanding equation (19a) we find 2(n-r) terms of a^r, where r = 1, 2,...., n-1, therefore equation (18) becomes

$$V(\hat{x}) = \frac{1}{n^2}\left[n\sigma^2 + 2\sigma^2 \sum_r (n-r)a^r \right] \tag{20}$$

Using the following results from GRADSHTEYN & RHYSIK

$$\sum_r a^r = \frac{a(1-a^n)}{(1-a)} \tag{21}$$

$$\sum_r ra^r = a\left[\frac{1-(n+1)a^n + na^{n+1}}{(1-a)^2}\right] \tag{22}$$

equation (18) gives

$$V(\hat{x}) = \frac{\sigma^2}{n^2}\left[n + \frac{2a}{(1-a)^2}\{n(1-a) + a^n - 1\} \right] \tag{23}$$

Since a < 1, it can be deduced that $\hat{x}$ is a consistent estimator because $V(\hat{x}) \to 0$ as $n \to \infty$. It is noted that when the samples $\{x(t_K)\}$ are independent, ie when a = 0, then $V(\hat{x}) = \sigma^2/n$. This is the standard result for the variance of the mean estimate of n independent samples. For large n,

$$\frac{V(\hat{x})}{(\sigma^2/n)} \simeq \frac{1 + a}{1 - a} \tag{24}$$

Figure (2) shows $V(\hat{x})/\sigma^2$ plotted against n for various values of a.

5.2 Variance Estimator and its Variance

The unbiased variance estimator which will be considered in this section is given by

$$\hat{v} = \frac{1}{N} \sum_i (x_i - \hat{x})^2 \tag{25}$$

where N has to be determined such that $E(\hat{v}) = \sigma^2$

$$E(\hat{v}) = \frac{1}{N} \sum_i E(x_i - \hat{x})^2 \tag{26}$$

$$E\left[(x_i-\hat{x})^2\right] = E\left[\{(x_i-\mu) - (\hat{x}-\mu)\}^2\right] = E\left[(x_i-\mu)^2\right] + E\left[(\hat{x}-\mu)^2\right] - 2E\left[(x_i-\mu)\ (\hat{x}-\mu)\right] \tag{27}$$

By using equation (14), equation (26) becomes.

$$E(\hat{v}) = \frac{1}{N} \sum_i \left(\sigma^2 + V(\hat{x}) - 2E\{(x_i-\mu).\frac{1}{n}\sum_j (x_j-\mu)\}\right)$$

$$= \frac{1}{N}\left[n\sigma^2 + nV(\hat{x}) - \frac{2}{n}\sum_i \sum_j \sigma^2\ a^{|i-j|}\ \right] \tag{28}$$

$$= \frac{1}{N}\left[n\sigma^2 + nV(\hat{x}) - 2\sigma^2 - \frac{2\sigma^2}{n}\sum_{i\neq j}\sum a^{|i-j|}\ \right]$$

Using equations (19) and (20) we get

$$E(\hat{v}) = \frac{1}{N}\left[n\sigma^2 + nV(\hat{x}) - 2\sigma^2 - \frac{4\sigma^2}{n}\sum_r (n-r)a^r\right] \tag{29}$$

$$= \frac{1}{N}\left[n\sigma^2 - \sigma^2 - \frac{2\sigma^2}{n}\sum_r (n-r)a^r\ \right]$$

For $\hat{v}$ to be unbiased, $E(\hat{v}) = \sigma^2$, hence

$$N = n-1-\frac{2}{n}\sum_r (n-r)a^r \tag{30}$$

Using equation (20), N can be expressed as a function of $V(\hat{x})$, ie

$$N = n - nV(\hat{x})/\sigma^2 = n - V(\hat{x})/(\sigma^2/n) \tag{31}$$

When the samples are independent it can be shown that $N = n - 1$ by putting $a = 0$ in equation (29) or substituting $V(\hat{x}) = \sigma^2/n$ in equation (31). In its simplified form

$$N = n - 1 - \frac{2a}{n(1-a)^2}\{n(1-a) + a^n - 1\} \tag{32}$$

Having found the unbiased estimator we will now find its variance

$$V(\hat{v}) = E\left[(\hat{v}-\sigma^2)^2\right] = E(\hat{v}^2) - \sigma^4 \tag{33}$$

$$E(\hat{v}^2) = E\left[\{\frac{1}{N}\sum_i (x_i-\hat{x})^2\}^2\right] = \frac{1}{N^2}\sum_i\sum_j E\left[(x_1-\hat{x})^2(x_j-\hat{x})^2\right] \tag{34}$$

Assuming Gaussian statistics for x_i and letting $z_i = x_1 - \hat{x}$, then z_i has zero mean and

$$E\left[z_i^2 z_j^2\right] = E\left[z_i^2\right] E\left[z_j^2\right] + 2E^2(z_i z_j) \tag{35}$$

It can be shown that $\sum_i E(z_i)^2 = N\sigma^2$.

Also,

$$E(z_i z_j) = E\left[(x_i-\mu)(x_j-\mu)\right] + E\left[(\hat{x}-\mu)\ (\hat{x}-\mu)\right] - E\left[(x_i-\mu)(\hat{x}-\mu)\right] - E\left[(x_j-\mu)\ (\hat{x}-\mu)\right] \tag{36}$$

Let $$A(i) = E\left[(x_i-\mu)(\hat{x}-\mu)\right] = \frac{1}{n}\sum_j E\left[(x_i-\mu)(x_j-\mu)\right] = \frac{1}{n}\sum_j \sigma^2 a^{|i-j|} = \frac{\sigma^2}{n}\left[n + \sum_{r=1}^{n-i} a^r + \sum_{r=1}^{i-1} a^r\right] \tag{37}$$

Then, $$\sum_i A(i) = nV(\hat{x}). \tag{38}$$

Substituting equation (37) in (36)

$$E(z_i z_j) = \sigma^2 a^{|i-j|} + V(\hat{x}) - A(i) - A(j) \tag{39}$$

$$\therefore \sum_i \sum_j E^2\left[(z_i z_j)\right] = \sum_i \sum_j \left(\sigma^2 a^{|i-j|} + V(\hat{x}) - A(i) - A(j)\right)^2 \tag{40}$$

Using equation (37), equation (40) can be simply written as

$$\sum_i \sum_j E^2\left[(z_i z_j)\right] = I_1 + I_2 + I_3 \tag{41a}$$

where $$I_1 = \sum_i \sum_j \sigma^4 a^{2|i-j|},\ I_2 = n^2 V^2(\hat{x}),\ I_3 = -2n\sum_i A_i^2 \tag{41b}$$

Substituting equations (34) and (41) into equation (33) we obtain

$$V(\hat{v}) = \frac{2}{N^2}\left[I_1 + I_2 + I_3\right] \tag{42}$$

where $$I_1 = \sigma^4\left[n + \frac{2a^2}{(1-a^2)^2}\{n(1-a^2) + a^{2n}-1\}\right] \quad (43a)$$

$$I_2 = \frac{\sigma^4}{n^2}\left[n + \frac{2a}{(1-a)^2}\{n(1-a) + a^n-1\}\right]^2 \quad (43b)$$

and $$I_3 = -\frac{2\sigma^4}{n(1-a)^2}\left[n(1+2a+a^2+2a^{n+1}) - 4\frac{(1+a)a(1-a^2)}{(1-a)} + 2\frac{a^2(1-a^{2n})}{(1-a^2)}\right] \quad (43c)$$

The equations (43a, b and c) are obtained using equations (19), (23) and (21) respectively in equation (41b). When a = 0, $V(\hat{v}) = \frac{2\sigma^4}{(n-1)}$, which is the same result as given by HALD for independent samples. It will be noticed that only I_1 contributes significantly to $V(\hat{v})$ for large n. A result similar to equation (24) can be obtained in this case for large n

$$V(\hat{v})/(2\sigma^4/n-1) \simeq \frac{1 + a^2}{1 - a^2} \quad (44)$$

This equation can be verified by considering $V(\hat{v})$ in figure (3) for $n = 10^4$ with a = 0 and a = 0.9. From the curves

$$\frac{V(\hat{v},\ a = 0.9)}{V(\hat{v},\ a = 0)} = \frac{1.9 \times 10^{-3}}{2 \times 10^{-4}} \simeq 10$$

and using equation (44) we obtain

$$\frac{1 + (0.9)^2}{1 - (0.9)^2} = \frac{1.81}{0.19} \simeq 10$$

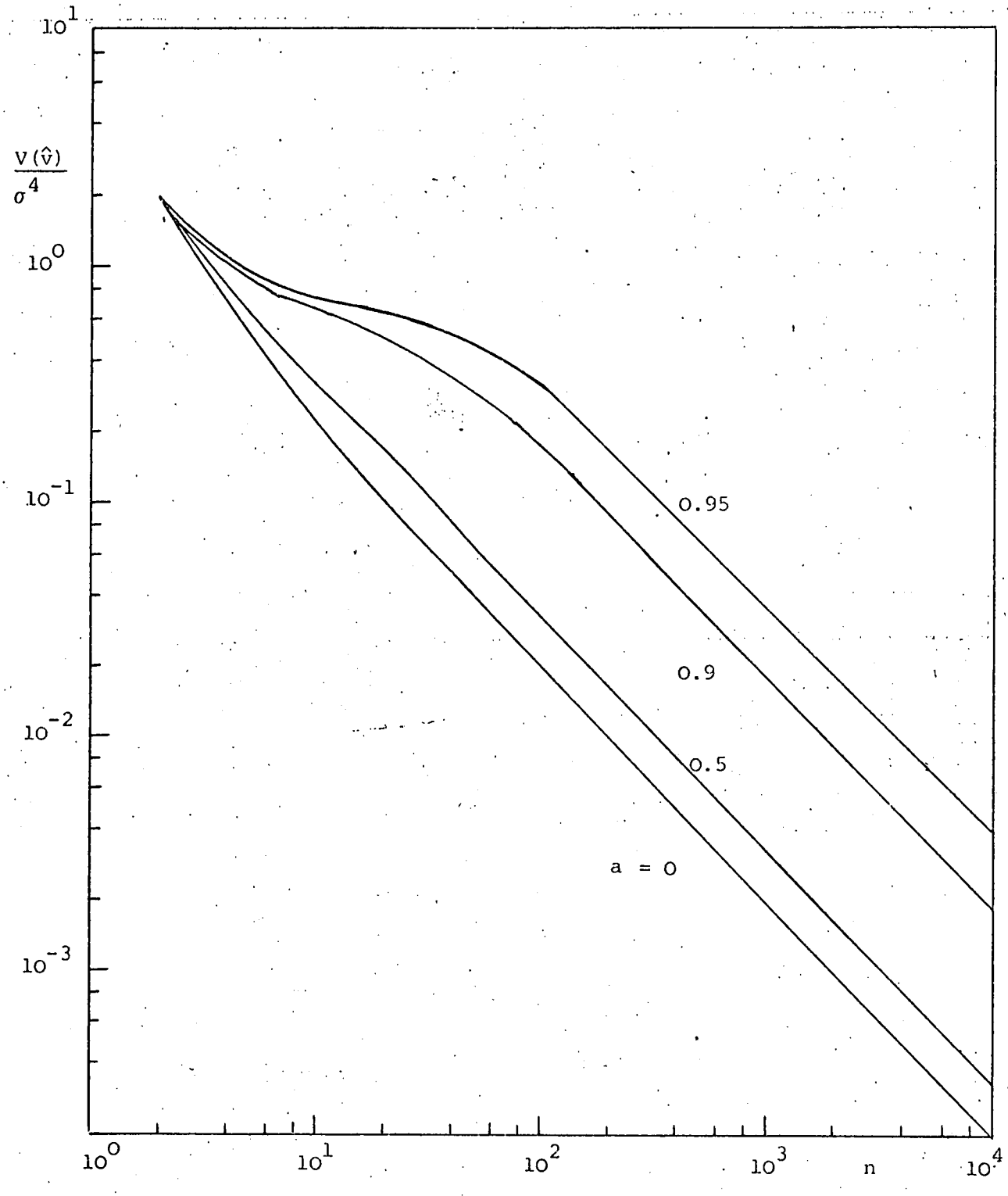

FIG (3) $\frac{V(\hat{v})}{\sigma^4}$ versus n for various values of a = $\frac{\nu}{\nu+\alpha}$

$$c.f. = \sigma^2 \exp(-\alpha|\tau|)$$

The variance estimator is consistent since $V(\hat{v})$ approaches zero as n increases (see figure (3) and equation (44)').

§ 6. $\underline{\text{C.F.} = \sigma^2 \exp(-\alpha|\tau|)\cos\omega\tau}$

As indicated in § 3, all the results obtained in § 5 can be directly extended to the present c.f.

For example, using equation (23) the variance of the mean estimator is

$$V(\hat{x}) = \text{Re}\left[\frac{\sigma^2}{n^2}\left(n + \frac{2a}{(1-a)^2}\{n(1-a) + a^n - 1\}\right)\right] \qquad (45)$$

where $a = \left[\frac{\nu}{\nu+(\alpha+i\omega)}\right]$

Similarly the variance of the variance estimator can be obtained.

By setting $\alpha = 0$, a periodic covariance function can be considered.

§ 7. $\underline{\text{C.F.} = \sigma^2 \exp(-\lambda\tau^2)}$

In this case the variance of the estimators cannot be obtained analytically, however, the results are easily obtained numerically.

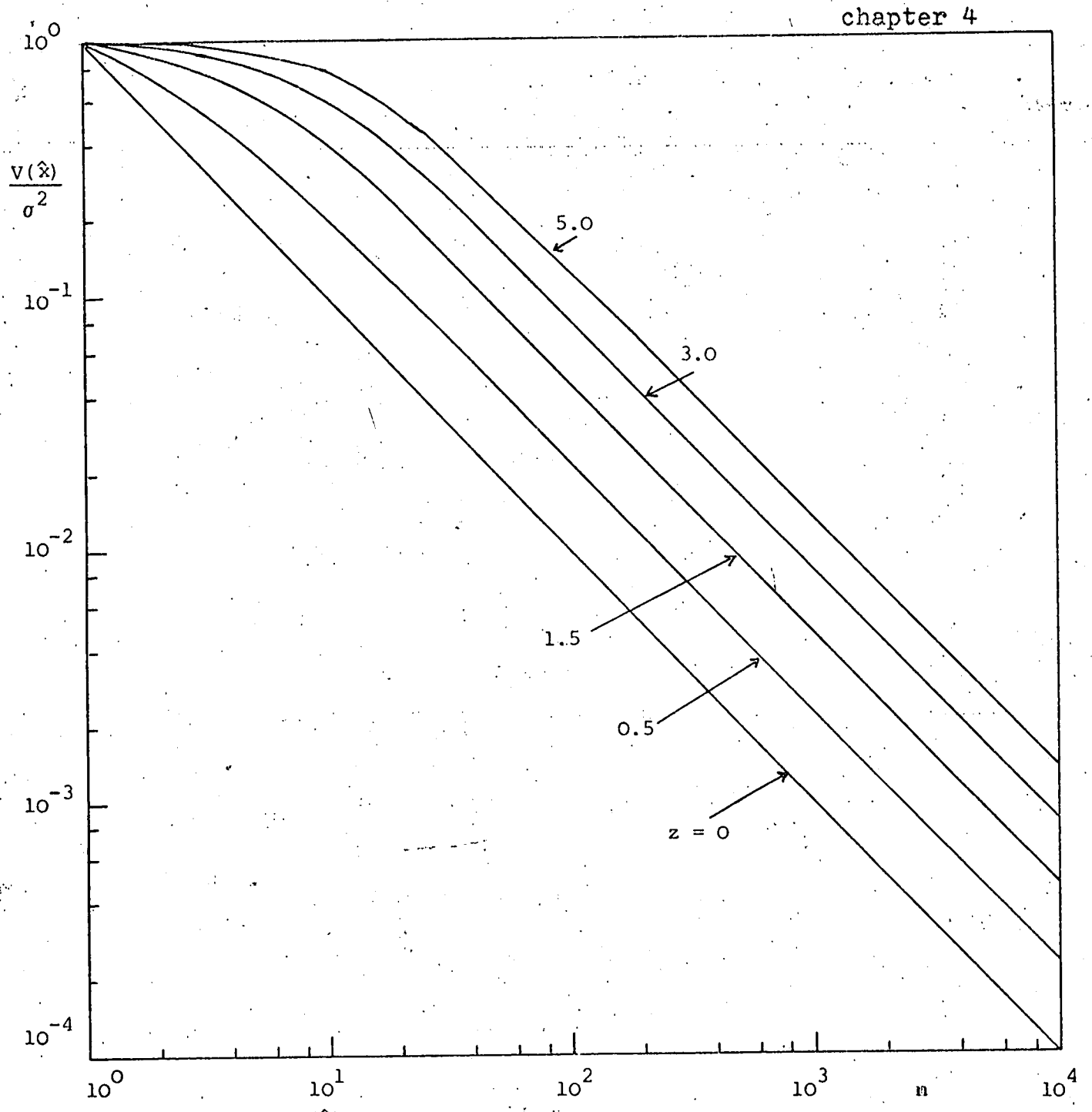

FIG(4) $\frac{V(\hat{x})}{\sigma^2}$ versus n for various values of $z = \frac{\nu}{\sqrt{2\lambda}}$

c.f. $= \sigma^2 \exp(-\lambda\tau^2)$

7.1 Variance of the Mean Estimator

By comparing equation (11) with equation (7) we can see that $a^n \equiv z^n \exp(z^2/4) D_{-n}(z)$. Using this similarity we can get the variance of the mean estimate by using equation (20).

$$V(\hat{x}) = \frac{1}{n^2}\left[n\sigma^2 + 2\sigma^2 \sum_{i>j}\sum z^{i-j} \exp(z^2/4) D_{-(i-j)}(z)\right]$$
$$= \frac{\sigma^2}{n^2}\left[n + 2 \exp(z^2/4) \sum_r (n-r)\, z^r D_{-r}(z)\right] \qquad (46)$$

The summation in equation (46) is convergent. The value of $z^r D_{-r}(z)$ can be computed using the following recurrence relation:

$$z^{r+2} D_{-(r+2)}(z) = \frac{z^2}{r+1}\left[z^r D_{-r}(z) - z^{r+1} D_{-(r+1)}(z)\right] \qquad (47)$$

Care need be taken when using this recurrence formula because of the round-off errors in computation. A backward reccurence technique should be used to avoid such errors, (ABRAMOWITZ & STEGUN). For values of r beyond a certain value k (dependent on z) $z^k D_{-k}(z)$ is approximately zero. We let $z^k D_{-k}(z)$ and $z^{k+1} D_{-(k+1)}(z)$ be 1 and 0 respectively. Backward recurrence is then used until the value of $zD_{-1}(z)$ is obtained, which is then compared with the standard tabulated values. The ratio of the tabulated to the computed value for r = 1 is obtained. Multiplication of all the computed values by this ratio gives the correct value for all $r \leq k + 1$.

The curves in figure (4) are for $V(\hat{x})/\sigma^2$ versus n for various values of z. It should be noticed that the z = 0 curve corresponds to the independent samples case and is the same as that obtained for

a = 0 when considering the exponentially decaying correlation (see figure (2)).

For large n, $V(\hat{x})/\sigma^2$ decreases linearly with n. The variance of the mean estimate as n approaches infinity can be obtained analytically. Rewriting equation (46)

$$V(\hat{x}) = \frac{\sigma^2}{n^2}\left[n + 2\exp(z^2/4)\sum_r (n-r)\, z^r D_{-r}(z)\right] \tag{48}$$

Using equation (10) we get

$$\begin{aligned}\sum_r z^r D_{-r}(z) &= \exp(-z^2/4)\sum_r z\int_0^\infty \frac{(xz)^{r-1}}{(r-1)!}\exp(-zx-\frac{x^2}{2})dx \\ &= \exp(-z^2/4).z.\int_0^\infty \sum_r \frac{(xz)^{r-1}}{(r-1)!}\exp(-zx-\frac{x^2}{2})dx\end{aligned} \tag{49}$$

as n approaches infinity

$$\sum_r (xz)^{r-1}/(r-1)! \simeq e^{xz}$$

$$\therefore \quad \sum_r z^r D_{-r}(z) = z.\exp(-z^2/4).\int_0^\infty \exp(-x^2/_2)dx$$

$$= z\exp(-z^2/4).\sqrt{\pi/2} \tag{50}$$

Interchanging the order of summation and integration

$$\sum_r r\, z^r D_{-r}(z) = \exp(-z^2/_4)z.$$

$$\int_0^\infty \sum_r r\frac{(zx)^{r-1}}{(r-1)!}\exp(-zx-\frac{x^2}{2})dx$$

From GRADSHTEYN & RHYSIK we have

$$\sum_{r} \frac{r(zx)^{r-1}}{(r-1)!} \simeq zx \exp(zx) + \exp(zx) \quad (\text{as } n \to \infty) \tag{51}$$

Substituting equations (50) and (51) in equation (48) we get

$$V(\hat{x}) = \frac{\sigma^2}{n}\left[1 + z\sqrt{2\pi} + \frac{1}{n}(2z^2 + z\sqrt{2\pi})\right]$$

By neglecting the $1/n^2$ term

$$V(\hat{x}) \quad \frac{\sigma^2}{n}\left[1 + z\sqrt{2\pi}\right] \tag{52}$$

This relationship can be verified easily by using the graphs in figure (4).

7.2 Variance of the Variance Estimator

A simple extension of the results of § 5 can be applied to the Gaussian c.f. in this section. From equation (42)

$$V(\hat{v}) = \frac{2}{N^2}\left[I_1 + I_2 + I_3\right] \tag{53a}$$

where
$$I_1 = \sigma^4\left[n+2\exp(z^2/2) \sum_{r}(n-r) \ (z^r D_{-r}(z))^2\right] \tag{53b}$$

$$I_2 = \{\sum_{i} A(i)\}^2 \tag{53c}$$

$$I_3 = n \sum_{i} A^2(i) \tag{53d}$$

and
$$A(i) = \frac{\sigma^2}{n}\{1 + \exp(z^2/4)\left(\sum_{r=1}^{n-i} z^r D_{-r}(z) + \sum_{r=1}^{i-1} z^r D_{-r}(z)\right)\} \tag{53e}$$

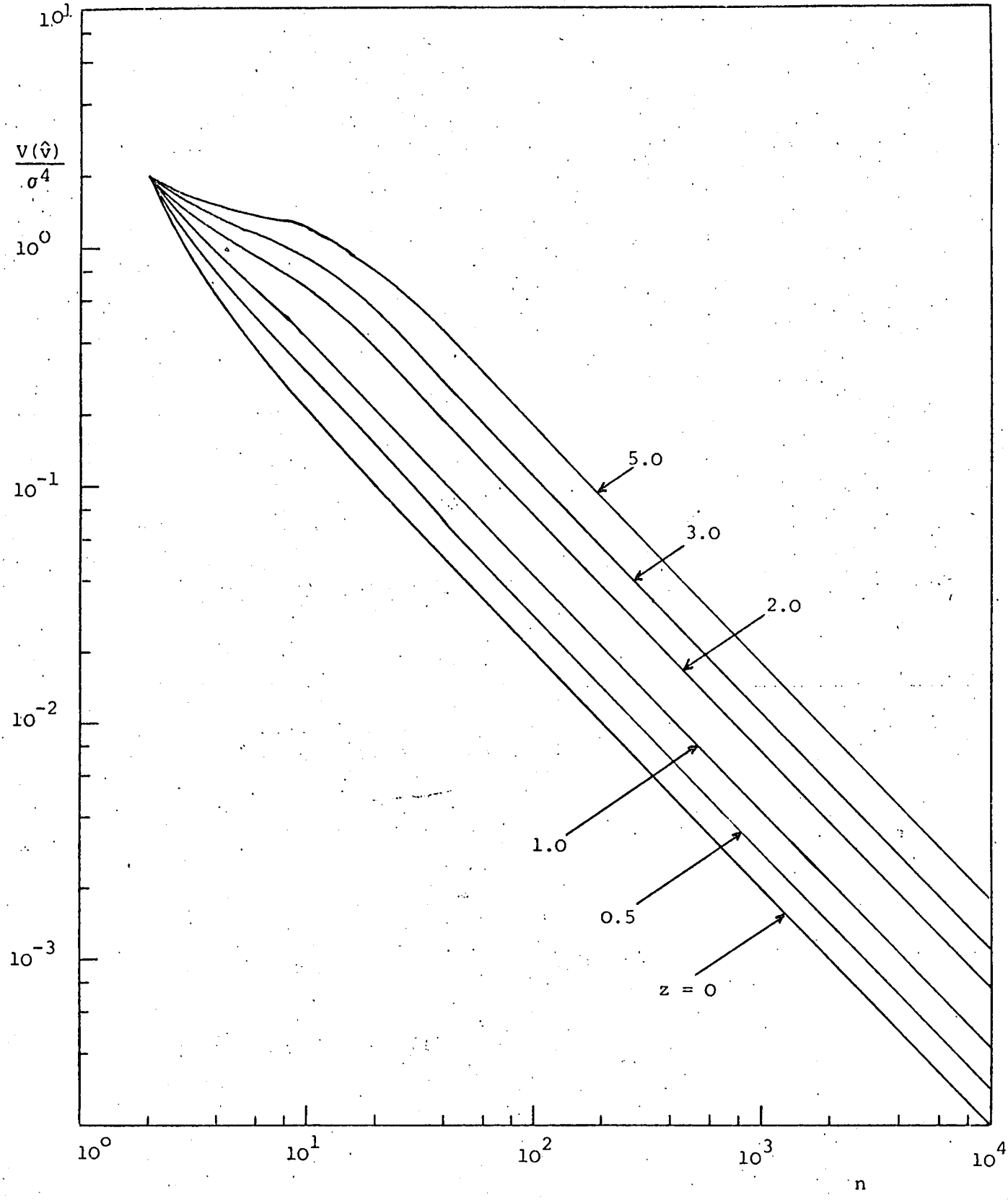

FIG (5) $\frac{V(\hat{v})}{\sigma^4}$ versus n for various values of $z = \frac{\nu}{\sqrt{2\lambda}}$

c.f. $= \sigma^2 \exp(-\lambda\tau^2)$

From equation (30)

$$N = n-1 - \frac{2}{n} \exp(z^2/4) \sum_r (n-r)\ z^r D_{-r}(z) \qquad (53f)$$

As in § 2.2 only I_1 contributes significantly to $V(\hat{v})$ for large n, and hence

$$V(\hat{v}) \simeq \frac{2\sigma^4}{(n-1)^2}\left[n + 2n \exp(z^2/2) \sum_r (z^r D_{-r}(z))^2\right] \qquad (54)$$

The factor $\sum_r (z^r D_{-r}(z))^2$ in equation (54) converges very quickly to zero when $z < 1$ hence it is justifiable to retain only two terms of the summation,

$$\therefore V(\hat{v}) \simeq \frac{2\sigma^4 n}{(n-1)^2}\left[1 + 2 \exp(\frac{z^2}{2})\{z^2 D^2_{-1}(z) + z^4 D^2_{-2}(z)\}\right] (\text{for } z<1) \qquad (55)$$

figure (5) shows graphs of $V(\hat{v})/\sigma^4$ versus n for different values of z.

§ 8. CONTINUOUS AVERAGING

The results obtainable by continuous averaging (hot wire anemometry) will be compared with those obtained by averaging a Poisson sampled signal (laser anemometry). The latter has been discussed in the previous sections. A commonly used model for the c.f. of the velocity is $\sigma^2 \exp(-\alpha|\tau|)$ and hence we shall consider this one for comparison.

The estimators of mean and variance for continuous averaging are respectively

$$\hat{x}_c = \frac{1}{T}\int_o^T x(t)dt$$

$$\hat{v}_c = \frac{1}{P}\int_o^T \left[x(t) - \frac{1}{T}\int_o^T x(t)dt\right]^2 dt$$

where x(t) is the continuous velocity record of length T. P is such that the variance estimator is unbiased.

Using a procedure similar to that given by BENDAT & PIERSOL we find the variance of these estimators for large T to be

$$V(\hat{x}_c) = \frac{2}{T}\int_o^\infty C(\tau)\, d\tau = \frac{2}{T}\int_o^\infty \sigma^2 \exp(-\alpha\tau)d\tau = \frac{2\sigma^2}{T\alpha} \qquad (56)$$

$$V(\hat{v}_c) = \frac{2T}{P^2}.2\int_o^\infty C^2(\tau)d\tau = \frac{4T}{P^2}\int_o^\infty \sigma^4 \exp(-2\alpha\tau)d\tau$$

$$= \frac{2\sigma^4 T}{P^2\alpha}$$

It can be shown that $P = T - \frac{2}{\alpha}$, hence

$$V(\hat{v}_c) = \frac{2\sigma^4}{\alpha T} \qquad (57)$$

Although, as expected, the variances of the estimators for the sampled process are higher than those for continuous averaging, it will be shown that the results for the sampled process approach those of the latter as the rate of the Poisson process, $\nu = n/T$, approaches infinity. See equations (58) and (59).

Rewriting equation (24) and using the definition of a

$$V(\hat{x}) = \frac{\sigma^2}{n}\frac{1+a}{1-a} = \frac{\sigma^2}{n}\left[\frac{\alpha/\nu+1+1}{\alpha/\nu+1-1}\right] = \frac{\sigma^2}{n}\left[\frac{2}{\alpha/\nu}\right] = \frac{2\sigma^2}{\alpha T} \qquad (58)$$

From equation (44)

$$V(\hat{v}) = \frac{2\sigma^4}{n}\frac{1+a^2}{1-a^2} = \frac{2\sigma^4}{\alpha T} \qquad (59)$$

§ 9. PHYSICAL SIGNIFICANCE of the METHOD of AVERAGING

It was shown in § 8 that if the continuous velocity record is available the mean velocity is given by $\hat{x}_c = \int_o^T x(t)dt/T$. In burst counter experiments, however, only point estimates of the velocity are available and hence a discretized form of this integral has to be considered in order to compute the mean. In evaluating the discretized version of the mean, some assumptions must be made regarding the relationship between the velocity record and the sampling process.

Since the flow is sampled as described in § 4, the simplest approximation to the sampled flow is to hold x_k constant for the period $\Delta t_k = t_{k+1} - t_k$. The estimated mean then becomes, $\hat{x} = \sum_{k=1}^{n} x_k \Delta t_k / T$. It is necessary to assume a relationship between the velocity, x_k and the time Δt_k between consecutive particles to evaluate the summation.

When the turbulence level is not very high, ($\lesssim$20%), the sampled velocity estimates $\{x_k\}$ and the times between particles $\{\Delta t_k\}$ can be assumed to be uncorrelated. In such a situation the estimate of the mean velocity can be easily shown to be $\sum_{k=1}^{n} x_k/n$. This is the arithmetic mean of the sequence $\{x_k\}$ obtained from (n) samples and has been used in the previous sections as an estimate of the mean velocity.

It has been argued by McLAUGHLIN & TIEDERMAN that using an arithmetic mean to determine the average velocity gives a biased estimate of mean velocity, higher than the true value. This situation can be explained as follows. When the instantaneous velocity of the fluid exceeds the true mean velocity **V**, say, more particles pass through the scattering volume than if the fluid velocity was a constant = V. Similarly, there are fewer particles that traverse the scattering volume when the fluid velocity is below V. The probability density of the velocity obtained will be biased towards the higher velocities because a greater proportion of particles passing through the scattering volume have higher velocities and hence contribute more to the right hand side tail of the velocity probability density function.

SMITH & MEADOWS have observed experimentally that the estimate of mean velocity obtained by the arithmetic mean is correlated with the sampling rate ν. While this corroborates the results of McLAUGHLIN & TIEDERMAN it has been shown that there is only a very low correlation between these quantities. This low

value justifies the use of the arithmetic mean as an estimate of the mean velocity in the previous sections. For high turbulence levels it may be necessary to correct for the biasing effect. It has been suggested by KREID that an unbiased estimate of the mean velocity can be evaluated using $\{n \sum_{k=1}^{n} (1/x_k)\}^{-1}$. This estimate is an approximation of the integral $\int_0^T x(t)dt/T$ if there is a positive correlation between x_k and ν (or $1/\Delta t_k$), ie, $x_k . \Delta t_k = P$, where P is a constant.

§ 10. DETERMINATION of the PROBABILITY DENSITY FUNCTION

In most burst counter systems, the probability density function (p.d.f.) of the velocity is obtained by constructing a histogram. Since the velocity is a continuous variable, the probability distribution function and the probability density function need to be smooth functions. It is therefore necessary to

i. draw a smooth line through the histogram

ii. fit a model to it or

iii. use a non-parametric method for smoothing as suggested by PARZEN

The latter two methods have had considerable success in pattern recognition research and it has been suggested that these could be useful complements or alternatives to the "raw" or manually smoothed histogram. As yet, however, the application of these techniques to burst counter data or the analysis of digitized velocity records

obtained from a hot wire anemometer has not been reported.

KASHYAP & BLAYDON have shown that if the velocity p.d.f. or distribution function can be represented as $\sum_{i=1}^{n} \alpha_i \phi_i(x)$ where $\{\phi_i(x), i=1,....,n\}$ is a set of independent functions, then the unknown parameters $\{\alpha_i, i = 1, ...,n\}$ can be obtained on-line using a stochastic recursive technique. In addition to requiring very little storage, this method facilitates the continual examination of the parameter values and once these values stabilize, the data collection can be terminated. It is noted, however, that a fair amount of computation is required at each iteration and hence this technique would not be feasible when the average data rate is much greater than 1/T, where $\bar{T}$ = time required for each iteration.

PARZEN has suggested a class of p.d.f. estimators based on n independent observations (velocity estimates) x_i, $i = 1, ..., n$,

$$f(x) = \frac{1}{nh} \sum_{i=1}^{n} K\left(\frac{x - x_i}{h}\right)$$

These estimators were shown to be consistent and asymptomatically normal subject to certain conditions on h, the parameter which determines the smoothness of f(x). The drawback in using these estimators is that all the n observations have to be stored and the evaluation of f(x) for a particular value of x requires a long computation involving all the observations. By expanding K(.) as a Taylor series, SPECHT has suggested a method which considerably

reduces the computation needed in the original method of PARZEN, however, all the observations still need to be stored. In the burst counter experiments reported by MAYO *et al* and SMITH and MEADOWS all the velocity estimates are stored so that spectral analysis can be carried out off-line, hence the storage requirement of SPECHT's method is not necessarily special. It is noted that although PARZEN's results require that the observations be independent, there is no reason why f(x) will not provide reasonable estimates of the probability density function if the observations are correlated.

It will suffice to say here that K(.) is analogous to the impulse response of a low pass electrical filter where the variable, time, is replaced by x. A detailed discussion of the form of K(.) and its parameter (h) is given in SPECHT's article and an up-to-date analysis and bibliography of this subject is presented by KRONMAL & TARTER.

§ 11. POWER SPECTRUM ESTIMATION

The analysis of continuous records is in many instances most conveniently carried out by digital means on a computer. Much effort has been devoted to the development of digital techniques for estimating spectra from equi-spaced samples, based either on the Blackman-Tukey correlation and transform method or on the periodogram F.F.T. method, (BENDAT and PIERSOL).

When a burst counter is used, estimates of the velocity are obtained randomly in time. Because of the unequally spaced data, conventional spectral analysis techniques cannot be used. The spectrum of such processes was first analysed by SHAPIRO & SILVERMAN and they showed that if a continuous process is Poisson sampled, then the spectrum of the resulting process does not suffer from aliasing. Beutler and Leneman in a series of papers have considered the spectra for a large variety of point processes (see BEUTLER for a survey of this work). MASRY has described a class of sampling schemes which lead to alias-free spectral estimates. It is only recently that the original ideas of SHAPIRO and SILVERMAN have been shown to apply in practice and on-line processors have been shown to be possible for stationary processes, (MAYO *et al*) and (GASTER and ROBERTS). In this section the theory of this type of spectral analysis and some practical details will be briefly discussed. It will be shown that a biased spectral estimate can be obtained and its variance will be given. As expected the variance is higher than that expected for the spectrum that would be obtained when the continuous record is available. Throughout the discussion the sampling times are assumed to be Poisson distributed. As mentioned in the previous section, this is a reasonable approximation.

The correlation coefficient $r(n)$ of the sampled process is defined as the average of the lagged products $x_m\, x_{m+n}$, where $m = 1,2 \ldots$, The relationship between these coefficients and the correlation function $R(\tau)$ of $x(t)$, can be obtained by the following relation:

$$r(n) = \int_0^\infty R(\tau)\ p_n(\tau)\ d\tau \tag{60}$$

where $p_n(\tau)$ has been given by equation (3) for Poisson sampling. Since $R(\tau)$ and $S(\omega)$ the spectrum of $x(t)$ are Fourier transform pairs,

$$r(n) = \int_{-\infty}^{\infty} S(\omega)\ \left(\frac{\nu}{\nu - i\omega}\right)^n d\omega \tag{61}$$

SHAPIRO & SILVERMAN have shown that the solution of this integral equation gives an alias-free estimate of the spectrum given by

$$S(\omega) = \frac{1}{\pi} \sum_{n=1}^{\infty} b(n)\psi_n(\omega) \tag{62}$$

where
$$\psi_n(\omega) = \mathrm{Re}\left\{\frac{\sqrt{2\nu}(i\omega+\nu)^{n-1}}{(i\omega-\nu)^n}\right\} \tag{63}$$

and
$$b(n) = \sqrt{\frac{2}{\nu}} \sum_{k=0}^{n-1} (-2)^k \binom{n-1}{k} r(k+1) \tag{64}$$

In practice the r(n) coefficients are estimated from an experiment of say duration T to give

$$\hat{r}(n) = \frac{1}{N} \sum_{m=1}^{N} x_m x_{m+n} \tag{65}$$

where N is a random variable equal to the number of samples in time T. It can be shown that $\hat{r}(n)$ is an unbiased estimate of r(n), ie $E\left[\hat{r}(n)\right] = r(n)$.

In practice $\hat{r}(n)$ and hence $\hat{b}(n)$ will only be computed for a finite number of n. A 'truncated' estimate is then given by

$$\hat{S}_M(\omega) = \frac{1}{\pi} \sum_{n=1}^{M} \hat{b}(n)\psi_n(\omega) \tag{66}$$

The expected value of $\hat{S}_M(\omega)$ is

$$S_M(\omega) = \frac{1}{\pi} \sum b(n)\psi_n(\omega) \tag{67}$$

where (see equations (61) and (64))

$$b(n) = \int_{-\infty}^{\infty} S(\omega)\psi_n(\omega)d\omega \tag{68}$$

From these results it can be shown that $S_M(\omega)$ is a weighted integral of $S(\omega)$:

$$S_M(\omega) = \int_{-\infty}^{\infty} S(\omega')\alpha_M(\omega,\omega')d\omega' \tag{69}$$

where the kernel

$$\alpha_M(\omega,\omega') = \frac{1}{\pi} \sum_{n=1}^{M} \psi_n(\omega)\psi_n(\omega') \tag{70}$$

GASTER & ROBERTS have shown that this kernel (window) has a pronounced tendency to broaden the spectrum as ω/ν increases. They have also demonstrated that an extremely large amount of data is necessary for obtaining high resolution and low variance spectral estimates and hence deriving them from the coefficients $\hat{r}(n)$ is not practicable.

All practical systems for the analysis of burst counter data are based on digital techniques. It is therefore inevitable that slotting (quantizing) will have to be used. The velocity estimates as well as the sampling time have to be quantized. Only the quantization of the sampling times will be discussed. One approach is to approximate the mean autocorrelation function by a Dirac comb of period $\Delta\tau$. The values of the spikes of this comb are taken as being equal to the average of the values of the neighbouring randomly spaced estimates. This is effectively the same as saying that the time axis has been quantized. It is necessary that the quantizing interval $\Delta\tau$ satisfies two conditions: it is much less than the mean sample period $(1/\nu)$ and that it also satisfies the Nyquist criterion in the usual manner with $(1/\Delta\tau)$ being the equivalent rate of uniform sampling. The spectrum can be obtained conveniently using F.F.T. followed by smoothing.

The result of an error analysis of the spectral estimator is given by MAYO *et al.* Assuming that x(t) is a stationary broad band (spectrum S(f)) Gaussian process the expression for the normalised r.m.s. variability error, ε, is given by

$$\varepsilon = \left[1/n. \sum_{i=m}^{n+m-1} (\hat{S}(i\Delta f) - S(i\Delta f))^2\right]^{\frac{1}{2}}/S(0) \qquad (71)$$

$$\simeq (2/3)^{\frac{1}{2}}\ 2B\left(\frac{M\Delta\tau}{N\lambda}\right)^{\frac{1}{2}} \qquad (72)$$

where m = first point in the pass band

n = number of points in the pass band over which the summation is taken

B = equivalent bandwidth of $S(f)$

N = number of sampled points

λ = rate of the sampling process

M = maximum lag of the correlation function

Equation (72) was derived assuming that $\lambda/2B << 1$, $N >> M\lambda\Delta\tau$ and that the Bartlett window is used for smoothing. It has been verified by MAYO *et al* by using a simulation. JONES has also obtained error estimates of similar spectral ordinates but his results differ from those of MAYO *et al*. For a detailed discussion and derivation of practicable estimates of randomly sampled processes, the reader is referred to the original papers.

APPENDIX A

EXPERIMENTS on SINUSOIDAL FLUCTUATIONS

In order to test the validity of the theory presented in § 9 of Chap.2 and the practical utility of the results, two sets of experiments were performed. The first involved simulating the velocity fluctuations occurring in the flow with a mechanical system. This consisted of a perspex disc which was rotated in a vertical plane whilst being oscillated horizontally. The usefulness of the mechanical simulator lies in the fact that variable parameters are known precisely and can be altered at will. The second set of experiments involved measurements in the wake of a circular cylinder set in a steady airstream. In this case the sinusoidal velocity fluctuations were produced by the shed eddies. In both cases the crossbeam optical configuration was used.

By observing both the frequency of the cosinusoidal waveform and the positions of the zeros of the damping Bessel function, both the mean velocity and the amplitude of the velocity fluctuation can readily be determined. Note that the first zero of the Bessel function J_o occurs when its argument $\frac{2\pi a}{s}\tau = 2.4$, (c.f. eq.32 of Chapter 2). Hence if there are n cycles between the zero lag and the first zero of the Bessel function, the ratio (a/u) of peak deviation to mean velocity is $2.4/(2\pi n)$. The period of the cosine term gives the Doppler frequency and u can be determined since the velocity to frequency conversion constant, 1/s, is known from the optical geometry.

The measurement of the streamwise velocity using a hot-wire anemometer in the flow experiment gave a comparison with the correlator results.

i. Mechanical Simulation

The mechanical simulator was an 18cm. diameter perspex disc rotated inthe vertical plane by a synchronous motor at approximately 1 Hz. Using a 1 mW He-Ne laser and a DISA beam splitter, a fringe pattern was formed at a short distance from the periphery of the disc, the fringes being aligned in the horizontal transmission plane at the same level as the centre of the disc. The beam separation at the transmission lens was 5cm. The focal length of the transmission lens was 30cm. . The disc was painted matt black in order to reduce the back scattered light to a level low enough for photon counting. The back scattered light was imaged through a lens onto a photomultiplier and discriminator unit adjusted for single photon response, the resulting pulse train being processed with a digital correlator (Precision Devices). The instantaneous measured velocity with this configuration is governed by the distance of the fringe pattern from the centre of the disc since the rotation is maintained at a constant speed. A fluctuating velocity can therefore be achieved by moving the centre of the disc relative to the optical system. The required simple harmonic movement was achieved by moving the complete disc and synchronous motor using a variable speed motor and a crank mechanism. The frequency of oscillation was set at approximately 1 Hz, this value being chosen as very small in comparison with the disc frequency to avoid any non-linear interactions between the two motions. By setting a range of amplitudes for the disc oscillation, photon

correlation records were obtained from different a/u ratios. Good agreement was found between the results obtained from the correlograms and direct measurement. For $a/\bar{u} > 0.2$ the correlograms showed some distortion. This is to be expected since eq.(32) of Chapter 2 holds for $u >> a$.

ii. Wind Tunnel Experiment

In the wake of a circular cylinder in the Reynolds Number range 40 to 150 (say) is a regular street of shed vortices. Measurements of the streamwise component of velocity in this type of wake show that the mean flow is perturbed by the passage of each vortex and it is found that in the periphery of the wake the perturbation is approximately sinusoidal. Measurements of values of mean and fluctuating velocities were made in the wake of a circular cylinder using both a photon-correlation anemometer and a hot-wire anemometer.

The experiment was conducted in the 1 m x 1 m working section of a low turbulence wind-tunnel whose flow was steady at the very low speeds required by the experiment. Previous work in a small open-circuit tunnel had proved unsuccessful because of flow instabilities. The cylinder was a 0.47 cm diameter brass rod which was moved vertically by a traversing arrangement attached to a vertical aerofoil in a working section. The cylinder position was measured to 0.5 mm on a scale on the wind-tunnel window.

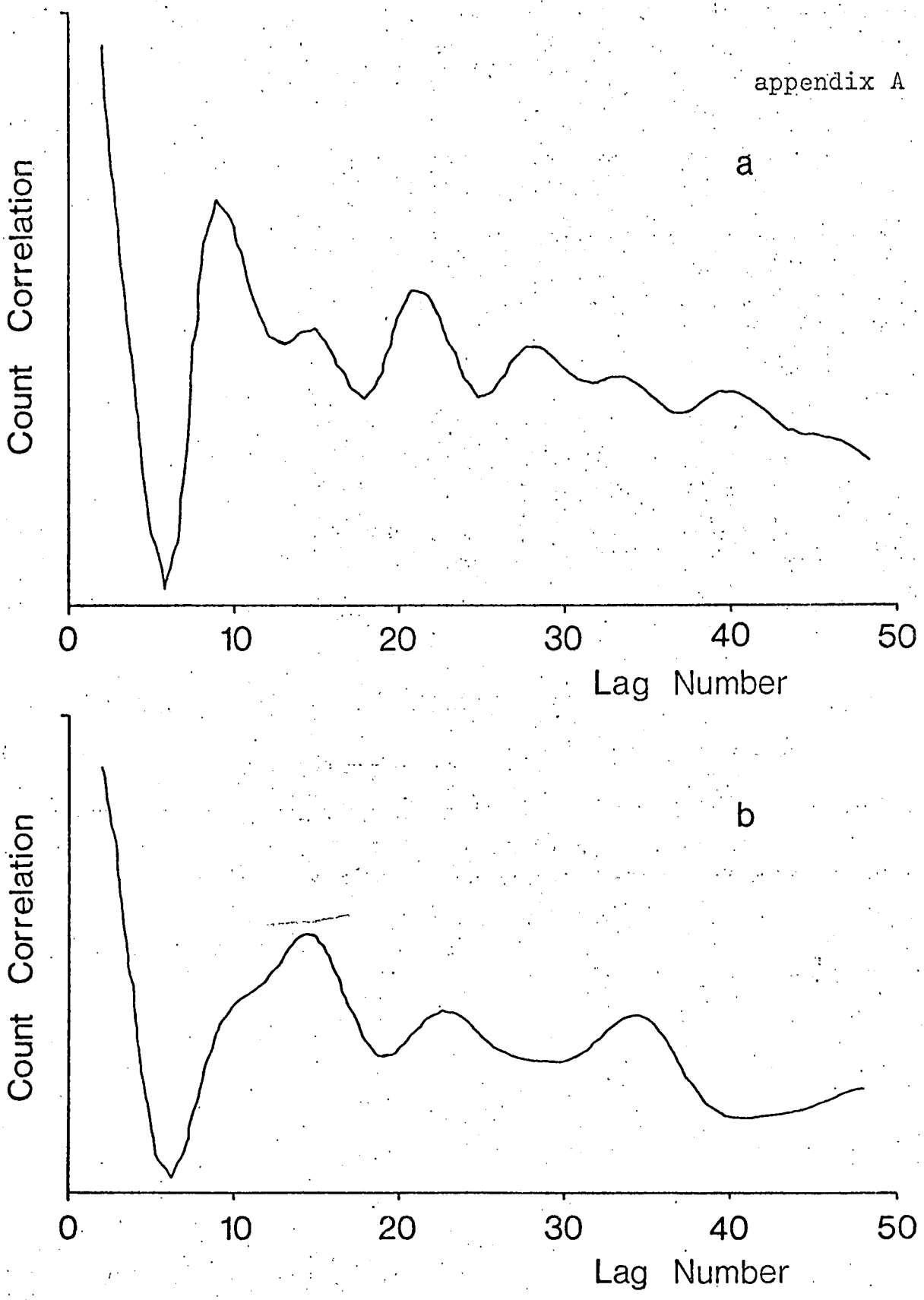

Fig.(1) Correlogram for a flow where the ratio of the fluctuating velocity to the local mean velocity (a) small, (b) large.

The hot-wire probe was held firmly 2 cm behind the leading edge of the cylinder. A 15 mW laser was used to form a probe volume at the same height as the hot-wire but approximately 1 mm upstream of it.

The windspeed was selected so that the vortex street detected by the hot-wire was stable. The free stream velocity was measured with the photon correlator and found to be 0.39 m sec^{-1}, giving a Reynolds number based on cylinder diameter (0.47 cm) of 124. The frequency of shedding measured on a spectrum analyser was found to be 13.3 Hz giving a Strouhal number of 0.157.

The wake was traversed by moving the cylinder while keeping the hot-wire and interference volume stationary. Correlation records were taken at twenty-two stations at 1 mm intervals distributed symmetrically through the wake. Hot-wire measurements of the mean velocity and the rms of the streamwise fluctuating velocity were made at each station. Measurements of positive and negative peak fluctuating velocities were made at a number of stations in the wake.

Calculation of turbulence levels from the correlograms was only possible at the outer part of the vortex street where the ratio of the fluctuating velocity to the local mean velocity was small, ie less than say 15% (fig.1(a)). For larger levels difficulties are seen in identifying $J_o = 0$ (fig. 1(b)) when the beating becomes so rapid that the sinusoid is not easily identified.

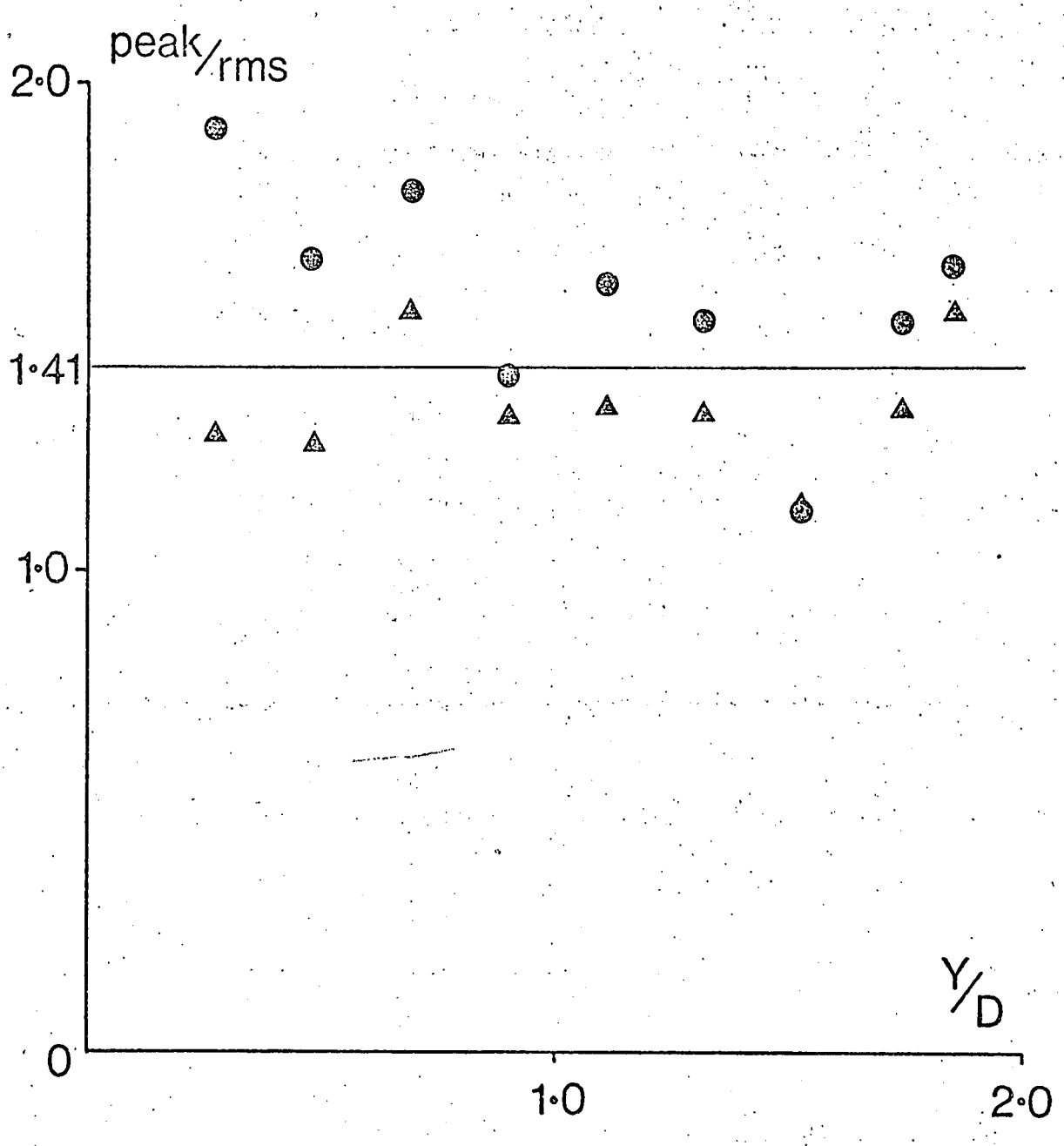

Fig.(2) Graph of crest factor against non-dimensional distance, where Y is the distance from the centre line of the wake and D is the diameter of the cylinder

● Positive peak

▲ Negative peak

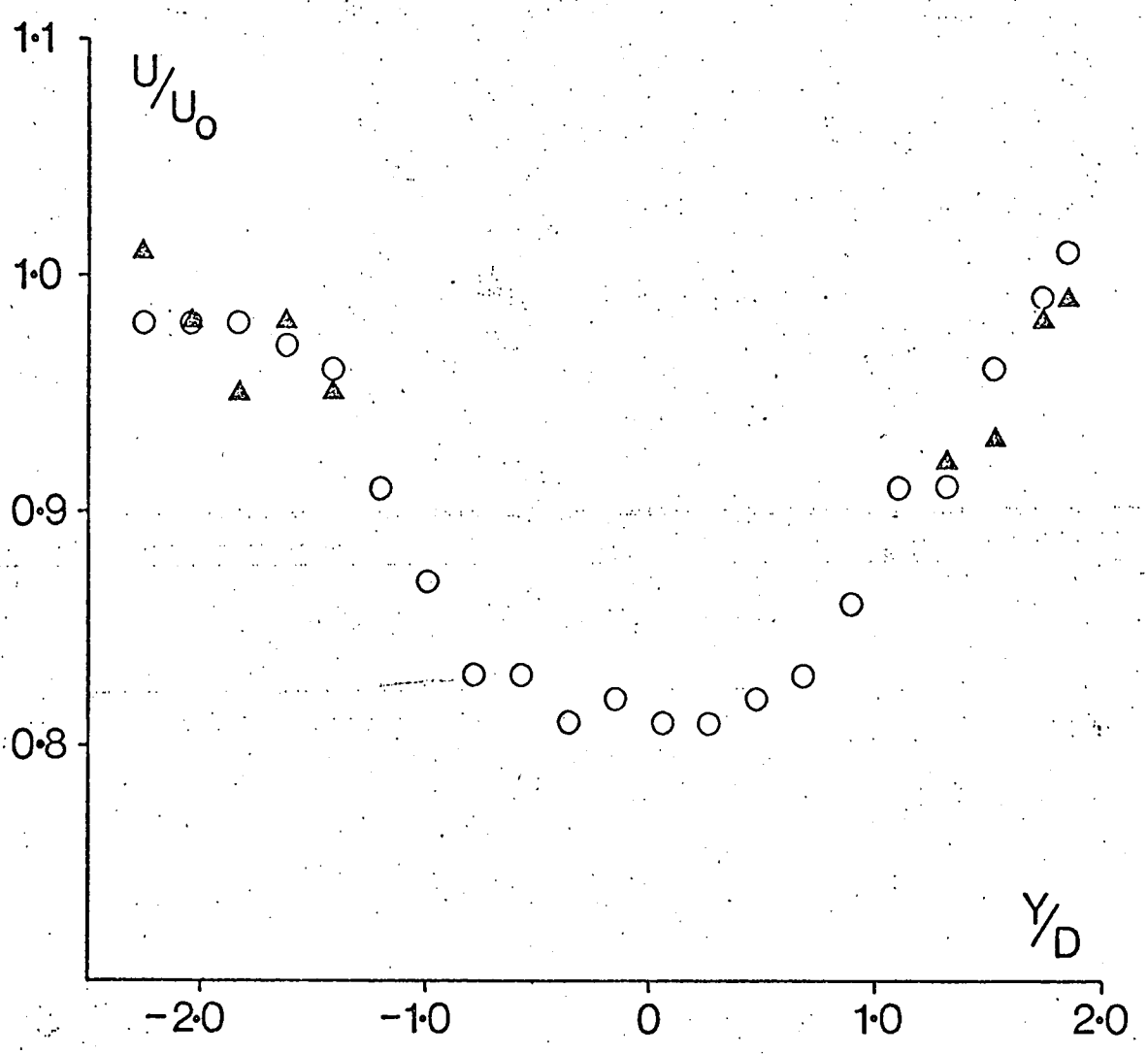

Fig.(3) The mean velocity in the wake of the cylinder. U is the local velocity and U_o the free-stream velocity.

○ Hot-wire results

△ Laser Doppler results

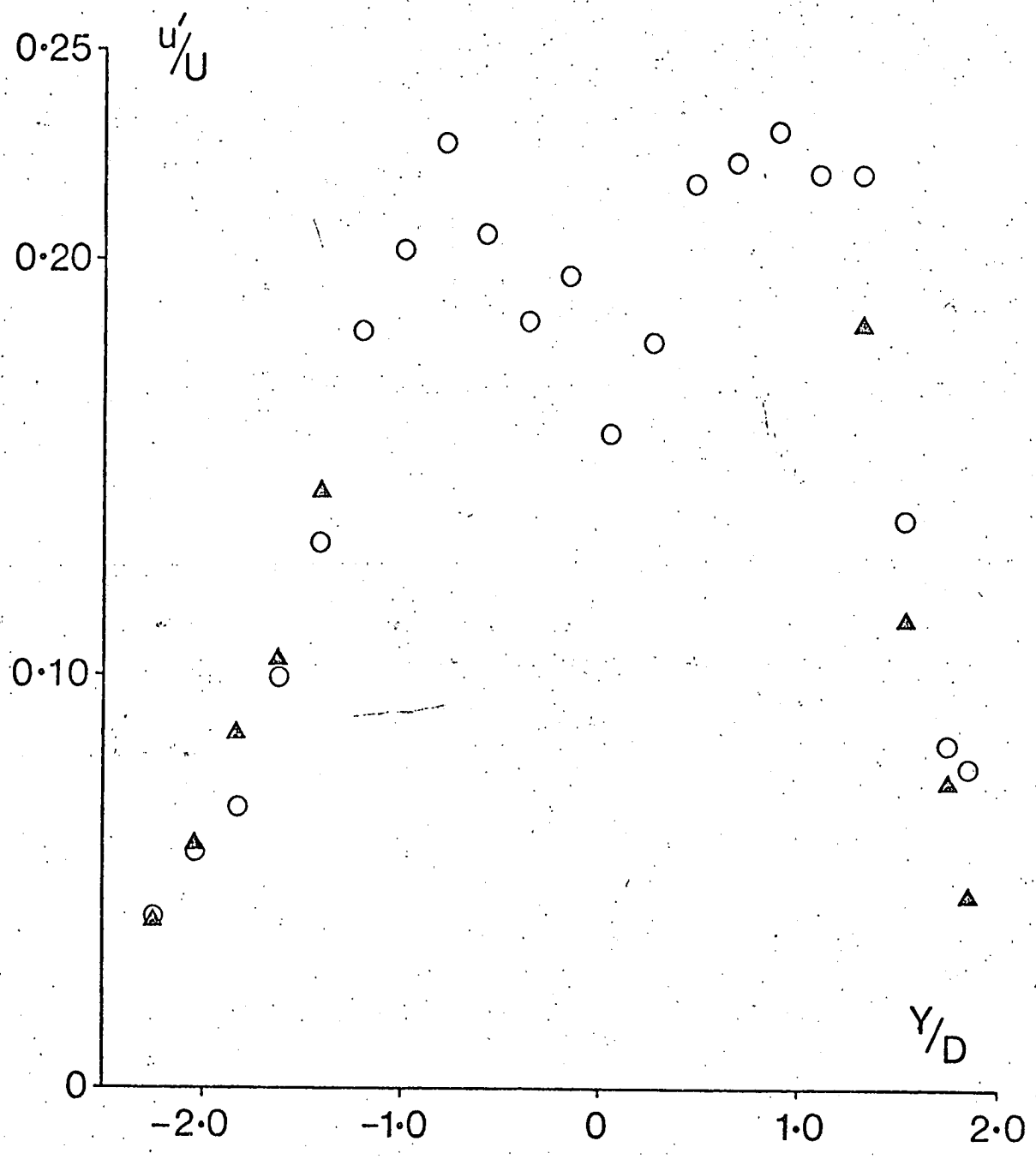

Fig.(4) The fluctuating velocity in the wake of the cylinder. u′ is the rms of the fluctuating velocity.

o Hot-wire results

△ Laser Doppler results

The crest factor (peak fluctuating velocity/rms fluctuating velocity) for both positive and negative half-cycles is plotted in fig. 2 for one side of the symmetrical wake in the range defined above. The crest factor for a sine wave (1.414) is also shown on this diagram. The wave is seen to be closely sinusoidal at the wake periphery but becomes distorted as the core is approached. This is due to the growing contribution from the second harmonic. Fig. 3 shows a comparison of the mean velocities measured by the hot-wire and from the correlograms, while fig. 4 shows fluctuating levels measured by the two methods. It is seen that there is close agreement in both cases. The most significant cause of discrepancy between the two measurements appeared to arise through misalignment of the measuring positions. Alignment was difficult because in a plane perpendicular to the cylinder axis the hot-wire had an effective diameter of 5 μm whilst the diffraction limited laser spot diameter was approximately 7×10^{-4} m. It is worth noting, however, that in the direction of the cylinder axis the dimensions of the measuring regions for the two systems were comparable.

APPENDIX B

Volume 17, number 2 OPTICS COMMUNICATIONS May 1976

ERROR ANALYSIS OF RANDOMLY CLIPPED PHOTON COUNT CORRELATION ESTIMATOR

Q. ISA DAUDPOTA
Dept. of Physics, Edinburgh University, Scotland, UK

Received 23 January 1976, revised version received 1 March 1976

The use of uniform random clipping makes the one-bit correlation function independent of the statistics of the incident field. It has therefore been used in optical spectroscopy to measure the intensity spectrum of non-gaussian fields. This note shows that for a correctly chosen range of clipping, the difference in the error of the estimator and the error expected in a full (multi-bit) correlator decreases inversely as the number of samples. The analysis also applies to one-bit scaling and other methods of uniform random clipping.

The single clipped photon correlation technique has been applied in many scientific spheres to obtain the intensity autocorrelation function of optical fields. This method is attractive because a high speed of operation can be achieved with simple digital circuits. For some fields the analytic relations that exist between the one-bit correlation function and the true correlation function of intensity are quite complicated [1]. In the case of gaussian fields the relation is very simple and the single clipped photon correlation has been successfully used to investigate scattered fields where the gaussian assumption is valid [2].

It is now well known that in certain experimental situations the observed fields deviate significantly from the gaussian. Among the cases in which this happens are light scattered by particles carried by turbulent fluids [3] and scattering from a small number of particles undergoing motion of some kind [4]. For such experiments, unlike those with gaussian fields, the self-beat (homodyne) spectrum provides additional information to the heterodyne measurement [5].

The field statistics are usually not known a priori and many methods have been proposed for making the count correlation function independent of them. These methods have been described and compared in [6]. Apart from full digital correlation, the other methods basically rely on clipping each sample at a randomly selected level. An alternative method has been analysed [7] in which a uniformly distributed signal is added before double clipping at a fixed level is carried out. This method can be easily modified to operate in the single clipped mode, in which case it becomes equivalent to uniform random clipping which will be considered below.

Scaling and uniform random clipping are equivalent when the scaling factor and the range of clipping levels are identical and greater than the expected maximum number of photon counts per sample time. This condition is always necessary for both methods to the give a correct estimate of the intensity correlation function [8].

The variance of the correlation function obtained using uniform random clipping will now be compared with the error expected with full correlation. The estimate of the full count correlation function is

$$r_f(\tau, N) = N^{-1} \sum_{t=1}^{N} n_t n_{t+\tau} , \qquad (1)$$

where n_t is the number of counts in sample time T centred at time t. Similarly the uniform randomly clipped correlation function estimate is

$$r_u(\tau, N) = N^{-1} \sum_{t=1}^{N} [n_t]^c \, n_{t+\tau} , \qquad (2)$$

where

$$[n_t]^c = 1, \quad \text{if } n > c,$$

$$= 0, \quad \text{if } n_t \leqslant c,$$

c is uniformly distributed with probability density

$$f(c) = 1/S, \quad 0 \leqslant c \leqslant S-1,$$

$$= 0, \quad \text{otherwise}. \tag{3}$$

The mean square error criterion is most conveniently applied and very useful for a comparison of different measuring methods. For the complete correlation function we have

$$\sigma_f^2(\tau, N) = \mathrm{E}[r_f(\tau, N) - R(\tau)]^2 \tag{4}$$

$$= \mathrm{E}[r_f^2(\tau, N)] - [R(\tau)]^2, \tag{5}$$

where $R(\tau) = \mathrm{E}[r_f(\tau, N)]$ and $\mathrm{E}[\cdot]$ denotes expectation. The error in the clipped case is

$$\sigma_u^2(\tau, N) = S^2 \mathrm{E}[r_u^2(\tau, N)] - [R(\tau)]^2, \tag{6}$$

since

$$\mathrm{E}[r_u(\tau, N)] = (1/S)R(\tau). \tag{7}$$

Eq. (7) can be easily shown by taking expectations on both sides of eq. (2) and noting that $\mathrm{E}[[n_t]^c] = \mathrm{E}[n]/S$, where $E[n]$ is the average number of counts per sample time. Now

$$\mathrm{E}[r_u^2(\tau, N)] = (1/N^2)$$

$$\times \sum_{p=1}^{N} \sum_{q=1}^{N} \mathrm{E}[[n_p]^{c_1} n_{p+\tau} [n_q]^{c_2} n_{q+\tau}], \tag{8}$$

which on simplifying gives

$$\mathrm{E}[r_u^2(\tau, N) = (1/NS)\, \mathrm{E}[n_p n_{p+\tau}^2]$$

$$+ (1/N^2) \sum_{p \neq q}^{N} \sum^{N} (1/S^2) \mathrm{E}[n_p n_{p+\tau} n_q n_{q+\tau}]. \tag{9}$$

In equivalent notation the mean square value of the full correlation function is

$$\mathrm{E}[r_f^2(\tau, N)] = (1/N)\, \mathrm{E}[n_p^2 n_{p+\tau}^2]$$

$$+ (1/N^2) \sum_{p \neq q}^{N} \sum^{N} \mathrm{E}[n_p n_{p+\tau} n_q n_{q+\tau}]. \tag{10}$$

Combining eqs. (5), (6), (9) and (10) gives

$$\sigma_u^2(\tau, N) = \sigma_f^2(\tau, N)$$

$$+ (1/N)(S\, \mathrm{E}[n_p n_{p+\tau}^2] - \mathrm{E}[n_p^2 n_{p+\tau}^2]). \tag{11}$$

Written in this form, the mean square error is seen to be equal to the error expected with full correlation in addition to a term inversely proportional to the number of samples N. Since the value of n cannot exceed S the upper bound on the error is

$$\sigma_u^2(\tau, N)|_{\max} = \sigma_f^2(\tau, N) + S^4/N. \tag{12}$$

By applying an argument similar to that used by Haus [9] it may be assumed that (n) is a Poisson variable when the S/N ratio is low, i.e. the photons detected by the photomultiplier are mainly due to background laser light. This is a familiar experimental situation and leads to a tighter bound than that obtained in eq. (12):

$$\sigma_u^2(\tau, N) = \sigma_f^2(\tau, N) + (1/N)\, \{\mathrm{E}[n] + (\mathrm{E}[n])^2\}$$

$$\times \{S\, \mathrm{E}[n] - \mathrm{E}[n] - (\mathrm{E}[n])^2\},$$

$$(\text{Poisson } n \text{ and } \tau \neq 0). \tag{13}$$

These formulae will be useful in determining the experimental time needed to achieve a desirable accuracy. If the precision required is such that it cannot be obtained with a reasonable value of N (proportional to experimental time), it would then be necessary to use full correlation.

References

[1] C. Bendjaballah, J. Phys. A.: Math. Nucl. Gen. 6 (1973) 837–842.
[2] H.Z. Cummins and E.R. Pike, (eds.), Photon Correlation and Light Beating Spectroscopy (Plenum Press, N.Y., 1974).
[3] B. Crosignani et al., Statistical Properties of Scattered Light (Academic Press, N.Y., 1975).
[4] D.W. Scheafer and B. Berne, Phys. Rev. Lett. 28 (1972) 475–478.
[5] H.Z. Cummins and H.L. Swinney, in: Progress in Optics, ed. E. Wolf, vol. 8 (North-Holland, Amsterdam, 1970).
[6] C.J. Oliver, in ref. [2].
[7] H. Berndt, IEEE Trans. Inf. Theory 14 (1968) 796–801.
[8] E. Jakeman et al. J. Phys. A.: Gen. Phys. 5 (1972) L93–6.
[9] H.A. Haus, in: Quantum Optics, Proc. E. Fermi School of Phys., Varenna, ed. R.J. Glauber (Academic Press, 1969).

REFERENCES

The numbers at the end of each article indicate the pages on which it is referred to.

ABBISS,J.B. et al.,1972,Laser anemometry in an unseeded supersonic wind tunnel by means of photon correlation spectroscopy of back-scattered light,J. Phys. D. : Appl. Phys.,5,L100-2,2.1 .

ABBISS,J.B.,T.W.CHUBB and E.R.PIKE,1974,Laser Doppler anemometry,Opt. Laser Tech.,6,249-61,2.18,2.19,2.23,2.27.

ABRAMOWITZ,M. and I.A.Stegun,1965,Handbook of mathematical functions,Dover Publ. Inc.,N.Y.,4.16.

ADRIAN,R.J. and R.J.GOLDSTEIN,1971,Analysis of a laser Doppler anemometer,J. Phys. E: Sci. Inst.,4,505-11,2.1,2.9.

AVIDOR,J.M.,1974,Novel instantaneous laser Doppler velocimeter,Appl. Opt.,13,280-5,2.5.

BECK,M.S.,K.T.LEE and N.G.STANLEY-WOOD,1973,A new method for evaluating the size of solid particles flowing in a turbulent fluid,Powder Tech.,8,85-90,2.30.

BENDAT,J.S. and A.G.PIERSOL,1971,Random Data: Analysis and measurement procedures,Wiley-Interscience,N.Y.,4.20,4.25.

BERGLAND,A.G.,1969,Fast Fourier Transform hardware implementations-an overview,IEEE Trans. Audio Electroacoust.,AU-17, 104-8,2.2.

BEUTLER,F.J.,1970,Alias free randomly timed sampling of stochastic processes,IEEE Trans. Info. Th.,IT 16,147-52,4.26.

BEUTLER,F.J. and O.A.Z.LENEMAN,1971,On the statistics of random pulse processes,Info. Control,18,326-41,2.3,2.15.

BEVINGTON,P.R.,1969,Data reduction and error analysis for the physical sciences,McGraw Hill,N.Y.,3.12.

BIRCH,A.D. et al.,1973,The application of photon correlation spectroscopy to the measurement of turbulent flows, J. Phys. D: Appl. Phys.,6,L71-3,3.6.

BIRCH,A.D.,D.R.BROWN and J.R.THOMAS,1975,Photon correlation spectroscopy and its application to the measurement of turbulence parameters in fluid flows,J. Phys. D:Appl. Phys., 8,438-47,3.11.

BOURKE,P.J. et al.,1970,A study of the spatial structure of turbulent flow by intensity-fluctuation spectroscopy, J. Phys. A:Gen. Phys.,3,216-28,2.1.

BRAYTON,D.B.,H.T.KALB and F.L.CROSSWY,1973,Two component dual-scatter LDV with frequency burst signal read-out, Appl. Opt.,12,1145-56,4.3.

CHU,B.,1974,Laser light scattering,Academic Press,N.Y.,2.11.

COX,D.R. and H.D.MILLER,1965,The theory of stochastic processes,Methuen,London,2.20.

CROSIGNANI,B.,P.DIPORTO and M.BERTOLOTTI,1975,Statistical properties of scattered light,Academic Press,N.Y.,2.23,2.24.

DONOHUE,G.L.,D.K.MCLAUGHLIN and W.G.TIEDERMAN,1972, Turbulence measurements with a laser anemometer measuring individual realizations,Phys. Fluids,15,1920-6,4.4.

DRAIN,L.E.,1972,Coherent and noncoherent methods in Doppler optical beat velocity measurement,J. Phys. D: Appl. Phys., 5,481-95,2.7,2.9.

DUBROFF,R.E.,1975,The effective autocorrelation function of maximum entropy spectra,Proc. IEEE,64 ,1622-23,3.18.

DURRANI,T.S. and C.GREATED,1974,Statistical analysis of velocity measuring systems employing the photon correlation technique,IEEE Trans. Aerosp. Electron. Syst.,AES-10,17-24, 2.20,2.23,2.24,2.26,2.27,2.31.

DURRANI,T.S. and C.GREATED,1975,Spectral analysis and cross-correlation technique for photon counting measurements on fluid flows,Appl. Opt.,14,778-86,2.31,3.18.

EDWARDS,R.V. et al.,1971,Spectral analysis of signal from the laser Doppler flowmeter: time independent systems, J. Appl. Phys.,42,837-50,2.1.

EDWARDS,R.V.,J.C.ANGUS and J.W.DUNNING Jr.,1973,Spectral analysis of signal from laser Doppler velocimeter: turbulent flows,J. Appl. Phys.,44,1694-8,2.1.

FARMER,W.M.,1972,Measurement of particle size, number density and velocity using a laser interferometer,Appl. Opt.,11, 2603-12,2.21.

FOORD,R. et al.,1974,A solid-state electro-optic phase modulator for laser Doppler anemometery,J. Phys. D:Appl. Phys.,7,L36-9,2.26.

FORRESTER,A.T.,R.A.GUDMUNDSEN and P.O.JOHNSON,1955, Photoelectric mixing of incoherent light,Phys. Rev.,99, 1691-1700,2.5,also see Forrester's article : Photoelectric mixing as a spectroscopic tool,J. Opt. Soc. Am.,1961,51,253-9.

GASTER,M. and J.B.ROBERTS,1973,Spectral analysis of randomly sampled signals,Nat. Physical Lab.,Teddington,Tech. Rept., 4.26,4.28. Published in J. Inst. Maths. Appl.,1975,15,p.195.

GRADSHTEYN,I.S. and I.M.RHYSIK,1966,Table of integral,series and products,Academic Press,N.Y.,4.8,4.10,4.17.

GRANT,I.,F.H.BARNES and C.GREATED,1975,Velocity measurements using the photon correlation technique in separated boundary layer,Phys. Fluids,18,504-7,2.27.

HALD,A.,1952,Statistical theory with engineering applications, Wiley,N.Y.,4.14.

HANSON,S.,1973,Broadening of the measured frequency spectrum in a differential laser anemometer due to interference plane gradients,J. Phys. D: Appl. Phys.,6,164-71,2.13.

HAYKIN,S. and C.THORSTEINSON,1974,Decision-directed delay-lock loop using fast Fourier transform crosscorrelation, Proc. IEE,121,245-8,2.30.

HIMMELBLAU,D.M.,1972,Applied nonlinear programming,McGraw Hill,N.Y.,3.11.

JAKEMAN,E.,1970,Theory of optical spectroscopy by digital autocorrelation of photon-counting fluctuations,J. Phys. A: Gen. Phys.,3,201-15,2.1.

JAKEMAN,E.,1972,The effect of heterodyne detection on the statistical accuracy of optical linewidth measurements, J. Phys. A: Gen. Phys.,5,L49-52,3.3.

JOHNSON,N. and S.KOTZ,1970,Continuous univariate distributions-1,Houghton Mifflin,Boston,2.31.

JONES,R.H.,1971,Spectrum estimation with missing observations, Ann. Inst. Statis. Math.,23,387-98,4.30.

KASHYAP,R. and C.BLAYDON,1968,Estimation of probability density and distribution functions,IEEE Trans. Info. Th., IT 14,549-56,4.24.

KLEIN,M.V.,1970,Optics,Wiley,N.Y.,2.11.

KREID,D.K.,1974,Error estimates for laser Doppler velocimeter in non-uniform flow,Appl. Opt.,13,1872-81,4.23.

KRONMAL,R. and M.TARTER,1974,The use of density estimates based on orthogonal expansions,in Exploring Data Analysis, ed. W. Dixon and W. Nicholson,U. Calif. Press,Berkeley,4.25.

LACOSS,R.T.,1971,Data adaptive spectral analysis methods, Geophysics,36,661-75,3.15.

LADING,L.,1973a,Analysis of signal-to-noise ratio of the laser Doppler velocimeter,Opto-electronics,5,175-87,2.21.

LADING,L.,1973b,Analysis of laser correlation anemometer, presented at Symp. on turbulence in liquids,Univ.Missouri, Rolla,2.31.

MAKHOUL,J.,1975,Linear prediction: a tutorial review, Proc. IEEE,63,561-80,3.16.

MARKEL,J.D. and A.H.GRAY Jr.,1973,On autocorrelation equations as applied to speech analysis,IEEE Trans. Audio Electro-acoustics,AU21,69-79,3.16.

MASRY,E.,1971,Random sampling and reconstruction of spectra, Info. Control,19,275-88,4.26.

MAYO Jr.,W.T.,M.T.SHAY and S.RITER,1974,Digital estimation of turbulence power spectra from burst counter LDV data, 16-26,in Proc. second int. workshop on laser velocimetry, vol.1,Purdue Univ.,4.25,4.26,4.29,4.30.

MENEELLY,C.T.,C.Y.SHE and D.F.EDWARDS,1972,Measurement of flow and turbulence distribution of free jet by laser photon spectroscopy,Opt. Commun.,6,380-2,2.1.

MCLAUGHLIN,D.K. and W.G.TIEDERMAN,1973,Biasing correction for individual realization laser anemometer in turbulent flows,Phys. Fluids,16,2082-88,2.25,4.22.

PAPOULIS,A.,1965,Probability,random variables and stochastic processes,McGraw Hill,N.Y.,2.22,2.26.

PARZEN,E.,1962,On estimation of a probability density function and mode,Ann. Math. Statist.,36,1065-76,4.23,4.24,4.25.

PENNER,S.S.,W.DAVIDOR and F.BIEN,1970,Determination of interference patterns from laser produced Schlieren interferometry,Am. J. Phys.,38,1413-15,2.7.

PIKE,E.R.,1969,Photon statistics,Riv. Del. Nuov. Cim.,1, Numero Speciale,277-314,2.14.

PISARENKO,V.F.,1973,The retrieval of harmonics from a covariance function,Geophys. J. R. Astro. Soc.,33,347-66,3.16.

ROY,L.K. and M.T.WASAN,1968,The first passage time distribution of Brownian motion with positive drift, Math. Biosci.,3,191-204,2.32.

SHAPIRO,H.S. and R.A.SILVERMAN,1960,Alias free sampling of random noise,J. Soc. Ind. Appl. Math.,8,225-48,4.26,4.27.

SHE,C.Y.,1973,Laser cross-beam intensity-correlation spectrum for a turbulent flow,12,2415-20,2.24,2.26.

SHE,C.Y. and J.A.LUCERO,1973,Simultaneous determination of velocity,turbulence and particle concentration of a turbulent flow using laser cross-beam photon-correlation spectroscopy, Opt. Commun.,9,300-3,2.10.

SHE,C.Y. and L.S.WALL,1975,Analytical evaluation of techniques for use of a laser Doppler velocimeter to measure flow and turbulence,J. Opt. Soc. Am.,65,69-77,2.9,2.11.

SMITH,D.M. and D.M.MEADOWS,1974,Power spectra from random time samples for turbulence measurements with a laser velocimeter,in Proc. second int. workshop on laser velocimetry, Purdue Univ.,4.3,4.22,4.25.

SNEDDON,I.N.,1966,Special functions of mathematical physics and chemistry,Oliver and Boyd,Edinburgh,3.14.

SPECHT,C.P.,1971,1971,Series estimation of a probability density function,Technometrics,13,409-24,4.24,4.25.

TAI,I.,K.HASEGAWA and A.SEKIGUCHI,1975,A real time correlator with peak detector,J. Phys. E: Sci. Inst.,8,206-8,2.30.

WANG,C.P.,1972,A unified analysis of laser Doppler velocimeters, J. Phys. E: Sci. Inst.,5,763-6,2.8,2.9.

WASAN,M.,1968,First passage time distribution of Brownian motion,monograph,Dept. of Maths, Queen's Univ,Kingston,Ontario, 2.31,2.32.

WATRASIEWICZ,B.M. and M.J.RUDD,1976,Laser Doppler measurements, Butterworths,London,3.6.

WAX,N.,Editor,1954,Selected papers on noise and stochastic processes,Dover,N.Y.,2.25. The paper referred to is by S. Rice.

YEH,Y. and H.Z.CUMMINS,1964,Localized fluid flow measurement with an He-Ne laser spectrometer,Appl. Phys. Lett.,4, 176-8,2.5.

Reports and papers written during the period Dec. '72 -Sept. '76

1. Assessment of photon counting technique (preliminary report), Sept.'73, 30 pages.

   An expression is derived relating the velocity variance for a uniform flow to the variance of the correlogram ordinates in the case of low scattered intensity. A direct expression for the variance of the ordinates, assuming Gaussian statistics for the scattered intensity, is derived and conditions for its validity presented.

2. Assessment of photon counting technique (report no. 2), Sept.'74, 24 pages.

   The count correlation function is derived for a velocity with sinusoid variation using two different methods. Experiments are described which show the usefulness of the theoretical results. These include an investigation of vortex shedding behind a cylinder in a uniform flow using photon correlation. The Maximum Entropy Method is described. The program listing for the ME method included in this report was modified in '76 and then used to obtain the spectra shown in chapter 3. A square root transformation for the reduction in variance of the correlogram ordinates is presented.

3. Application of photon correlation techniques to the measurement of flows with a sinusoidal perturbation, F.H.Barnes,Q.I.Daudpota,I.Grant and C.A.Greated. Accepted for publication in Physics of Fluids. A preliminary version of this paper was presented at the Fluid Dyn. Panel Symp. on Appl. of Non-Intrusive Instrum. in Fluid Flow Research, AGARD, French German Res. Inst., St. Louis, France, 3-5 May '76. See chapters 2,3 and Appendix A.

4. Estimation of moments of a Poisson sampled random process, Q.Isa Daudpota,Graham Dowrick and Clive A.Greated. Accepted for publication in J.Phys.A.:Math.Nucl.Gen. See chapter 4 §3-8.

5. Error analysis of randomly clipped photon count correlation estimator,Q.Isa Daudpota,Opt. Commun.,1976,17,143-4. See Appendix B.

6. A joint short note,with Dr. C. Greated, on the results of chapter 3 relating to the frequency transformation methods is planned.

IMPORTANT FORMULAE

1-Doppler frequency = $u/s = 2\,u \sin(\theta/2)/\lambda$ pg. 2.5

u = particle velocity, s = fringe spacing,

θ = angle between the beams.

2-Beam waist diameter at $1/e^2$ point: $d = 4\lambda f/(\pi D)$ pg. 2.11

3-Intensity scattered by a particle

$$I(t) = I_o \exp\left[-\frac{(t-t_o)^2 u^2}{2r^2}\right] \cos^2\left(\frac{\pi u t}{s}\right)$$ pg. 2.17

4-Correlation function for turbulent flow with Gaussian statistics and frequency shift f_s is

$$R(\tau) = D \exp\left(-\frac{u^2\tau^2}{4r^2}\right)\left[1 + \frac{m^2}{2}\exp\left(-\frac{2\pi^2\sigma^2}{s^2}\tau^2\right)\cos\left(2\pi\{u/s+f_s\}\tau\right)\right]$$

pg. 2.26

5-Correlation function for uniform velocity can be obtained from the previous formula by setting $\sigma=0$. pg. 2.19

6-Correlation function for a sinusoidally fluctuating flow is

$$R(\tau) = F \exp\left(-\frac{u^2\tau^2}{4r^2}\right)\left[1 + \frac{m^2}{2} J_o\left(\frac{2\pi a}{s}\tau\right)\cos\left(\frac{2\pi u}{s}\tau\right)\right]$$

pg. 2.29